

Copyright

by

Jordan Paul Lewandowski

2014

The Dissertation Committee for Jordan Paul Lewandowski Certifies that this is the approved version of the following dissertation:

Transcriptional regulation of sonic hedgehog target genes in the mammalian limb

Committee:

Steven Vokes, Supervisor

John Wallingford

Dean Appling

Vishwanath Iyer

Johann Eberhart

**Transcriptional regulation of sonic hedgehog target genes in the
mammalian limb**

by

Jordan Paul Lewandowski, B.A.

Dissertation

Presented to the Faculty of the Graduate School of
The University of Texas at Austin
in Partial Fulfillment
of the Requirements
for the Degree of

Doctor of Philosophy

The University of Texas at Austin

December 2014

Dedication

To Kirk Fleischauer,
For instilling an insatiable sense of curiosity

Acknowledgements

A doctoral degree is a consuming process that would not be manageable without the guidance and help from many people. Firstly, a graduate mentor is instrumental throughout the course of a doctoral program. I have had the privilege to study in Steven Vokes' lab. Steven has been incredibly supportive throughout my doctoral work, and I cannot express enough gratitude for his scientific and professional training. Secondly, the members of my dissertation committee – John Wallingford, Dean Appling, Vishy Iyer, and Johann Eberhart – have been essential in my scientific and professional development, and I cannot thank them enough. Along the same line, my undergraduate advisor, Robert Boswell, laid the foundation for my scientific training in ways that are too numerous to list here; so simply thank you for everything. Thirdly, scientific collaborations are excellent ways to engage in new problems and extend the breadth of a project. I am grateful to have been a part of a number of productive scientific collaborations and I would like to thank Dean Appling, Jessica Momb, Hongkai Ji, Fang Du, Shilu Zhang, Qiang Li, and Jacqueline Norrie. Lastly, I would like to thank the many people in the developmental biology community at the University of Texas at Austin who have been incredibly helpful providing material support, scientific discussion, and encouragement: Jacqui Tabler, Marian Powell, Taylor Pursell, Kayla Walter, Adam Rabinowitz, Simone Giovanetti, Susie Banks, and Kristen Falkenstein. The people I have engaged with along the way have been fantastic mentors, colleagues, and friends; for that, I am very grateful.

Transcriptional regulation of sonic hedgehog target genes in the mammalian limb

Jordan Paul Lewandowski, Ph.D.

The University of Texas at Austin, 2014

Supervisor: Steven A. Vokes

The Hedgehog (HH) family of secreted proteins are critical regulators of embryonic development. Dysregulation of the HH pathway results in a large class of developmental defects as well as several types of cancer. HH signaling elicits a transcriptional response by regulating GLI transcription factors. The mechanisms by which GLIs activate and sustain gene expression in response to HH are not well understood. To address this in the limb, we undertook a systems level analysis to determine the spatiotemporal kinetics of the GLI transcriptional response. In addition, we focus on the regulation of a single GLI-bound cis-regulatory module (CRM) associated with the GLI target gene, *Gremlin*. And lastly, we establish a primary limb cell culture method that can be utilized in a medium throughput manner to manipulate gene expression and test the activity of DNA elements. This work provides the first characterization of the spatiotemporal response of a large group of GLI target genes. Furthermore, this work lays the foundation for a systems-level understanding of the gene regulatory networks underlying SHH-mediated limb patterning.

Table of Contents

List of Tables	x
List of Figures	xi
Chapter 1: Hedgehog, limb development, and transcriptional control	1
1.1: Functions of Hedgehog signaling	1
1.1.1: Hedgehog signaling in limb development	1
1.1.2: Hedgehog signaling in human disease	4
1.2: Hedgehog signal transduction	5
1.3: Transcriptional control of GLI target genes	7
1.3.1: GLI co-factors	8
1.4.2: GLI DNA motif quality	9
1.4: Concluding remarks	10
Chapter 2: Spatio-temporal regulation of GLI target genes in the limb	11
2.1: Introduction	11
2.2: GLI target genes cluster into three domains	12
2.3: GLI target genes have different temporal requirements for SHH	18
2.4: DNA motif analysis in CRMs	24
2.5: Sp-mediated transcription	27
2.6: Discussion	34
2.6.1: Expression patterns of GLI target genes	35
2.6.2: Different temporal requirements for SHH	37
2.6.3: Regulatory inputs in GLI-bound CRMs	38
Chapter 3: A GLI silencer robustly represses <i>Grem1</i> in the limb bud	42
3.1: Introduction	42
3.2: GRE1 genomic landscape and activity domain	44
3.3: GRE1 activity is regulated by GLI	47
3.4: GRE1 requires sustained SHH signaling	50
3.5: WNT and FGF signaling do not regulate GRE1	53
3.6: GRE1 functions as a GLI-mediated silencer	55

3.7: Discussion.....	61
3.7.1: GRE1 enhancer activity	62
3.7.2: GRE1 and GLI repressors.....	64
3.7.3: GLI proteins generate asymmetric gene expression.....	65
3.7.4: Multiple CRMs regulate <i>Grem1</i>	66
3.7.5: GLI-bound CRMs and robust transcriptional control.....	68
Chapter 4: Manipulating gene expression in dissociated limb buds.....	70
4.1: Introduction.....	70
4.2: Assessment of differentiation in limb cell cultures	71
4.3: Purmorphamine promotes an increase in cell number.....	74
4.4: Limb cells are responsive to multiple signaling pathways	75
4.5: Characterization of GLI target genes in limb cell culture	77
4.6: Delivering plasmids and siRNA into limb cell cultures	80
4.7: Discussion.....	82
Chapter 5: Future directions and concluding remarks	85
5.1: Mechanisms mediating a temporal Hedgehog response.....	85
5.2: How does FGF integrate with SHH to regulate GLI target genes?	87
5.3: Dual functioning GLI-bound CRMs.....	88
5.4: Concluding remarks.....	89
Appendix A: GLI target gene expression patterns.....	90
A.1: Spatial distribution of GLI target genes.....	90
A.2: GLI target gene expression patterns	97
Appendix B: RNAseq	101
B.1: Differentially expressed genes in cyclopamine treated limbs.....	101
B.2: Differentially expressed genes in Shh-deficient limbs.....	104
Appendix C: Materials and methods.....	115
C.1: Mice and ethics statement	115
C.2: Whole-mount in situ hybridization	115
C.3: Riboprobes	115

C.4: Quantitative reverse-transcriptase PCR	121
C.5: Shh ^{-/-} forelimb RNAseq	122
C.6: Cyclopamine treated wild-type forelimb RNAseq.....	123
C.7: de novo motif discovery and Gli motif quality analysis	124
C.8: Sp1 motif meta analysis	124
C.9: Co-immunoprecipitation	125
C.10: Mouse forelimb trunk cultures	125
C.11: Dissecting, dissociating, and nucleofecting mouse limb cells	126
C.12: Gaussia luciferase assay	129
C.13: Flow cytometry analysis	129
C.14: Alcian blue staining and imaging.....	129
C.15: GRE1 mouse transgenics	130
C.16: Primers	131
Commonly used abbreviations.....	133
References.....	134

List of Tables

Table 2.1:	Classification and expression of GLI target genes	23
Table A1:	Classification of the spatial expression of GLI target genes.....	91
Table B1:	Cyclopamine RNAseq	101
Table B2:	Shh ^{-/-} RNAseq	104
Table C1:	Generating riboprobes against GLI target genes	115
Table C2:	Primers used in qRT-PCR experiments	131

List of Figures

Figure 1.1: Illustration of an E10.5 mouse embryo and forelimb	2
Figure 1.2: Schematic of SHH-GREM1-FGF signaling regulatory loop.....	3
Figure 1.3: Simplified illustration of the Hedgehog signaling pathway	6
Figure 1.4: Model of digit specification and growth.....	8
Figure 2.1: <i>in situ</i> hybridization screen for GLI target genes	13
Figure 2.2: GLI target genes cluster into three distinct domains	15
Figure 2.3: GO biological processes enrichment in expression domain	16
Figure 2.4: GLI target genes maintain early expression domain.....	17
Figure 2.5: Schematic depicting RNA-seq pipeline	19
Figure 2.6: GLI target genes have distinct temporal requirements for SHH.....	21
Figure 2.7: DNA motifs enriched in GLI-bound CRMs	25
Figure 2.8: Assessment of the quality of Gli motifs in GLI-bound CRMs	26
Figure 2.9: <i>Sp1</i> is expressed in the forelimb and is not regulated by SHH.....	28
Figure 2.10: SP-mediated transcription maintains GLI target genes	29
Figure 2.11: FGF inhibition does not downregulate most GLI target genes.....	31
Figure 2.12: Sp1 siRNA in micromass limb culture	32
Figure 2.13: SP-mediated transcription activates GLI target genes.....	34
Figure 2.14: Model illustrating the roles of GLI and SP1	40
Figure 3.1: GRE1 enhancer activity	45
Figure 3.2: GRE1 enhancer activity correlates temporally with Shh activity.....	46
Figure 3.3: GRE1 enhancer activity requires Gli-activation	48
Figure 3.4: <i>Gli1</i> is reduced in <i>Gli3</i> ^{-/-} forelimbs	49
Figure 3.5: GRE1 enhancer activity requires sustained Shh signaling	52

Figure 3.6: GRE1 enhancer activity is not negatively regulated by FGF	54
Figure 3.7: Inhibition of WNT signaling does not perturb GRE1 activity	55
Figure 3.8: GRE1 is not essential for limb development	57
Figure 3.9: Gremlin and GRE1 transheterozygote	58
Figure 3.10: GRE1 CRM interacts genetically with Gli3 to repress <i>Grem1</i>	59
Figure 3.11: Schematic models showing Gli3 repression of <i>Grem1</i>	61
Figure 3.12: GLI proteins generate asymmetric expression of <i>Grem1</i>	67
Figure 4.1: Assessment of limb cell differentiation	73
Figure 4.2: Individual and collective effects on cell number	74
Figure 4.3: Limb bud cells are responsive to multiple signaling pathways	76
Figure 4.4: Regulation of Shh target genes in primary limb bud cultures	79
Figure 4.5: Method to efficiently deliver plasmids and siRNA	82
Figure A1: Schematized spatial distributions of GLI target genes	90
Figure A2: Category 1 gene expression patterns.....	97
Figure A3: Category 2 gene expression patterns.....	98
Figure A4: Category 3 gene expression patterns.....	99
Figure A5: Multiple domain gene expression patterns	100

Chapter 1: Hedgehog, limb development, and transcriptional control

1.1: FUNCTIONS OF HEDGEHOG SIGNALING

The Hedgehog (HH) family of secreted proteins are critical regulators of embryonic development across a variety of metazoans. The responses elicited by the HH pathway vary greatly; HH signaling acts as an inductive signal for transcription, promotes cell proliferation, enables cell survival, and regulates tissue homeostasis (reviewed in Wilson and Chuang, 2010). In addition to the key roles in development, dysregulation of the HH pathway has been implicated in several types of cancer.

In mammals there are three homologs of HH: desert hedgehog (*Dhh*), Indian hedgehog (*Ihh*), and sonic hedgehog (*Shh*), each of which have key functions in organizing tissue growth and patterning during embryonic development. Among the key roles, *Dhh* regulates germ cell formation in the testis, *Ihh* regulates both bone and cartilage development, and *Shh* regulates neural, muscle, and limb development (reviewed in Jiang and Hui, 2008). Because the HH pathway is employed iteratively during development, it is feasible to utilize several developing tissues as a model to study the pathway.

1.1.1: Hedgehog signaling in limb development

The developing vertebrate limb bud, readily amenable to genetic and embryological approaches, is a well-established model system used to study the HH signaling pathway.

In the vertebrate limb bud, *Shh* is expressed in the posterior margin (termed the zone of polarizing activity) (Chang et al., 1994; Riddle et al., 1993) (Fig. 1.1). This region was identified in a series of tissue transplant experiments in chicken looking for limb tissue with anterior-posterior organizing activity (Saunders and Gasseling, 1968). Since *Shh* encodes a secreted protein, SHH activity reaches over half of the limb as indicated by the pathway target gene *Gli1* (Fig. 1.1).

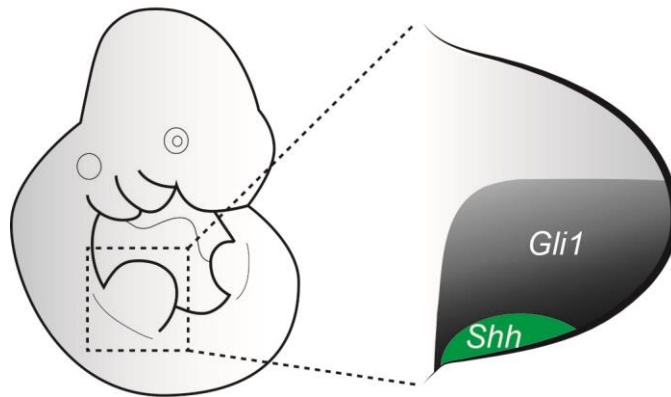


Figure 1.1: Illustration of an E10.5 mouse embryo and forelimb. *Shh* mRNA expression domain is shown in green. *Gli1* mRNA expression domain (SHH activity area) is shown in graded black.

In the developing vertebrate limb bud, *Shh* functions to regulate digit number and growth (Chiang et al., 1996; Towers et al., 2008; Zhu et al., 2008). This occurs through a signaling loop involving the regulation of a BMP inhibitor, gremlin 1 (*Grem1*) (Zuniga et al., 1999, Panman et al., 2006, Zuniga et al., 2012; Li et al., 2014; Vokes et al., 2008). GREM1 inhibits localized BMP activity, thereby maintaining the apical ectodermal ridge

(AER), which propagates a signaling loop between the mesoderm and the AER, thereby regulating limb growth and digit number (Khokha et al., 2003; Litingtung et al., 2002; Michos et al., 2004; te Welscher et al., 2002; Zuniga et al., 1999) (Fig. 1.2). The importance of regulating *Grem1* is discussed in Chapter 4.

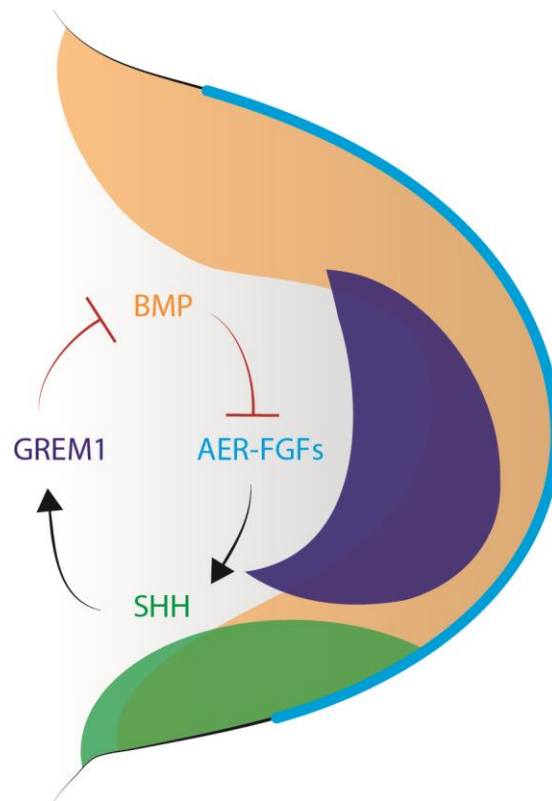


Figure 1.2: Schematic of SHH-GREM1-FGF signaling regulatory loop during limb development. Gene expression domains: green depicts sonic hedgehog (SHH), light orange depicts bone morphogenetic protein (BMP), dark blue depicts Gremlin 1 (GREM1), and light blue in the apical ectodermal ridge (AER) depicts FGF expression.

1.1.2: Hedgehog signaling in human disease

Considering the critical functions of HH signaling during development, it is not unexpected that dysregulation of the pathway's upstream or downstream components lead to a broad spectrum of human congenital birth defects and cancers. Major defects in the pathway lead to severe neural abnormalities (holoprosencephaly, exencephaly, and cyclopia) and ultimately embryonic lethality (reviewed in Murdoch and Copp, 2010). Less severe defects in the pathway are associated with human abnormalities including: extra digits (polydactyly), shorter limbs, missing digits, and craniofacial defects (reviewed in Anderson et al., 2012) . In addition to the variety of developmental deformities, dysregulation of the HH pathway is also implicated in several types of cancer. Mutations in the HH receptor, patched 1 (*Ptch1*), are found in human skin cancers (basal cell carcinomas) and aggressive brain tumors (medulloblastomas) (Kool et al., 2014, Pietsch et al., 1997; Fan et al., 1997; Gailani et al., 1996, Johnson et al., 1996). Taken together, defects in the HH pathway are critical drivers of various human pathologies.

The extensive connections between HH signaling and disease have generated much interest in determining how the HH pathway is regulated and its elicited cellular responses. The subsequent sections summarize of key aspects of HH signal transduction, temporal responses to HH ligand, and a compendium of the transcriptional control mechanisms used to regulate HH target genes.

1.2: HEDGEHOG SIGNAL TRANSDUCTION

The HH signaling pathway regulates growth and patterning in multiple tissues during embryogenesis. Secreted HH ligands can spread over several cell diameters, eliciting both short and long-range effects (Chamberlain et al., 2008; Li et al., 2006; Nahmad and Stathopoulos, 2009; Sanders et al., 2013). In vertebrates, the HH signaling pathway is regulated by the primary cilia, a microtubule-based cellular protrusion (reviewed in Goetz and Anderson, 2010) (Fig. 1.3). HH-receiving cells ultimately respond by modulating the activity of the downstream GLI transcription factors (GLI1-3, homologs of Ci in *Drosophila*). In the absence of HH ligand, GLIs are partially degraded by the proteasome, forming a truncated protein that functions as a transcriptional repressor (GLI-R). Conversely, in the presence of HH ligand, processing of GLI proteins to transcriptional repressors is inhibited, permitting the formation of full-length GLI activators (GLI-A) (Aza-blanc et al., 1997; Méthot and Basler, 1999; Pan et al., 2006; Wang et al., 2000) (Fig. 1.3). Reducing the levels of GLI-R and favoring GLI-A elicits a diverse transcriptional response of GLI target genes (further discussed in Chapter 2).

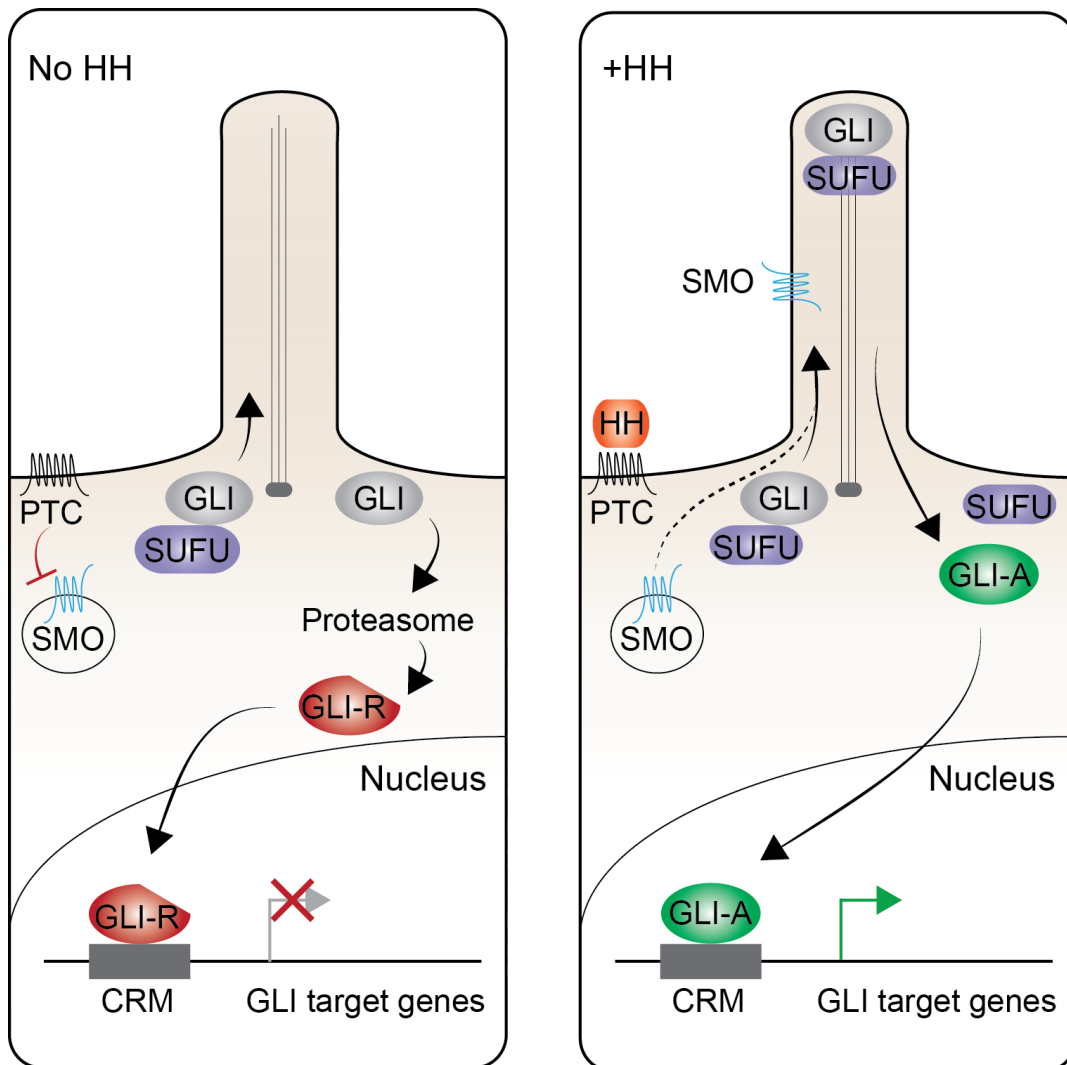


Figure 1.3: Simplified illustration of the Hedgehog signaling pathway. Patched 1 (PTCH1), suppressor-of-fused (SUFU), smoothened (SMO), cis-regulatory module (CRM), hedgehog (HH), Gli activator (GLI-A), Gli repressor (GLI-R). Cellular protrusion is the primary cilia.

1.3: TRANSCRIPTIONAL CONTROL OF GLI TARGET GENES

The timing and duration of SHH is important for establishing polarity within the limb bud (Li et al., 2014; Zhulyn et al., 2014), and there is some evidence suggesting that cells retain a memory of their exposure to SHH (Harfe et al., 2004). In addition, studies have indicated that a relatively brief exposure to SHH specifies digit patterning, while longer exposures are needed for subsequent growth and expansion of the autopod and digit progenitor cells (Towers et al., 2008; Zhu et al., 2008) (Fig. 1.4). The differential requirements of SHH for digit specification and growth suggest there are GLI target genes with distinct temporal requirements for SHH. While a few studies have determined the temporal requirement for HH signaling for a limited number of GLI target genes (further discussed in Chapter 2), a number of outstanding questions remain: What is the temporal requirement of HH signaling for a broad group of GLI target genes? What are the molecular mechanisms underlying the temporal transcriptional responses?

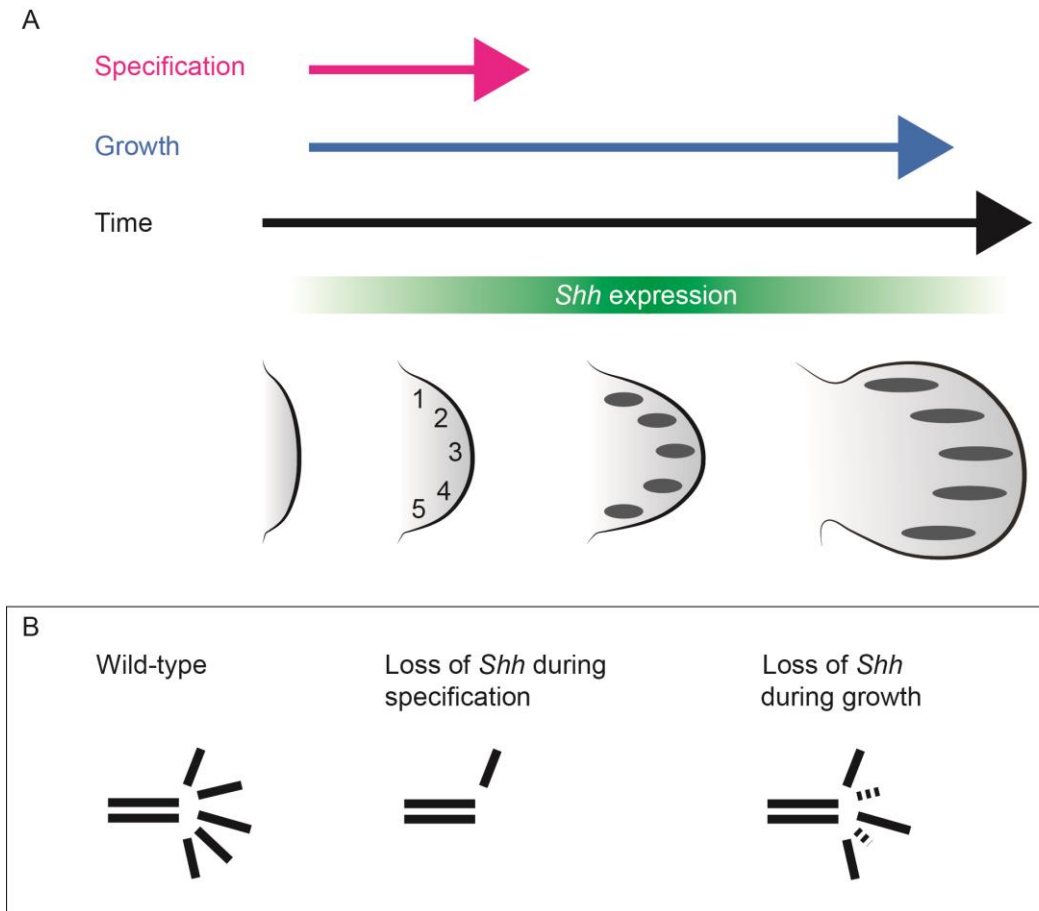


Figure 1.4: Model of digit specification and growth during limb development. (A) Schematized developing limb buds showing specification of early digit progenitors and subsequent expansion. (B) Schematized skeletal phenotypes when *Shh* is removed during the digit specification period and during the growth phrase. Gray ovals represent digit progenitors and growing digit rays, and dashed lines represent undergrown digits.

1.3.1: GLI co-factors

GLI proteins activate or repress target gene transcription by binding to a similar DNA sequence motif (TGGGTGGTC) within a cis-regulatory module (CRM) (Hallikas et al., 2006; Peterson et al., 2012). Transcriptional responses to the HH pathway can be

elicited either by de-repression of GLI-R or in other cases, by transcriptional activation through GLI-A (further discussed in Chapter 4) (reviewed in Falkenstein and Vokes, 2014). In addition, recent studies suggest that additional tissue-specific factors are necessary for activating appropriate GLI target genes (Biehs et al., 2010). In the neural tube, GLI-bound CRMs are enriched for SOX binding motifs, and SOX2 and SOXB1 acts as a neural-specific GLI co-factors (Oosterveen et al., 2012; Oosterveen et al., 2013; Peterson et al., 2012). The mechanisms underlying transcriptional specificity in other Hh-mediated developmental processes remain unknown.

1.3.2: GLI DNA motif quality

A recent study in the mouse neural tube suggests that the quality (with respect to the consensus sequence) of Gli binding sites (GBS) in CRMs function in a temporal response for GLI target genes (Peterson et al., 2012). In addition, evidence from several studies indicate that GBS quality is an important factor in the spatial readout of Shh signaling. In the chick neural tube, GLI target genes closest to the HH signaling source are associated with CRMs that have higher quality Gli binding sites (GBS), while genes farther away are associated with CRMs that contain lower quality GBS (Oosterveen et al., 2012). Similarly, in the *Drosophila* imaginal wing disc, a CRM that controls the expression of a broadly expressed gene, *Dpp*, contains multiple low quality Ci sites, whereas a CRM that controls the expression of a gene, *Ptc*, which is closer to the Hh signaling source, contains high quality Ci sites (Parker et al., 2011). It is interesting to speculate that the quality of

the GBS may play a role in the temporal response of target genes in the developing mouse limb.

1.4: CONCLUDING REMARKS

The iterative use of the Hedgehog signaling pathway throughout embryonic development highlights the importance of the pathway. Moreover, implications of the Hedgehog pathway in cancers, make understanding the molecular mechanisms regulating this pathway critical to human health. Over the past several decades much information has been discovered about the Hedgehog pathway; however, there are a numbers of outstanding questions pertaining to the transcriptional control mechanisms and tissue-specific responses.

Chapter 2: Spatiotemporal regulation of GLI target genes in the limb

Contributing to this work: Lewandowski, J.P., Du, F., Zhang, S., Powel, M.B., Ji, H., and Vokes, S. A. Spatiotemporal regulation of GLI target genes during mammalian limb development (manuscript in revision). J.P.L., F.D., S.Z., H.J., conceived experiments, and collected and interpreted data; M.B.P performed experiments.

2.1: INTRODUCTION

As mentioned in Chapter 1, GLI proteins convert Sonic hedgehog (Shh) signaling into a transcriptional output. The mechanisms by which GLI proteins activate and sustain gene expression in response to SHH are not well understood. The timing and exposure of SHH is clearly important; however, only a few studies have investigated the temporal requirement for SHH signaling on the level of individual genes (Bénazet et al., 2009; Drossopoulou et al., 2000; Panman et al., 2006; Scherz et al., 2007; Zuniga et al., 2004). To address this in the limb, we undertook a systems level analysis to determine the spatiotemporal kinetics of the GLI transcriptional response.

In previous work, we used chromatin immunoprecipitation (ChIP) to identify GLI binding sites and intersected these with microarray gene expression datasets from Shh mutants in order to predict a set of approximately 200 putative direct GLI target genes in the developing limb bud (Vokes et al., 2008). Here, we extend these studies and determine the expression domains of our predicted GLI target genes in the mouse limb. Using this approach we found three distinct expression domains for GLI target genes. We then show that genes within these domains have different temporal SHH signaling requirements for

establishing their expression. Further, we find that the GLI-bound CRMs associated with genes in each domain are enriched for both unique and common DNA motifs including one for SP-family transcription factors. Finally, we provide evidence that SP-mediated transcription is critical both for initiating and sustaining a subset of GLI target genes. We speculate that SP proteins may represent a way of transferring transcriptional control from transient inductive signals to ubiquitously expressed factors that maintain transcription. Collectively, these results provide the first characterization of the spatiotemporal response of a large group of GLI target genes, and lay the foundation for a systems-level understanding of the gene regulatory networks underlying SHH-mediated limb patterning.

2.2: GLI TARGET GENES CLUSTER INTO THREE DOMAINS

The expression patterns of 199 of 205 previously predicted GLI target genes (Vokes et al., 2008) were determined at E10.5 and E11.5 (Fig. 2.1A). Of the 199 genes analyzed, 96% ($n=191$) were detected in embryos at E10.5, and of these, 90% ($n=171$) were detected in the limb (13 of 19 genes not detected in the limb by *in situ* at E10.5 were detected at E11.5). We classified genes on the basis of their expression pattern in the limb at E10.5 (Fig. 2.1B, Table 2.1, Fig. A1, and Table A1) and subsequently focused on understanding genes predominately expressed in the SHH-responsive posterior limb (Fig. 2.2A and Table 2.1).

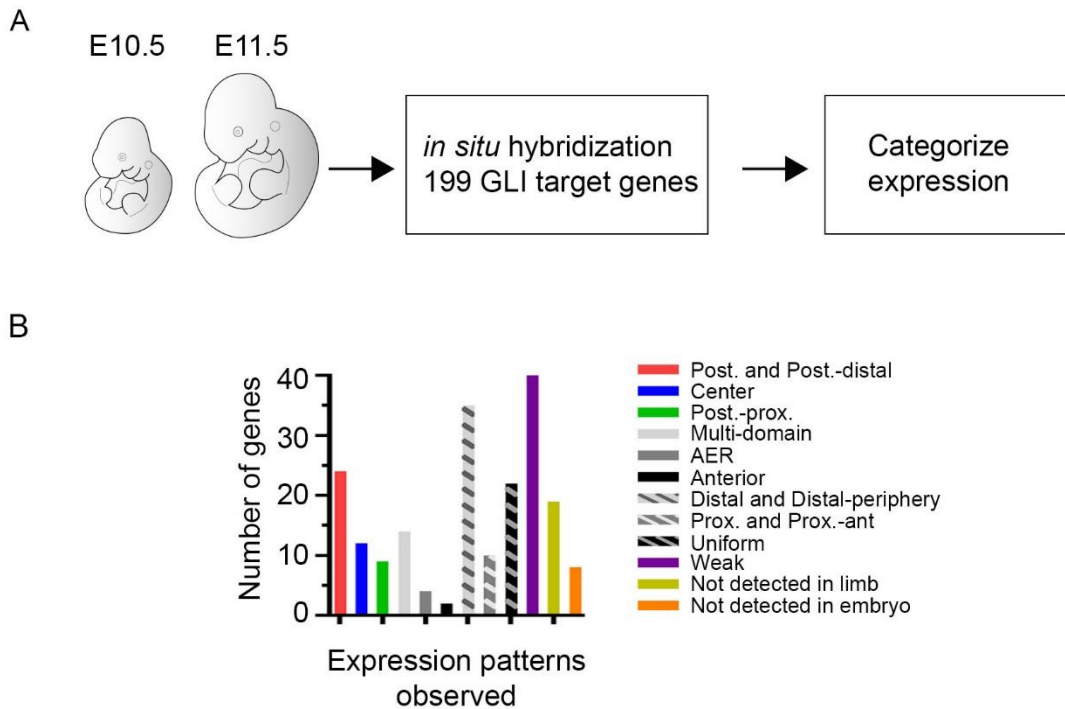


Figure 2.1: *in situ* hybridization screen for GLI target genes (A) *in situ* hybridization pipeline for 199 GLI target genes. (B) Distribution of expression patterns in the limb.

We searched for genes that were predominately expressed in the posterior limb bud, a region that is responsive to SHH signaling as defined by the expression of pathway target genes *Gli1* and *Ptch1* (Fig. 2.2A) (Litington et al., 2002; Marigo et al., 1996; te Welscher et al., 2002; Chiang et al., 2001; Ahn et al., 2004). Posteriorly expressed genes cluster into three broad domains (Fig. 2.2B-D, Table 2.1, Fig. A1, and Table A1). Category 1 contained 24 genes expressed in the posterior and posterior-distal limb bud (Fig. 2.2B). Genes in this category included the SHH pathway target genes *Gli1*, *Ptch1*, and *Ptch2* (Chiang et al., 2001; Litington et al., 2002; te Welscher et al., 2002; Marigo et al., 1996; Motoyama et al., 1998). Category 2 comprised 12 genes expressed in the central limb (Fig. 2.2C), and

category 3 contained 9 genes that were expressed in the posterior-proximal limb (Fig. 2.2D). Lastly, we identified 14 genes expressed in multiple domains, where at least one expression domain was spatially located within the SHH-responsive region. Because these may have more complex forms of regulation we excluded these genes from further analysis (Fig. A5). Altogether, we identified 45 genes that were expressed in three domains in the limb bud.

The identification of distinct expression domains in the limb suggested that these domains might have specific biological functions. We explored this possibility by determining enriched biological processes for each category using GO ontology term analysis (WebGestalt) (Zhang et al., 2005). Category 1 was notably enriched for transcriptional regulation and cell proliferation processes ($P \leq 0.000001$) (Fig. 2.3). In contrast, category 2 was notably enriched for cell differentiation, cell adhesion, and ossification processes ($P \leq 0.05$), and category 3 was enriched for skeletal development processes ($P \leq 0.05$) (Fig 2.3). Differential enrichment within these categories suggests that the three distinct SHH-mediated domains in the limb may have unique functions.

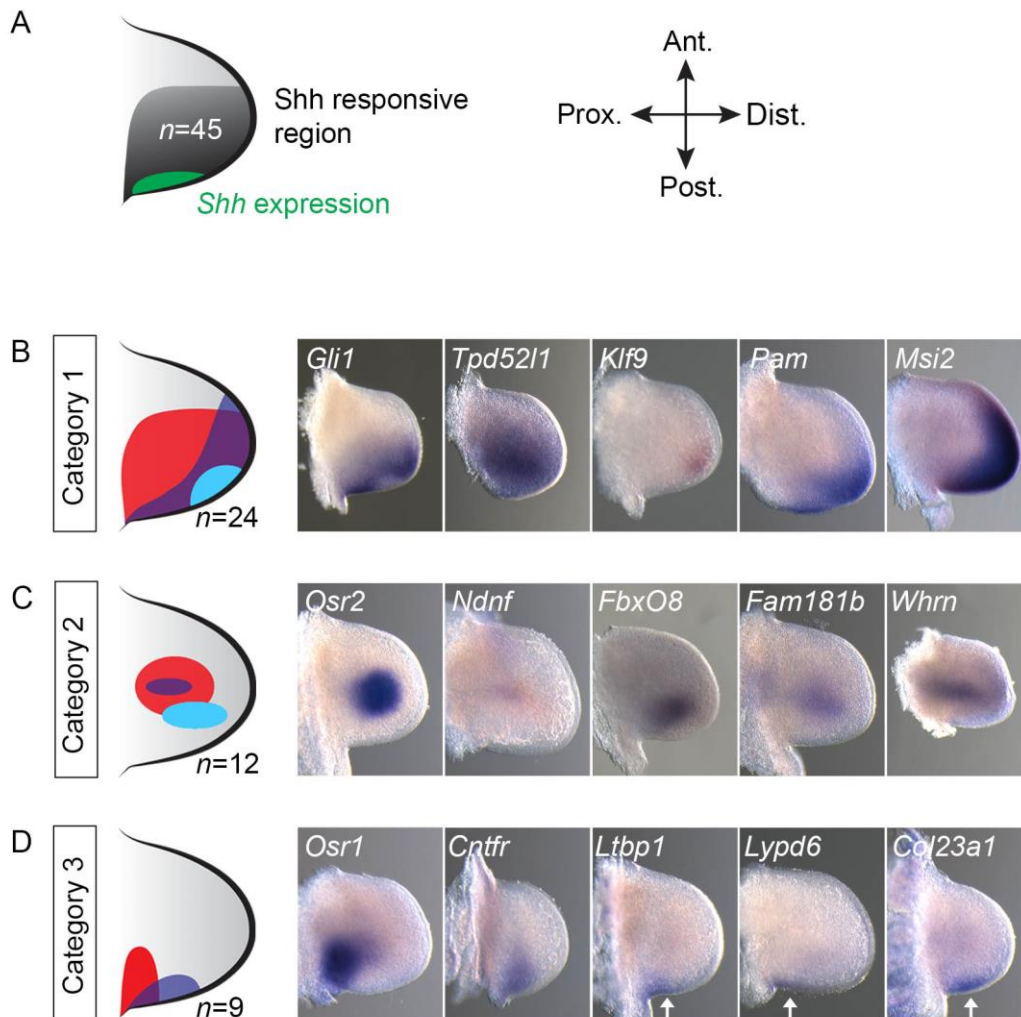


Figure 2.2: GLI target genes cluster into three distinct domains within the SHH-responsive region. (A) Schematic of E10.5 mouse limb showing *Shh* expression (green) and the SHH-responsive region (dark gray). (B-D) Schematized expression patterns observed for GLI target genes in individual categories depicted in red, light blue, and purple. Representative *in situ* images at E10.5 are shown. (B) Category 1 contains genes expressed in the posterior and posterior-distal limb ($n=24$), (C) Category 2 comprises genes expressed in the central limb ($n=12$), and (D) category 3 contains genes expressed in the posterior-proximal limb ($n=9$). White arrows indicate expression in the posterior-proximal domain.

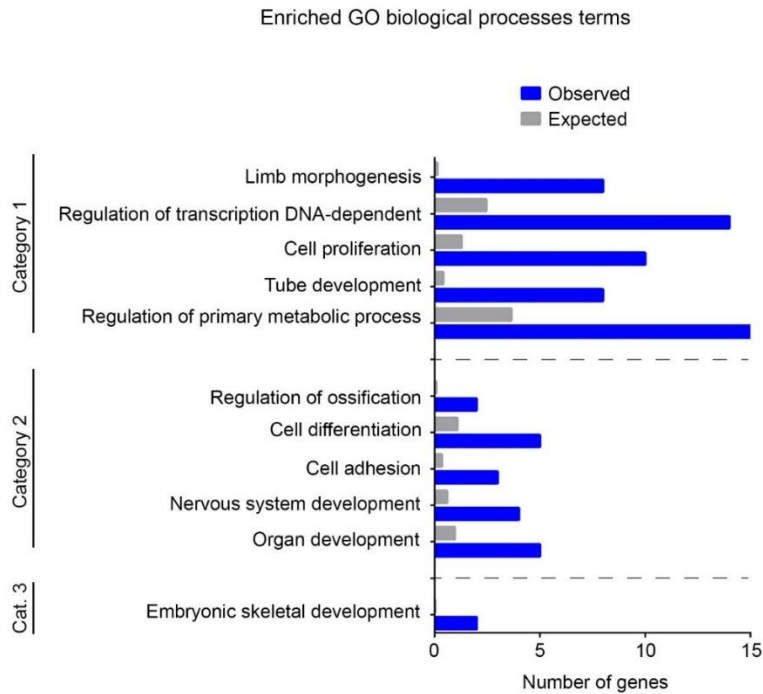


Figure 2.3: GLI target genes expressed in different domains in the limb are enriched for unique GO biological processes. Genes in each category were compared with the mouse reference sequences using GO ontology terms (WebGestalt). The expected number of terms for the given sample size are in gray, and observed terms from the input genes are in blue. The comparison used a hypergeometric distribution to calculate the statistic for each category. Terms in category 1 have a significance level of $P=0.000001$ with a minimum of 8 genes in each category. Terms in category 2 and 3 have a significance level of $P=0.05$ with a minimum of 2 genes in each category.

Our categorization of expression patterns was based on E10.5 limb buds. Because SHH signaling within the limb bud is dynamic, it is possible that the expression of GLI target genes within these domains could also be dynamic. To assess this, we examined the temporal changes in the expression domains of GLI target genes by comparing their expression patterns between E10.5 and E11.5. Most genes expressed in a particular domain at E10.5 remain expressed in a broader version of the same domain at E11.5 (category 1,

$n=18/24$; category 2, $n=9/12$; category 3, $n=8/9$) (Fig. 2.4 and Figs. A2-4). Taken together, these results indicate that the expression domains of GLI target genes are relatively stable despite the large changes in SHH signaling that occur during this period. In summary, we identified three stable domains of GLI target gene expression within the SHH-responsive region of the limb bud.

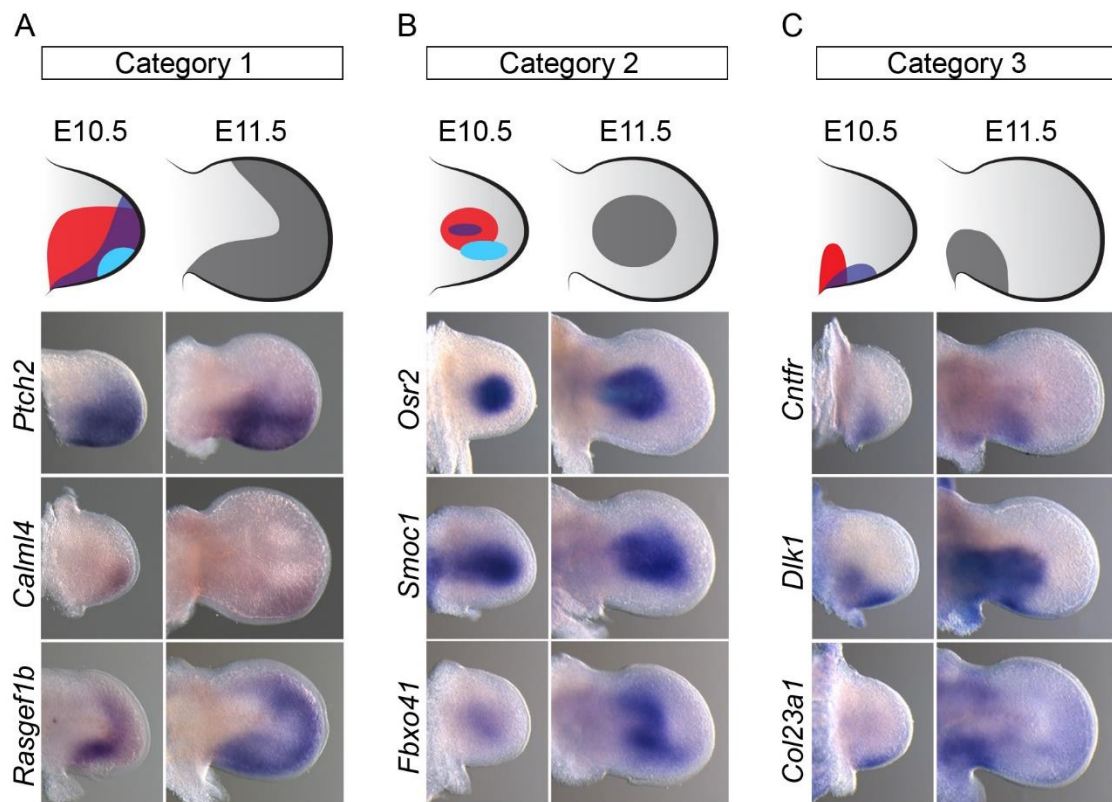


Figure 2.4: GLI target genes maintain early expression domain. (A-C) Schematized expression domains in E10.5 and E11.5 limbs for GLI target genes. Expression domains at E11.5 are broader (indicated in gray). Number of genes in each category expressed in the same domain at E10.5 and E11.5: (A) category 1, $n=18/24$, (B) category 2 ($n=9/12$), and (C) category 3 ($n=8/9$).

2.3: GLI TARGET GENES HAVE DIFFERENT TEMPORAL REQUIREMENTS FOR SHH

GLI target genes require SHH signaling for transcriptional activation or robust expression; however, subsequent requirements for SHH signaling have been determined for only a few GLI target genes. For example, *Hoxd13* requires SHH signaling for activation and continues to require SHH to maintain expression beyond E10.75 (Panman et al., 2006). In contrast, *Jag1*, requires exposure to SHH signaling through E10.25 before expression becomes independent of SHH signaling (Panman et al., 2006). We sought to determine the temporal requirement of SHH signaling for the group of 45 GLI target genes expressed in the posterior limb. To determine whether transient SHH activation was required for expression of GLI target genes, we cultured E10.25 wild-type limbs, which have already expressed *Shh*, in the presence of a HH pathway inhibitor, cyclopamine (Chen et al., 2002). If gene expression was maintained after transient SHH exposure, but downregulated in *Shh*^{-/-}, then SHH is required only transiently for GLI target gene expression. In contrast, if genes required continued exposure to SHH, they would remain downregulated in wild-type limb buds that received a brief exposure to SHH. While previous studies have identified SHH-responsive genes at E10.5 using microarrays (Probst et al., 2011; Shah et al., 2009), we decided to perform a new analysis using RNA-seq on E10.25 limb buds in order to make direct quantitative comparisons (Fig. 2.5).

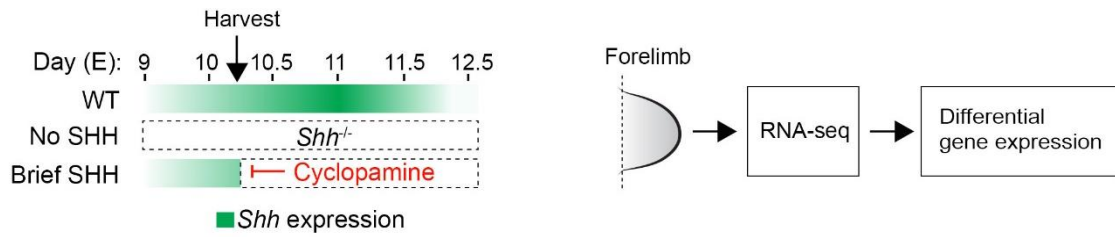


Figure 2.5: Schematic depicting RNA-seq pipeline. (A) *Shh* expression indicated in green. Forelimb samples with different SHH exposures indicated as WT, No SHH, and Brief SHH.

Using littermate E10.25 (32-35 somites) wild-type and *Shh*^{-/-} forelimbs, we identified 297 SHH-responsive genes downregulated $\geq 25\%$, ($\text{Log}_2\text{FC} \leq -0.4105$) with a false discovery rate (FDR) ≤ 0.05 (Table B2). Among these downregulated genes, we identified several known GLI target genes: *Gli1*, *Ptch1*, *Hhip*, *HoxD13*, *Grem1*, and *Hand2* (Table 2.1 and Table B2) (Bénazet et al., 2009; Chiang et al., 2001; Litingtung et al., 2002; Panman et al., 2006; Vokes et al., 2008; te Welscher et al., 2002). To determine which of these genes continue to require SHH, we cultured E10.25 (31-34 somites) wild-type forelimbs for 15 hours in either control media or media containing cyclopamine, a Hh pathway inhibitor which antagonizes Smoothened (*Smo*) (Chen et al., 2002; Panman et al., 2006). Within this dataset, we identified 61 genes downregulated $\geq 25\%$ ($\text{Log}_2\text{FC} \leq -0.4105$) with a $\text{FDR} \leq 0.05$. Consistent with previous reports, several genes that continue to require SHH at E10.25 were confirmed in our dataset: *Gli1*, *Hoxd11*, *Hoxd12*, and *Hoxd13* (Table 2.1 and Table B1) (Panman et al., 2006).

Next, we asked if the 45 GLI target genes predominately expressed in the posterior limb have differential requirements for SHH signaling. To determine genes that require

sustained SHH signaling, we identified genes that were downregulated $\geq 25\%$ ($\text{Log}_2\text{FC} \leq -0.4105$) with a $\text{FDR} \leq 0.1$ in both datasets (Fig. 2.6A). One gene, *Runx3*, was excluded from the analysis because of a low read count in one dataset. Among the group, 18 out of 44 genes were statistically downregulated in both *Shh*^{-/-} limbs and limbs treated with cyclopamine (Fig. 2.6B and Table 1, indicated with an asterisk). Interestingly, nearly all of the genes found downregulated in both datasets ($n=15$) were expressed in category 1 (posterior and posterior-distal), making it significantly enriched for genes requiring sustained SHH (two-sided Fisher's exact test, $P=0.0018$) (Table 2.1, indicated with an asterisk).

To determine the genes that require a transient exposure to SHH signaling, we identified genes downregulated $\geq 25\%$ ($\text{Log}_2\text{FC} \leq -0.4105$) with a $\text{FDR} \leq 0.1$ in *Shh*^{-/-} limbs that had unchanged expression relative to wild-type limbs cultured in cyclopamine. Among the group of 44 genes, 5 genes were statistically downregulated in *Shh*^{-/-} limbs but unchanged relative to controls in cyclopamine treated limb cultures (Fig. 2.6C and Table 2.1, indicated with a double dagger). All of these genes were expressed in categories 2 and 3, suggesting that in contrast to category 1, categories 2 and 3 have more transient requirements for SHH.

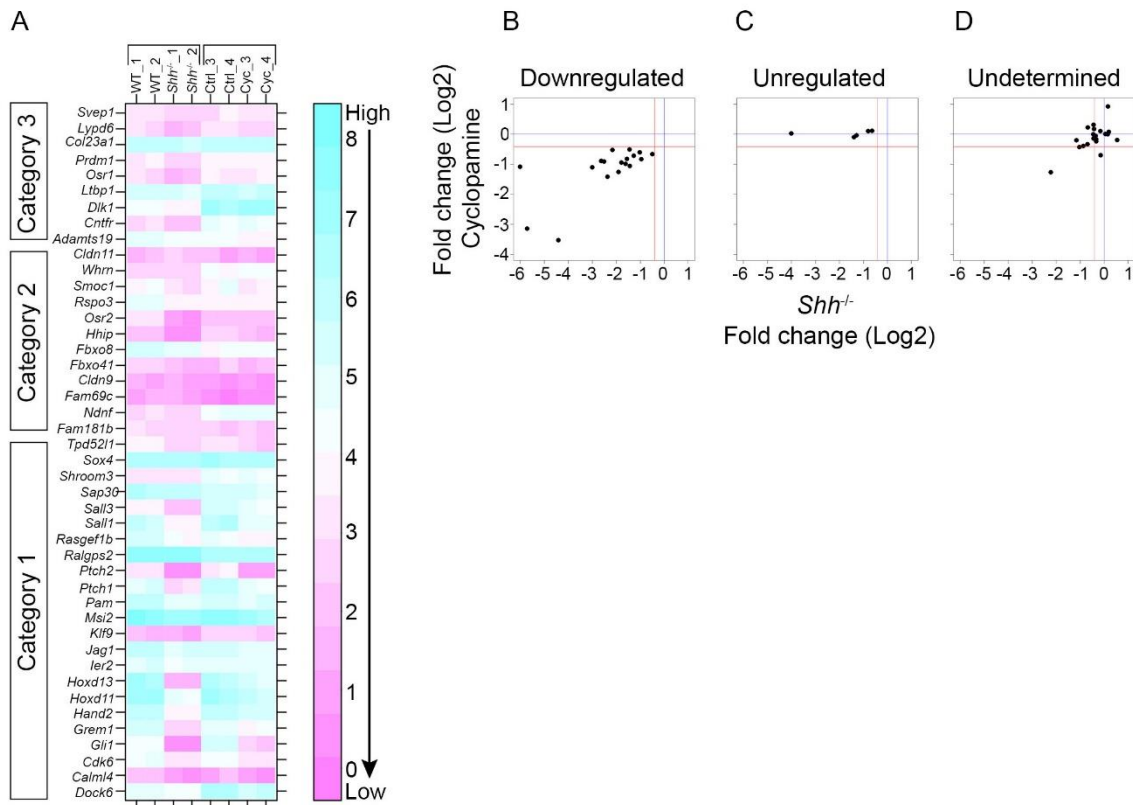


Figure 2.6: GLI target genes have distinct temporal requirements for SHH. (A) Heatmap showing expression for GLI target genes in categories 1-3 across eight RNA-seq samples: WT, wild-type; *Shh*^{-/-}; Ctrl, control; Cyc, cyclopamine. (B-D) Scatter plots showing expression (Log2FC) of GLI target genes in *Shh*^{-/-} (No SHH) and cyclopamine (Brief SHH) samples. Blue lines at 0 indicate no change in expression, and red lines indicate the downregulated cutoff (Log2FC = -0.4105). (B) Statistically downregulated GLI target genes in both *Shh*^{-/-} and cyclopamine samples ($n=18$). (C) GLI target genes statistically downregulated in *Shh*^{-/-}, but unregulated in cyclopamine sample ($n=5$). (D) GLI target genes unable to make a statistical determination ($n=21$). Expression values for genes in C-E indicated in Table 2.1.

The expression values for 21 out of the 44 genes were not different enough to make a statistical determination; they were neither significantly reduced nor statistically unchanged (Fig. 2.6D and Table 2.1). These genes, downregulated in *Shh*^{-/-} limb buds,

could represent a category that is in the process of becoming transcriptionally independent of SHH signaling. In summary, we found that genes expressed in the posterior and posterior-distal (category 1) tend to require a longer exposure to SHH signaling in order to maintain expression, while genes expressed in the central (category 2) and posterior-proximal (category 3) tend to require a shorter exposure to SHH before expression becomes independent. We conclude that GLI target genes have differential requirements for SHH signaling, and that the transcriptional regulation of GLI target genes correlates with where they are expressed.

Category 1			Category 2			Category 3		
Gene	FC <i>Shh</i> ^{-/-}	FC cyc	Gene	FC <i>Shh</i> ^{-/-}	FC cyc	Gene	FC <i>Shh</i> ^{-/-}	FC cyc
<i>Calml4</i>	-2.22	-1.27	<i>Cldn11</i>	0.55	-0.20	<i>Adamts19</i>	-0.15	-0.70
<i>Cdk6</i> *	-1.61	-0.99	<i>Cldn9</i>	0.20	0.07	<i>Cntff</i> *	-0.80	0.10
<i>Dock6</i> *	-0.49	-0.66	<i>Fam181b</i>	-0.45	0.00	<i>Dlk1</i>	-0.41	0.17
<i>Gli1</i> *	-5.71	-3.14	<i>Fam69c</i>	0.17	0.92	<i>Ltbp1</i>	-0.33	-0.17
<i>Grem1</i> *	-2.63	-0.89	<i>Fbxo41</i>	-0.69	-0.34	<i>Osr1</i> *	-1.39	-0.10
<i>Hand2</i> *	-2.16	-0.53	<i>Fbxo8</i>	-0.68	0.22	<i>Prdm1</i>	-1.15	-0.21
<i>Hoxd11</i> *	-2.51	-0.91	<i>Hhip</i> *	-3.00	-1.10	<i>Col23a1</i>	-0.37	-0.12
<i>Hoxd13</i> *	-6.01	-1.09	<i>Ndnf</i>	-0.44	0.31	<i>Lypd6</i> *	-1.27	-0.72
<i>Ier2</i>	-0.43	-0.15	<i>Osr2</i> [‡]	-4.01	0.02	<i>Svep1</i> [‡]	-0.63	0.11
<i>Jag1</i>	-0.86	-0.40	<i>Rspo3</i> [‡]	-1.29	-0.04			
<i>Klf9</i>	-1.03	-0.43	<i>Smoc1</i> *	-1.43	-1.06			
<i>Msi2</i> *	-0.95	-0.84	<i>Whrn</i>	-0.16	0.10			
<i>Pam</i> *	-1.01	-0.61						
<i>Ptch1</i> *	-2.37	-1.42						
<i>Ptch2</i> *	-4.41	-3.52						
<i>Ralgps2</i>	-0.32	-0.24						
<i>Rasgef1b</i> *	-1.44	-0.51						
<i>Sall1</i> *	-1.90	-1.26						
<i>Sall3</i> *	-1.79	-0.95						
<i>Sap30</i>	-0.35	-0.05						
<i>Shroom3</i>	0.05	0.01						
<i>Sox4</i>	0.16	-0.01						
<i>Tpd52l1</i> *	-1.56	-0.82						

Table 2.1: Classification and expression of GLI target genes. Schematized expression patterns of GLI target genes found in categories 1-3. List of GLI target genes found in each category. Gene expression values in log₂ fold change (FC) from RNA-seq experiments (shown in Fig. 3). Hedgehog pathway targets are underlined. Genes downregulated $\geq 25\%$ ($\text{Log}_2\text{FC} \leq -0.4105$) in both *Shh*^{-/-} limbs and cyclopamine treated limbs are indicated with an asterisk (*) and shown in red. Genes downregulated $\geq 25\%$ ($\text{Log}_2\text{FC} \leq -0.4105$) in *Shh*^{-/-} limbs but unregulated ($\text{Log}_2\text{FC} \geq 0$) in the cyclopamine experiment are indicated with a double dagger (‡).

2.4: DNA MOTIF ANALYSIS IN CIS-REGULATORY MODULES

The 45 genes defined above are highly likely to be directly regulated by SHH signaling through their associated GLI-bound CRMs. To identify co-factors potentially involved in mediating the GLI response, we searched the GLI-bound CRMs associated with these genes for enriched DNA motifs using *de novo* motif analysis (Ji et al., 2008; Ji et al., 2006). We uncovered novel DNA motifs enriched in categories 1 and 2. No enriched motifs were uncovered for CRMs associated with genes in category 3 due to the small sample size (Fig. 2.7A,B). The most enriched motif in any category was Gli, which was substantially enriched in GLI-bound CRMs associated with category 1 genes compared to matched genomic controls (Fig. 2.7A). We also identified a GC rich motif which corresponded to the known binding motif for the SP1 transcription factor (Fig.2.7A) (Gidoni et al., 1984; Ji et al., 2006). In addition to being enriched in category 1, the Sp1 motif was the most enriched motif found in category 2 (Fig. 2.7B). We also identified several novel motifs that are highly sequence specific; however, they do not correspond to any known transcription factor binding sites (Fig. 2.7A,B). Thus, DNA motif analysis identified both unique and common motifs among two of the expression categories.

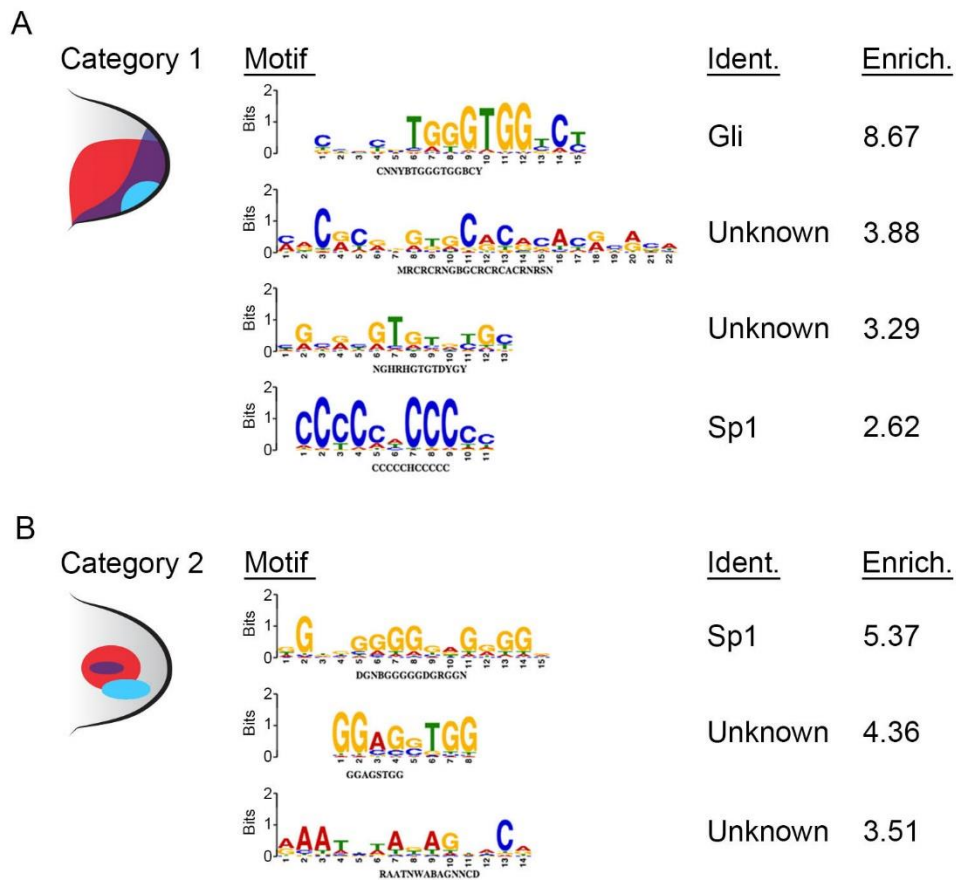


Figure 2.7: DNA motifs enriched in GLI-bound CRMs. (A) Enriched DNA motifs in GLI-bound CRMs associated with category 1 and (B) category 2 genes. Known and unknown protein binding motifs and the enrichment value are indicated. No statistically enriched DNA motifs were identified in category 3.

The quality of Gli motifs have been shown to function in differential interpretation of HH signaling in the developing mouse neural tube and *Drosophila* imaginal wing disc (Oosterveen et al., 2012; Parker et al., 2011; Peterson et al., 2012). We asked if the different expression categories had differences in Gli motif quality. We chose the Gli motif with the highest motif score in our dataset and mapped the position weight matrix of the Gli motif

to GLI-bound CRMs associated with genes expressed in categories 1, 2, and 3. Gli motifs associated with genes expressed in category 1 and 3 have higher means of log-likelihood, indicating higher quality Gli motifs (Fig. 2.8). In contrast, Gli motifs associated with category 2 have a lower (although not statistically significant) mean of log-likelihood, indicating lower quality Gli motifs (Fig. 2.8). Interestingly, genes in categories 1 and 3 are expressed overlapping or are adjacent to the *Shh* expression domain in the posterior limb, while genes in category 2 are expressed further from the *Shh* expression domain. This suggests that long-range SHH signaling could regulate category 2 genes. The same trends in Gli motif quality were also observed in the mouse neural tube and *Drosophila* imaginal wing disc for short and long range GLI target genes (Oosterveen et al., 2012; Parker et al., 2011).

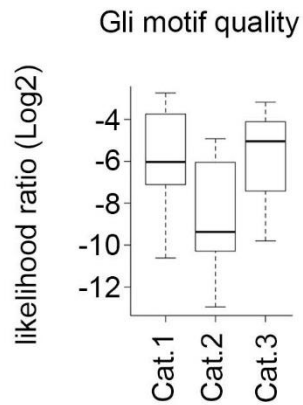


Figure 2.8: Assessment of the quality of Gli motifs in GLI-bound CRMs. CRMs associated with genes found in categories 1-3 shown as log₂ likelihood ratio. Reported p-values using a Welch's t-test for comparing Gli motif quality between the categories: Category 1 to 2 (P=0.083); category 1 to 3 (P=0.776); category 2 to 3 (P=0.144).

2.5: SP-MEDIATED TRANSCRIPTION

As an initial step towards determining the functional importance of these motifs, we decided to focus on the Sp1 motif, which was identified in both categories 1 and 2. In the limb mesenchyme *Sp1*, *Sp2*, and *Sp3* are expressed in a mostly uniform pattern at E10.5 (Saffer et al., 1991; Yokoyama et al., 2009; Baur et al., 2010). Both SP1 and SP3 bind to the same DNA motif with similar affinities, suggesting that both could be binding this motif in the limb (Hagen, Muller, Beato, Suske, & Marburg, 1992). While roles for SP-family proteins in the early limb bud mesenchyme have not been studied, several Sp members have been characterized within the ectoderm, including *Sp6*, which has been proposed to regulate Wnt expression in the AER (Talamillo et al., 2010), and *Sp8* and *Sp9*, which regulate *Fgf8* expression in the AER and likely bind a similar DNA motif sequence as SP1 (Bell et al., 2003; Kawakami et al., 2004; Sahara, Kawakami, Izpisua Belmonte, & O'Leary, 2007; Treichel, Schöck, Jäckle, Gruss, & Mansouri, 2003).

Consistent with previous reports, *Sp1* is expressed throughout much of the embryo, including the forelimbs (Fig. 2.9A). Although the *Sp1* locus has a closely associated GLI-bound CRMs and was initially predicted to be a GLI target gene (Vokes et al., 2008), *Sp1* gene expression is not affected in *Shh*^{-/-} forelimbs (Fig. 2.9B). In addition, SP1 does not co-immunoprecipitate with GLI1 in the mouse limb (Fig. 2.9C).

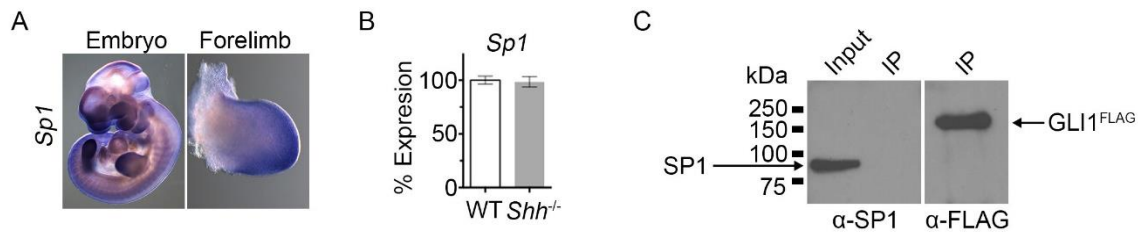


Figure 2.9: *Sp1* is expressed in the forelimb and is not regulated by SHH. (A) *in situ* hybridization for *Sp1* in wild-type (WT) E10.5 embryo and forelimb. (B) qRT-PCR for *Sp1* in 33-35 somite WT (open bar) and *Shh*^{-/-} (gray bar) forelimbs. Error bars indicate the standard error of the mean ($n=3$). (C) Western blot of GLI1^{FLAG} co-immunoprecipitation (co-IP) for SP1 in E10.5 mouse forelimbs from PrxCre; RosaGli1-Flag embryos. SP1 is detected in the input sample, but is not detected in the co-IP sample. As a control, GLI1^{FLAG} is detected in the co-IP sample.

To determine if SP-mediated transcription contributed to the regulation of GLI target genes, we cultured contralateral mouse forelimbs in media with or without 300nM mithramycin A (Fig. 2.10), an antibiotic that has been shown to bind to GC rich DNA sequences and selectively inhibit SP-mediated transcription (Blume et al., 1991; García-Huerta et al., 2012; Guo, Rödelberger, Digweed, & Robinson, 2013; Snyder, Ray, Blume, & Miller, 1991; Van Dyke & Dervan, 1983). To assess the level of inhibition for SP-mediated transcription, we determined the expression levels of *Fgf8* and found it was strongly downregulated, which is consistent with its regulation by *Sp8* and *Sp9* (Fig. 2.10B,C). Next, we assessed the expression levels for a selected group of GLI target genes from categories 1, 2 and 3. Limb buds cultured in media containing mithramycin A have reduced expression levels of selected GLI target genes across all expression categories (Fig. 2.10C). Consistent with the reductions observed by qRT-PCR, limb buds cultured in

FGFs in the AER are essential for maintaining *Shh* expression (Laufer, Nelson, Craig, Johnson, Morgan, & Tabin, 1994; Niswander, Jeffrey, Martin, & Tickle, 1994). Since *Ptch1* and *Gli1* are reduced by approximately 50%, this downregulation could be due to sensitivity to SHH pathway inhibition and/or by inhibition of mesodermal SP protein activity. To distinguish between these, we first examined the 5 GLI target genes that did not require continued SHH signaling (Table 2.1, indicated with a double dagger). From this group, 4 out of 5 genes were downregulated, 3 of them significantly ($P \leq 0.05$) in mithramycin A treated limb bud cultures. To ensure that reduction of these 4 genes (and the broader group) was not due to reduced FGF expression in the AER, we cultured limb buds in the presence of an FGF receptor antagonist, SU5402 (Mohammadi et al., 1997) (Fig. 2.11A). As expected, the FGF target genes sprouty 4 (*Spry4*) and dual specificity phosphatase 6 (*Dusp6*) were significantly reduced at 4, 8, and 15 hours (Fig. 2.11B-D) (Minowada et al., 1999). While *Shh* expression was also reduced at 4, 8, and 15 hours, the pathway target genes *Gli1* and *Ptch1* were not significantly reduced, although showed variable expression (Fig. 2.11B-D). The majority of GLI target genes were not greatly reduced, and several genes that were strongly downregulated by mithramycin A were generally unaffected or even upregulated when cultured in SU5402 (Fig. 2.11E). This suggests that mithramycin A mediated reduction in GLI target gene expression is not solely due to the abrogation of the SHH-FGF signaling loop.

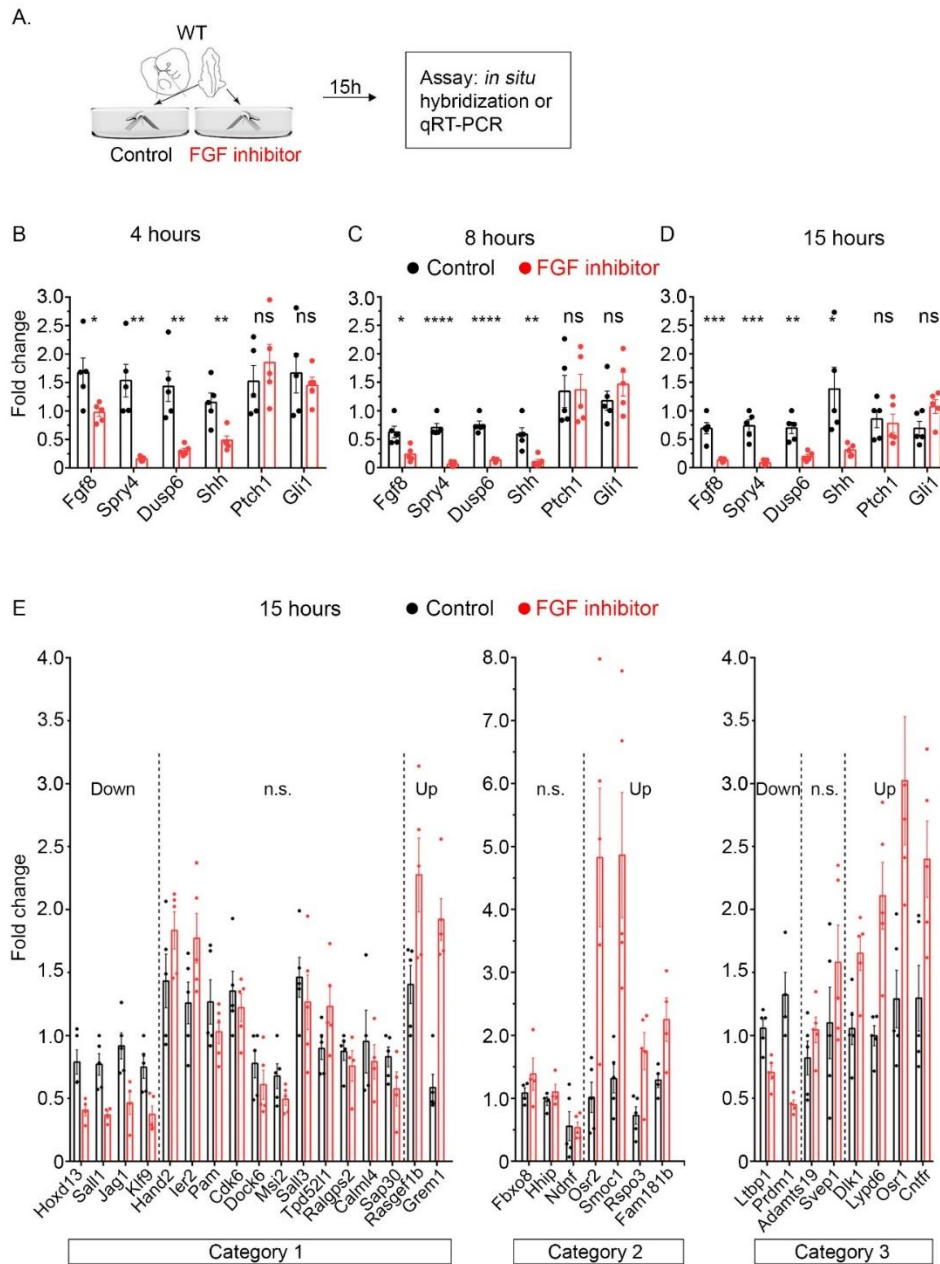


Figure 2.11: FGF inhibition does not downregulate most GLI target genes. Wild-type (32-35 somites) forelimb cultured in 0.1% DMSO and the contralateral limb cultured in media containing 10 μ M SU5042 (FGF inhibitor) for 4, 8, or 15 hours. (B-D) Kinetics of FGF inhibition. qRT-PCR for FGF and SHH pathway targets. (E) q-RT-PCR for GLI target genes at 15 hours. $n=5$ individual forelimb pairs. An asterisk indicates a statistically significant difference (two-tailed unpaired t-test, $P \leq 0.05$). The mean value is plotted at the top of the bar and error bars are the standard error of the mean.

To assess the specificity of mithramycin A and circumvent secondary effects caused by reduced SHH and FGF activity, we utilized a modified-micromass culture method for Shh-responsive genes that allows efficient knock-down of genes by siRNA while preventing differentiation of limb bud cells (Lewandowski, Pursell, Rabinowitz, & Vokes, 2014) (Fig. 2.12A). Limb cells electroporated with a *Sp1* siRNA showed a 69% reduction in *Sp1* expression at 48 hours compared to cells electroporated with a negative control siRNA (Fig. 2.12B). The expression of four independent GLI target genes were reduced >25% (Fig. 2.12C). This suggests that SP1, in the limb bud mesenchyme, contributes to maintain expression of GLI-target genes.

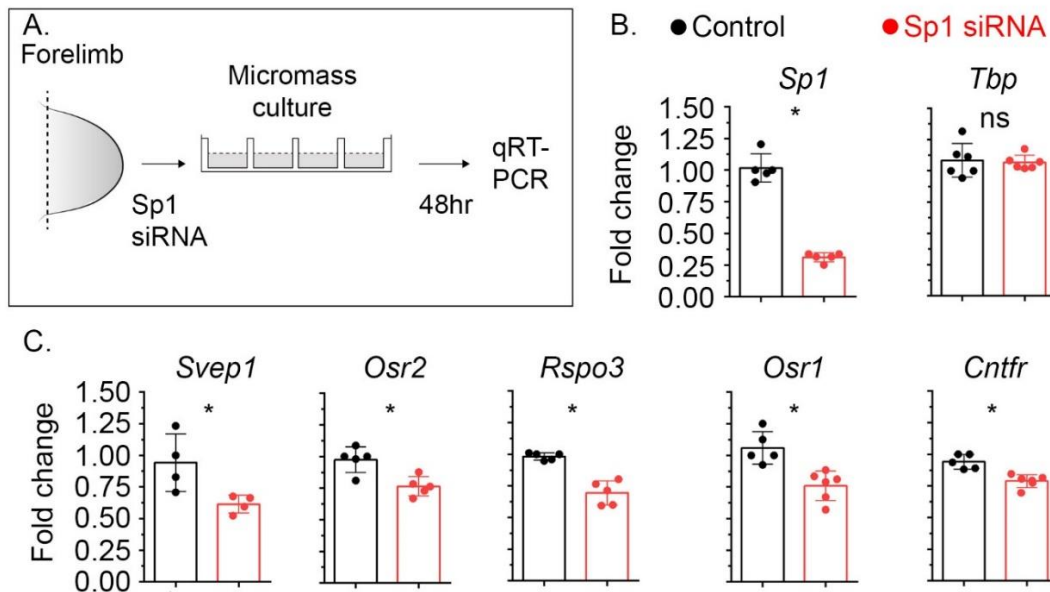


Figure 2.12: *Sp1* siRNA in micromass limb culture and qRT-PCR for GLI target genes. (A) Experimental pipeline. (B) qRT-PCR for *Sp1* and *Tbp* (negative control gene) in control (black) and *Sp1* siRNA (red) cultures. (C) qRT-PCR for GLI target genes. Statistical significance determined using an unpaired two-tailed T-test. Asterisk (*) indicates Pvalue <0.05.

We then asked if SP-mediated transcription is also required for SHH-dependent transcriptional activation of GLI target genes. Although *Shh*^{-/-} forelimbs have reduced or absent expression of GLI target genes, they are capable of activating expression in response to exogenous SHH protein (Panman et al., 2006). We cultured forelimbs from E10.25 (32-34 somite) *Shh*^{-/-} embryos and heterozygous or wild-type littermates in the presence of the HH pathway activator (purmorphamine) (Sinha et al., 2006), mithramycin A, or both small molecules (Fig. 2.13A). As expected, the GLI-target genes *Ptch1*, *Msi2*, *Cdk6* and *Osr2* were reduced in *Shh*^{-/-} forelimbs while a control gene, *Tbp*, was unchanged (Fig. 2.13B, white bars). Conversely, *Shh*^{-/-} forelimbs cultured in the presence of purmorphamine had upregulated expression of *Ptch1*, *Msi2*, *Cdk6*, and *Osr2* (Fig. 2.13B, blue bars). When *Shh*^{-/-} forelimbs were cultured in mithramycin A alone or together with purmorphamine, gene expression remained at levels comparable to control cultured *Shh*^{-/-} forelimbs (Fig. 2.13B, red and yellow bars). These results suggest that activation of GLI target genes requires SP-mediated transcription. In summary, SP proteins act as GLI transcriptional co-regulators that are required for both the transcriptional activation as well as for maintenance of GLI target genes.

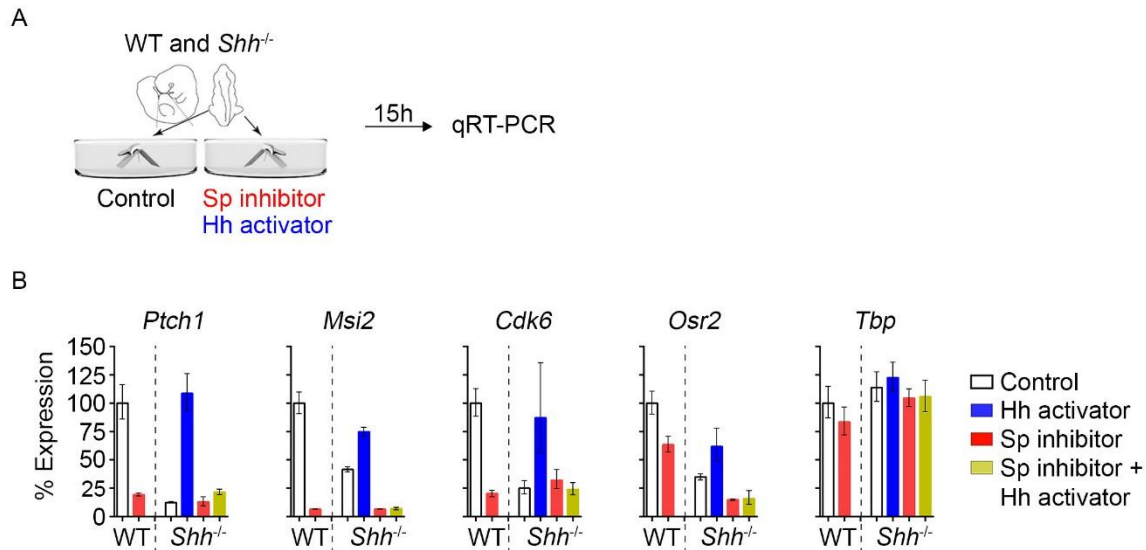


Figure 2.13: SP-mediated transcription is necessary for transcriptional activation of GLI target genes (A) Schematic of contralateral mouse forelimb culture. Littermate wild-type or heterozygous (indicated as WT) and *Shh*^{-/-} contralateral forelimbs (31-33 somites) cultured for 15 hours in control media (open bars), 300 nM mithramycin A (Sp inhibitor) (red bars), 10 μ M purmorphamine (Hh activator) (blue bars), or both (yellow bars). (B) qRT-PCR for select GLI target genes: *Ptch1*, *Cdk6*, *Msi2*, and *Osr2* as well as a control gene, *Tbp*. Gene expression is normalized to *Gapdh* and error bars indicate a 95% confidence interval (per genotype, 3 contralateral limb buds for each condition).

2.6: DISCUSSION

In this study, we have identified a set of genes that by multiple criteria are direct GLI targets in the developing limb bud. These genes are expressed in three domains, which have distinct temporal requirements for SHH signaling in order to maintain expression. The GLI binding regions associated with genes in two of the domains are also enriched for additional motifs, representing binding sites for potential transcriptional co-regulators. One of these motifs corresponds to the binding sequence for SP1, which we show is important

for co-regulating a broad subset of GLI target genes in the limb bud. The identification of distinct transcriptional domains has greatly improved the understanding of HH patterning in the *Drosophila* imaginal wing disc and vertebrate neural tube. The presence of analogous domains within the limb bud (this study) should enable the determination of the gene regulatory networks underlying SHH-mediated limb patterning.

2.6.1: Expression patterns of GLI target genes

Whole-genome approaches, using DNA microarrays, have been used to identify SHH-responsive genes during limb development (Bangs et al., 2010; Hu, McGlinn, Harfe, Kardon, & Tabin, 2012; McGlinn et al., 2005; Probst et al., 2011; Shah et al., 2009; Vokes et al., 2008). Combining this approach with three-dimensional spatial information from whole-mount embryo *in situ* hybridization, has been successfully used to identify genes regulated in distinct domains (Bangs et al., 2010; Probst et al., 2011; Welten et al., 2011). Here, we focused on genes that were previously identified as likely GLI target genes and performed a comprehensive *in situ* hybridization screen to determine the limb expression patterns for nearly all of the 205 GLI target genes at two developmental stages. The previous studies were unable to distinguish direct and indirect effects in *Shh*^{-/-} limb buds. By examining GLI targets, this study improves our understanding of the genes and processes directly controlled by SHH.

While our analysis identified a group of high confidence SHH regulated genes, a number of additional candidate GLI target genes did not show spatially restricted

expression in the posterior limb. Some of the genes that have uniform expression patterns are still likely to be SHH-responsive. For example, *Rab34* has relatively uniform limb expression but is nonetheless SHH-responsive, containing a GLI binding site with posterior-specific activity (Vokes et al., 2007). Similarly, we detected many GLI target genes expressed in the distal limb and excluded them from further analysis because they were not primarily expressed within the SHH-responsive region (Fig. 2.1B and Table A1). A previous study classifying SHH-responsive genes suggested that *Cyp26b1*, a distally expressed gene and reduced in *Shh*^{-/-} limbs, is primarily regulated by FGFs because of a breakdown in the SHH-FGF signaling loop (Probst et al., 2011). Since many of these distally expressed genes are in proximity to GLI binding regions, it is possible that they are co-regulated by SHH and FGF in a feed-forward loop. By restricting our analysis to spatially restricted genes in the posterior limb, we are therefore likely excluding many bona-fide GLI target genes that have more complex regulatory inputs.

We identified three broad expression domains of GLI target genes (Fig. 2.2B-D). The coordinated expression of developmentally expressed genes, termed syn-expression groups, has been proposed to be involved in regulating common biological pathways (Gawantka, Pollet, Delius, Vingron, & Pfister, 1998; Ramialison et al., 2012; Visel et al., 2007). Category 1 genes, expressed in the posterior and posterior-distal limb, are enriched for GO processes involved in transcriptional regulation and cell proliferation (Fig. 2.3). Consistent with these processes, the posterior-distal domain undergoes significant proliferative expansion during limb bud development, ultimately giving rise to most of the developing digits (reviewed in Zeller et al., 2009). If SHH acts as a morphogen in the limb

bud, it would likely be doing so through these category 1 genes. Interestingly, besides SHH pathway feedback components, we did not identify GLI target genes that had obvious graded expression in the limb. In contrast to category 1, GLI target genes expressed in category 2 (the central limb) are enriched for skeletal differentiation markers and BMP inhibitors (Fig. 2.3) (Hsu et al., 1998; Khokha et al., 2003; Rainger et al., 2011). Cells in this domain primarily contribute to the forearm (zeugopod) (Vargesson et al., 1997). Similarly, genes expressed in category 3 are enriched for skeletal pathway genes (Fig. 2.3). In addition, lineage tracing experiments demonstrate that this region primarily contributes to the presumptive forearm (Vargesson et al., 1997).

2.6.2: Different temporal requirements for SHH

Previous reports identified four GLI target genes within the limb bud that require sustained SHH signaling beyond E10.5 (Panman et al., 2006). Our analysis of the temporal requirement of SHH signaling for GLI target genes extends these results and provides quantitative measurements of the response, identifying a total of 18 GLI target genes that require sustained SHH signaling beyond E10.25 (Table 2.1, indicated in red and an asterisk). These genes are nearly all expressed in category 1, which might comprise a gene regulatory module that is important for mediating limb growth during the period when SHH signaling is required for expansion of the cartilage progenitors (Towers et al., 2008; Zhu et al., 2008). It is not clear why genes in categories 2 and 3 generally require a briefer exposure to SHH. One possibility is that since genes in categories 2 and 3 are expressed in

more proximal regions, their transient need for SHH signaling reflects the earlier differentiation of more proximal limb elements compared to distal elements (Roselló-Díez et al., 2014). It is also possible that the lower Gli motif quality observed in GLI-bound CRMs associated with genes in category 2, reflects a requirement for regulating long-range target genes as has been suggested in the neural tube (Oosterveen et al., 2012).

Although the RNA-seq analysis was specifically applied to a group of previously defined GLI target genes, the analysis also identified a larger SHH-responsive group of genes that require transient or continued SHH signaling. In future studies it would be interesting to identify the expression pattern of this larger group of SHH-responsive genes and determine to what extent they conform to the expression categories as described in this work. Based on our finding that the regulation of GLI target genes correlates with where they are expressed, we predict that genes requiring sustained SHH signaling will be predominately expressed in the posterior and posterior-distal limb (category 1), while genes that require transient SHH signaling will be expressed in the central (category 2) or posterior-proximal limb (category 3).

2.6.3: Regulatory inputs in GLI-bound CRMs

In current ChIP approaches, it is difficult to distinguish between transcriptionally relevant binding sites from the majority of inert sites in a particular tissue (Shlyueva et al., 2014). We previously estimated that only 15% of GLI-bound CRMs are likely be transcriptionally relevant (Vokes et al., 2008). The GLI-bound CRMs associated with

genes in the domains identified in this study are a significant improvement on our previous approach, which only considered gene response irrespective of their spatial expression domains.

From this set of GLI-bound CRMs we identified both unique and common DNA motifs. The unique motifs do not correspond to known transcription factor binding sites and might represent binding sites for unidentified co-factors that confer specific expression. After the Gli motif, the Sp1 motif was the most common motif identified in categories 1 and 2 (Fig. 2.7A,B). While *Sp1* is a ubiquitously expressed gene, its expression levels are dynamic in different tissues and cell types (supplementary material Fig. S4A,B) (Saffer et al., 1991). Despite their reputation as ubiquitous transcription factors, several individual Sp-family genes have specific loss-of-function phenotypes, suggesting that they have specific roles in development (reviewed in Zhao and Meng, 2005; Suske et al., 2005). For example, *Sp1* has been shown to regulate several developmental pathways including neuronal differentiation (Okamoto, Sherman, Bai, & Lipton, 2002; Yoo et al., 2002), hematopoiesis (Gilmour et al., 2014), and most relevant to limb, cartilage and bone differentiation (Kasaai et al., 2013; Gene et al., 2006; Zhang et al., 2009). Moreover, previous studies have demonstrated that SP1 can mediate the interaction of distal regulatory elements with the proximal promoter region of a gene (Deshane et al., 2010; Su, Jackson, Tjian, & Echols, 1991).

The Sp1 motif was also enriched in a GLI1 ChIP-seq dataset on ventral neural tissue (Peterson et al., 2012) as well as in several other published limb ChIP datasets, indicating that its enrichment is not specific to GLI CRMs. Our work suggests that SP1 is an

important co-regulator for GLI target genes in the limb. In future studies, it will be interesting to explore these interactions in more detail. In the absence of this information, we present a speculative model for these interactions (Fig. 2.14). Here, SP1 is depicted as an essential co-factor for activating GLI target genes as well as controlling their later maintenance after genes no longer require SHH. As GLI1 and SP1 do not bind to each other (Fig. 2.9C), it is possible that SHH signaling would activate GLI-dependent CRMs and upon activation, SP1 would facilitate interactions between the CRM and the promoter (Fig. 2.14).

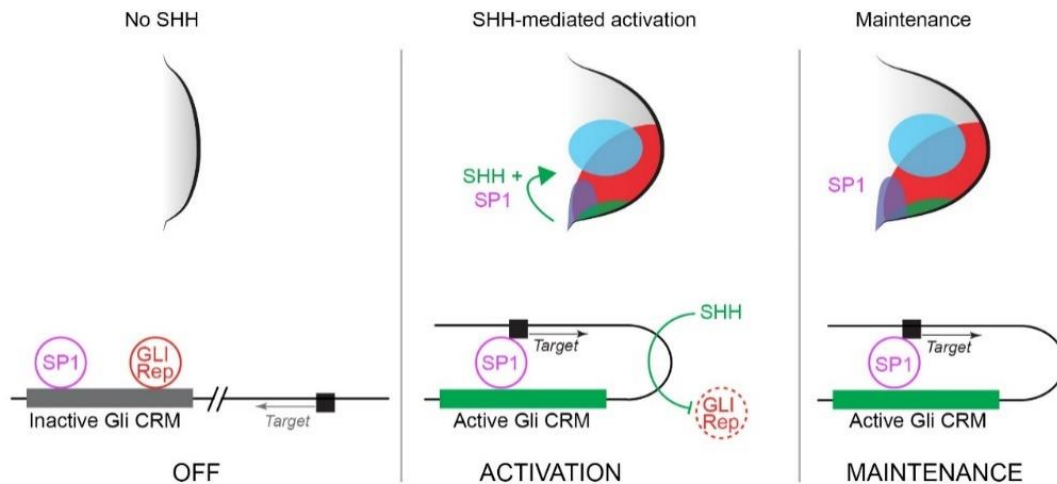


Figure 2.14: Speculative model illustrating the roles of GLI and SP1 in activating and maintaining GLI target gene expression. Prior to SHH, GLI dependent CRMs are inactive (depicted as gray in left panel). After the expression of SHH, GLI-R is inhibited, resulting in the activation of target gene expression by through physical interactions between the CRM and basal promoter that are facilitated by SP1. The length of the activation stage is variable, depending on the specific gene / domain. Ultimately, GLI target genes no longer require SHH signaling but many still require SP transcription, perhaps to maintain CRM-promoter interactions.

Interestingly, in *Drosophila*, *Sp1* is broadly expressed in the imaginal disc and is required for leg development (Estella and Mann, 2010; McKay et al., 2009; Estella et al., 2003). In this system, *Sp1* is involved in feed-forward loops that regulate specific enhancers that turn on genes involved in leg growth (Estella and Mann, 2010). Previous work has noted the presence of *Dlx*, *Hox* and *Meis* in both *Drosophila* and vertebrate limb development. Although *Drosophila* and vertebrate limbs evolved independently, the presence of these deeply homologous genes in both systems suggests they may be required for sub-circuits required for appendage formation (Shubin et al., 2009). *Sp1* may therefore represent an additional deeply homologous gene required for appendage development in vertebrates.

Chapter 3: A GLI silencer robustly represses gremlin in the limb bud

Portions of this chapter are modified with permission from the authors. Li, Q, Lewandowski, J. P*, Powell, M. B., Norrie, J. L., Cho, S. H., & Vokes, S. A. A Gli silencer is required for robust repression of gremlin in the vertebrate limb bud. Development (2014) 141(9)1906-19014. Q.L., J.P.L. and J.L.N conceived experiments, collected and interpreted data. M.B.P and S.H.C performed experiments.*

3.1: INTRODUCTION

Gli transcriptional targets fall into two distinct groups: genes that require Gli activation for transcription (Gli activator genes), and genes that are transcribed in the absence of Gli repression (Gli derepression genes). Gli activators could potentially play quantitative roles in regulating the expression levels of a subset of this latter class. The behavior of target genes in response to a gradient of Hh signaling suggests that competition between Gli activators and repressors could drive threshold responses that restrict the boundary of Gli-activator target gene expression (Jacob and Briscoe, 2003; Ruiz i Altaba, 1997; Wang et al., 2000). Studies that have manipulated Gli expression levels in the chick neural tube support this competition model (Oosterveen et al., 2012). The mechanism by which Gli repression prevents expression of its target genes is poorly understood, but in some cases relies on interactions between Gli repressors and specific transcription factors (Oosterveen et al., 2012). Mouse neural tubes lacking the major Gli transcriptional repressor Gli3 have a relatively modest change in target gene expression boundaries with no change in ventral neural fates and more subtle changes to intermediate identities, an

effect that could be due to the robustness of the neural-specific downstream regulatory network (Balaskas et al., 2012; Persson et al., 2002).

Sonic hedgehog (Shh), the Hh ligand expressed in the limb bud, has graded activity emanating from the most posterior region of the limb bud. The dose and duration of Shh signaling are critical for specifying digits and regulating growth (Ahn and Joyner, 2004; Harfe et al., 2004; Towers et al., 2008; Yang et al., 1997; Zhu et al., 2008). When compared to *Shh*^{-/-} embryos, *Shh*^{-/-};*Gli3*^{-/-} embryos have a substantial rescue in limb growth and digit formation. The expression of many genes that are lost in *Shh*^{-/-} limb buds are restored in *Shh*^{-/-};*Gli3*^{-/-} embryos but with symmetrical gene expression patterns along the anterior-posterior axis. This contrasts with their asymmetric expression in wild-type embryos and is exemplified by *Gremlin*, an important Shh target gene that encodes a protein playing key roles in regulating differentiation (reviewed in Rabinowitz and Vokes, 2012). Expression of *Gremlin* in the limb expands anteriorly in *Gli3*^{-/-} embryos, is severely downregulated in *Shh*^{-/-} embryos, and is rescued in *Shh*^{-/-};*Gli3*^{-/-} embryos (Aoto et al., 2002; Litingtung et al., 2002; Panman et al., 2006; te Welscher et al., 2002; Zuniga et al., 1999). Collectively, these studies illustrate the profound importance of Shh in counteracting Gli3-mediated repression of target genes.

Despite the central role of Gli proteins in regulating Hh signaling responses, the mechanism by which Gli activator and repressor proteins collaboratively regulate target genes remains poorly understood and is an impediment to defining target genes and gene regulatory networks. We used a Gli cis-regulatory module (CRM) that is embedded within a global control region for the *Gremlin* locus to perform the first genetic characterization

(loss-of-function) of a Gli-responsive CRM. We find that the GRE1 (Gli responsive element 1) acts as both an enhancer and a silencer. GRE1 enhancer activity requires sustained Hh signaling to drive activity. In the anterior limb bud, GRE1 acts as a Gli-dependent silencer. The silencer activity is necessary for providing robust repression of *Gremlin* in the distal-anterior limb.

3.2: GRE1 GENOMIC LANDSCAPE AND ACTIVITY DOMAIN

In a genome-wide chromatin immunoprecipitation study, we previously identified a 438-bp Gli3 binding region located over 100kb downstream of *Gremlin* (Fig. 3.1A) that exhibited enhancer activity in transient transgenic limb buds in a region partially overlapping with *Gremlin* gene expression (Fig. 3.1B-F) (Vokes et al., 2008). Enhancer activity is dependent on the presence of at least one Gli motif as mutations of the motif resulted in a complete lack of enhancer activity in G0 transgenic embryos (Vokes et al., 2008). We sought to characterize Gli enhancer regulation in the context of this CRM, which is henceforth referred to as GRE1 (Gli responsive element 1). Embryos derived from three founder lines of stable transgenics had β -galactosidase activity in posterior limb bud mesenchyme in an identical domain to that previously reported for transient transgenics (Fig. 3.1B-F) (Vokes et al., 2008).

We selected one line, Tg(Rr26-lacZ)438Svok, henceforth referred to as *GRE1lacZ*, for further analysis. β -galactosidase activity was first detected in embryos at E10.0 (31-32 somites) (Fig. 3.2A), well after the reported onset of *Gremlin* expression at ~E9 (Benzet

et al., 2009; Zúñiga and Zeller, 1999). The enhancer had activity in the posterior limb within a subregion of the Shh-responsive domain. *Shh* expression initiates in the limb bud around 28 somites (E9.75) (Charité et al., 2000), and the lag in reporter expression is consistent with the reported kinetics of Shh-mediated induction of *Gremlin* (Benazet et al., 2009). By E10.5, β -galactosidase activity was strongly upregulated and persisted until late E11.5 (Fig. 3.2B,C). By E11.75 expression was reduced and had retreated from the distal limb mesenchyme (Fig. 3.2D). Expression was nearly absent by E12.0 except for faint staining in the proximal middle of the condensing digit mesenchyme (Fig. 3.2E). No expression was detected after E12.0, correlating with the termination of Shh activity in the limb (Echelard et al., 1993; Harfe et al., 2004). Although the enhancer analyses focused on forelimb expression, we observed similar domains in the hindlimbs (Fig. 3.1C).

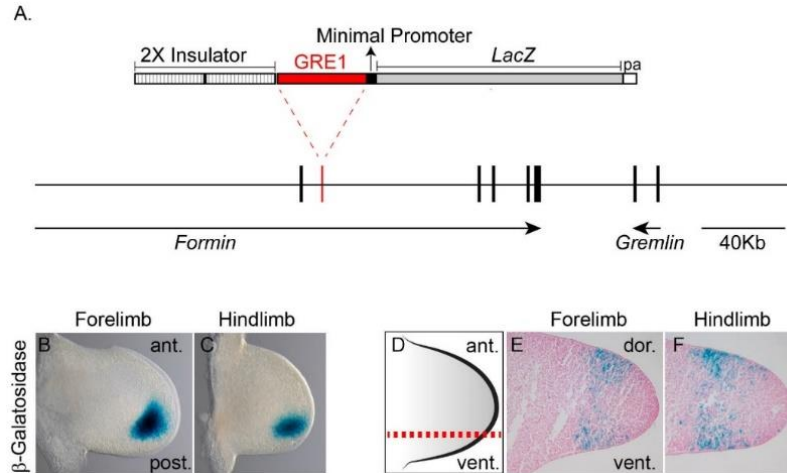


Figure 3.1: GRE1 enhancer activity. (A) Schematic showing the location of GRE1 in relation to the *Gremlin* locus and the GRE1LacZ transgenic construct. (B,C) *GRE1LacZ*^{+/-} E10.5 forelimb and hindlimb stained for β -galactosidase. (D) Illustration of a forelimb indicating the level of sectioning with a dashed red line. (E,F) Cryosections of *GRE1LacZ*^{+/-} E10.5 forelimb and hindlimb stained for β -galactosidase and nuclear fast red. Anterior (ant.), posterior (post.), dorsal (dor), and ventral (vent.).

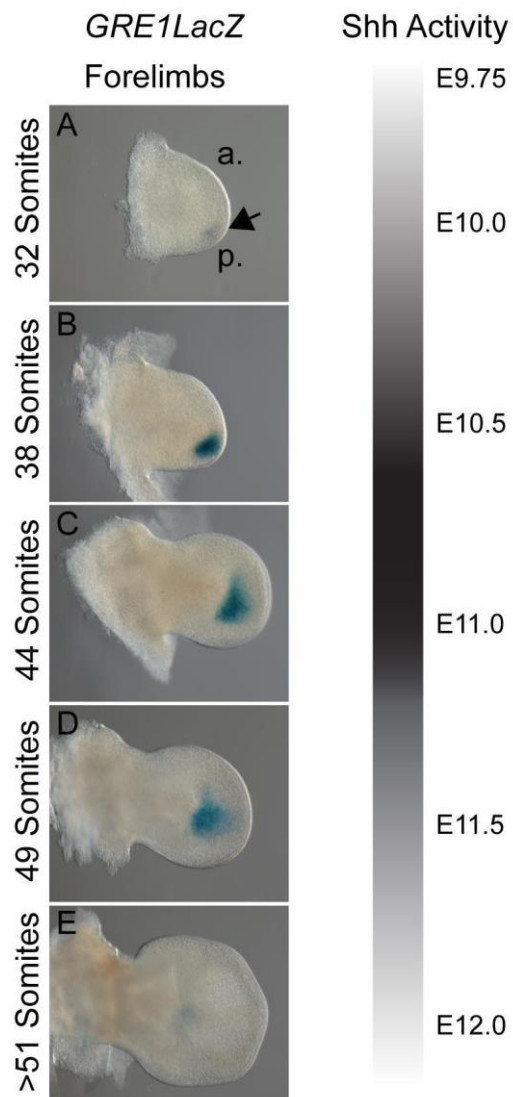


Figure 3.2: GRE1 enhancer activity correlates temporally with Shh activity. (A-E) *GRE1LacZ*^{+/+} forelimbs stained for β -galactosidase activity from days E10 – E12. The somite stage is indicated to the left of each image. Expression activity in the limb correlates with *Shh* expression in the limb bud (indicated by the bar in the center). ‘a.’, anterior; ‘p.’, posterior; black arrow indicates β -galactosidase.

3.3: GRE1 ACTIVITY IS REGULATED BY GLI

To determine if GRE1 is responsive to Shh signaling, we examined enhancer activity at E10.5 in Shh gain and loss-of-function backgrounds. In contrast to wild-type or heterozygous littermates (Fig. 3.3A,A'), *Shh*^{-/-};*GRE1LacZ*^{+/-} embryos had no detectable β -galactosidase activity (6/6 embryos) and, consistent with previous studies, *Gremlin* gene expression was highly downregulated (Fig. 3.3B,B') (Zúñiga and Zeller, 1999). We also examined expression by activating high levels of Hh signaling throughout the limb bud using a Cre inducible, dominant active allele, *Rosa*^{SmoM2} (Jeong et al., 2004). *Prx1Cre*;*Rosa*^{SmoM2c/+};*GRE1LacZ*^{+/-} embryos expressed both the *Gremlin* transcript and β -galactosidase activity throughout the entire distal limb bud (11/11 embryos; Fig. 3.3C, C'), indicating that high levels of Hh pathway activity were sufficient to activate *GRE1LacZ* along the anterior-posterior axis. *Gremlin* gene expression appeared patchy (Fig. 3.3C'), and while the reason for this expression is unclear, it is consistent with observations from another study that also activated the Hh pathway throughout the limb bud (Butterfield et al., 2009). Because *Prx1Cre* is active throughout the limb mesenchyme (Logan et al., 2002), the distal restriction of GRE1 enhancer activity suggested that additional, distal factors are also required for *Gremlin* expression. We concluded that Shh is both necessary and sufficient for enhancer activation.

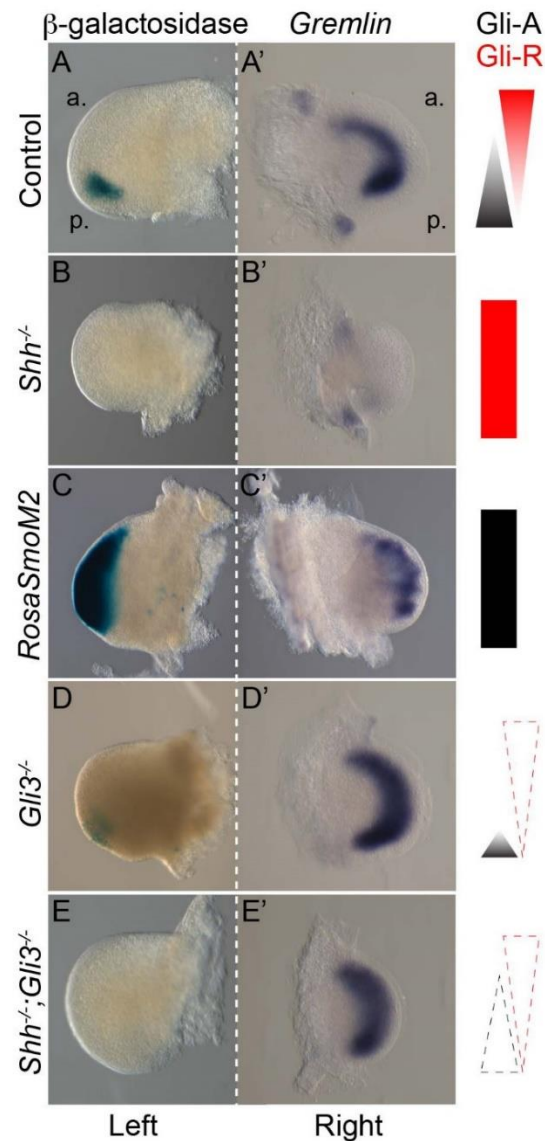


Figure 3.3: GRE1 enhancer activity requires Gli-activation. E10.5 *GRE1LacZ* forelimbs indicating enhancer activity in various genetic backgrounds. The corresponding Gli gradient status (Gli-activator in black, Gli-repressor in red) is indicated to the right of each set of images. (A-E') Embryos were dissected into halves, and the left forelimb (left column) was stained for enhancer activity (β -galactosidase) while the corresponding right forelimb (right column) was assayed for *Gremlin* gene expression. Limbs on the left appear larger than their contralateral right side due to differences in how they are fixed. The genotypes at the left correspond to (A-A') Control (*GRE1LacZ*^{+/-}), (B-B') *Shh*^{-/-}; *GRE1LacZ*^{+/-}, (C-C') *GRE1LacZ*^{+/-}; *PrxCre*^{+/-}; *Rosa*^{SmoM2c/+}, (D-D') *Gli3*^{-/-}; *GRE1LacZ*^{+/-}, (E-E') *GRE1LacZ*^{+/-}; *Shh*^{-/-}; *Gli3*^{-/-}. 'a.', anterior; 'p.', posterior.

We next examined enhancer activity in *Gli3^{-/-};GRE1LacZ^{+/+}* embryos at E10.5. Consistent with previous reports, *Gremlin* gene expression expands anteriorly in *Gli3^{-/-}* embryos (Fig. 3.3D'). In contrast the enhancer activity domain, marked by β -galactosidase staining, does not expand anteriorly (Fig. 3.3D). Instead, the domain is significantly reduced in all *Gli3^{-/-}* embryos (5/5) compared to heterozygous littermates ($p = 0.0007$). The reduction in enhancer activity suggests a role for Gli3 activator in the posterior limb. Consistent with this, *Gli3^{-/-}* limbs at this stage had significantly reduced levels of the Gli activator target gene *Gli1* (Fig. 3.4A). There was also a trend toward a 25% reduction in *Shh* levels that did not reach statistically significant levels (Fig. 3.4B). These results are consistent with previous studies that have shown that *Gli3^{-/-}* limb buds have reduced Gli activator levels as a combination of the direct reduction in Gli3 activator and reduced levels of *Shh* (Bai et al., 2004; Galli et al., 2010; Wang et al., 2007).

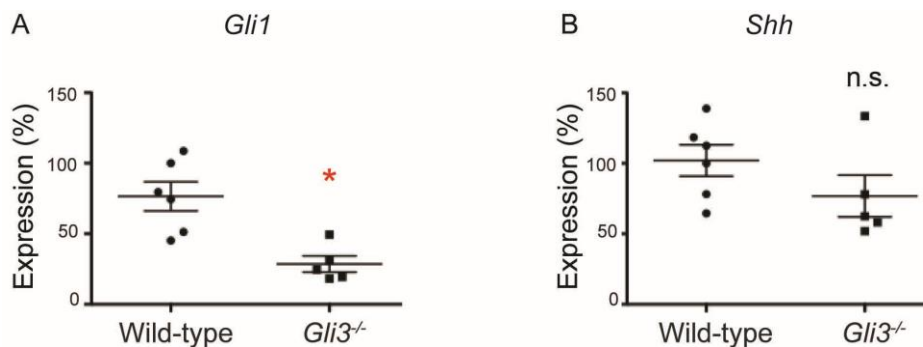


Figure 3.4: *Gli1* is reduced in *Gli3^{-/-}* forelimbs. qRT-PCR for (A) *Gli1* and (B) *Shh* in pairs of forelimbs from wild-type and *Gli3^{-/-}* embryos (32-34 somites), n=6 forelimb pairs per genotype. (A) Red asterisk indicates that *Gli1* expression is significantly reduced in *Gli3^{-/-}* forelimbs (Mann-Whitney U Test; U=1.000, $p = 0.0087$). (B) In the same samples, *Shh* levels tend to be reduced although not to statistically significant levels (Mann-Whitney U Test; U=6.000, $p = 0.1255$). The bars indicate the mean and standard error of the mean.

In *Shh*^{-/-};*Gli3*^{-/-};*GRE1LacZ*^{+/-} embryos at E10.5, *Gremlin* expression persists in limb buds in a depolarized fashion as shown previously (Fig 3.3E') (Aoto et al., 2002; Litingtung et al., 2002; te Welscher et al., 2002). However, the limb buds had an absence of β -galactosidase staining (3/3 embryos; Fig. 3.3E), indicating that Gli activation is required for GRE1 enhancer activity. This is consistent with our previous work that identified a Gli motif that was essential for driving enhancer activity (Vokes et al., 2008).

3.4: GRE1 REQUIRES SUSTAINED SHH SIGNALING

To determine the time period during which GRE1 requires Gli-activator for enhancer activity in the posterior limb, we used an established *ex vivo* limb bud culture assay, treating *GRE1LacZ*^{+/-} limb buds with the Hh pathway inhibitor cyclopamine (Panman et al., 2006). We cultured one forelimb in media containing cyclopamine while the contralateral side was cultured in control media, providing an internal control for staging and embryo variability (Fig. 3.5B). As expected from the lack of activity in *Shh*^{-/-} embryos (Fig. 3.3B), limb buds cultured in cyclopamine at stages before enhancer activity is detected (29-30 somites) resulted in a complete loss of β -galactosidase (Figs. 3.5A, A'). In limb buds cultured at 31-32 somites, there is a strong reduction (61%) in the size of the enhancer activity domain when compared to the control side (Fig. 3.5C-C''; p = 0.0004). Limbs cultured from 33-34 somites have more modest reductions (39%) in the size of the enhancer domain (Fig. 3D-D''; p = 0.0065). The domain size no longer depends on Shh

signaling from 35-36 somites onwards (Figs. 3.5E-E'' p = 0.3333). These results indicated that Shh signaling is required for expanding the domain of enhancer activity until 35-36 somites.

Since residual β -galactosidase protein could persist after the cessation of transcriptional activity from the reporter, it was not possible to determine if Shh is required to maintain enhancer activity with this approach. To circumvent this problem we performed additional limb bud cultures on 32 and 38 somite embryos and measured *LacZ* expression by qRT-PCR. As a control to ensure that the experimental conditions resulted in robust inhibition of Shh signaling, we measured the expression of the obligate Shh target gene *Gli1* (Panman et al., 2006). When forelimbs from 32 somite embryos were cultured, they had an 84% reduction in *Gli1* gene expression and a 75% reduction in *LacZ* expression. Similarly, forelimbs cultured from 38 somites embryos had a 70% reduction in *Gli1* and also had a 64% reduction in *LacZ* (Fig. 3.5F). The change in gene expression at later stages contrasts with the stable expression domains indicated by β -galactosidase staining (Fig. 3.5E-E''). We concluded that establishing the enhancer domain requires Shh signaling transiently until 35 somites, while enhancer activity within the domain continues to require sustained Shh signaling.

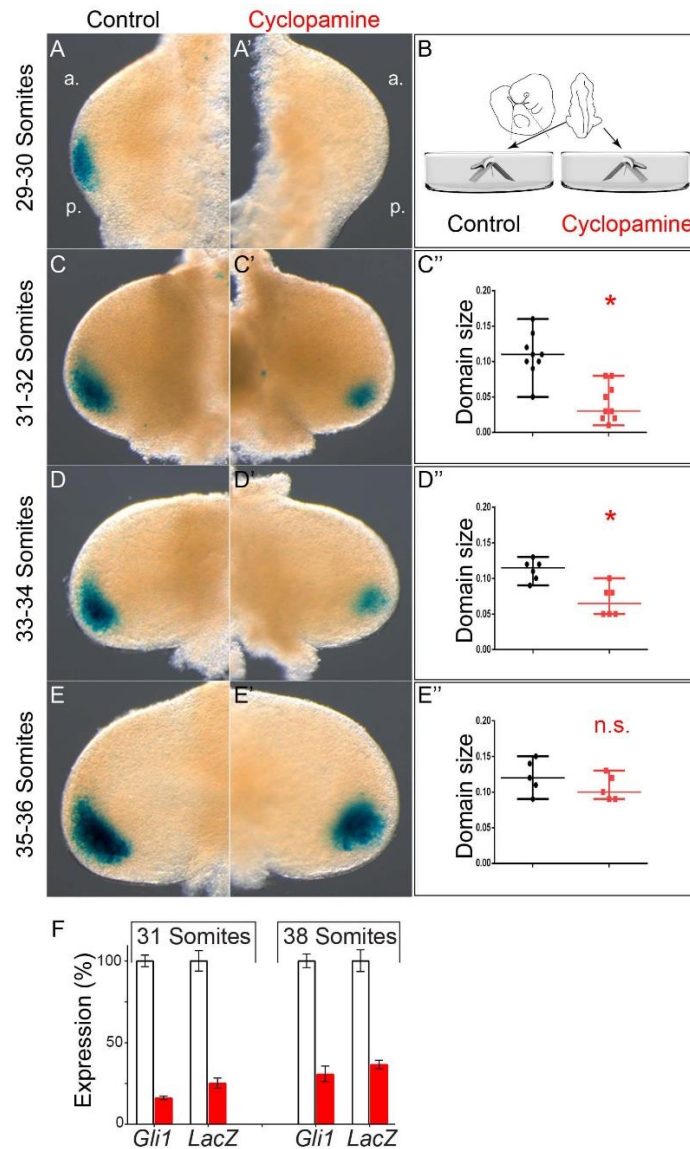


Figure 3.5: GRE1 enhancer activity requires sustained Shh signaling. *GRE1LacZ*^{+/-} forelimbs were cultured in vehicle-containing control media (A-F) while their contralateral forelimbs were cultured in cyclopamine (A'-F') as shown in (B). The stage of the limb buds at the start of the experiment is indicated on the left. (C''-E'') Graphs indicating the domain size measured by the ratio of the β -galactosidase stained area to the total limb bud area for control (black) or cyclopamine treated (red) limb buds. Data points indicate the median and range of values. The presence of an asterisk indicates statistically significant difference (Mann-Whitney U test). Specific values are: C'' U=3.5, p =0.0004; D'' U=1.5, p = 0.0065; E'' U=7.5, p = 0.3333. qRT-PCR in *GRE1LacZ*^{+/-} cultured forelimbs (as shown in (B)). Error bars indicate the standard error of mean, 'a.', anterior; 'p.', posterior.

3.5: WNT AND FGF SIGNALING DO NOT REGULATE GRE1

Previous work demonstrate that FGF signaling represses *Grem1* expression in the anterior-distal limb (Verheyden and Sun, 2008). In addition to requiring Hh signaling, GRE1 could potentially be negatively regulated by FGF signaling. To test this, we cultured *GRE1LacZ* limb buds in the presence and absence of the FGF inhibitor, SU5402 (Mohammadi et al., 1997). Consistent with previous results, inhibiting FGF signaling resulted in the expansion of *Gremlin* into the distal-anterior limb (Fig. 3.6E,F); however, *GRE1LacZ* activity did not expand into the distal-anterior limb (Fig. 3.6A-D). We conclude that FGF signaling does not negatively regulate GRE1.

In addition, another possibility is that WNT signaling may play a role in regulating GRE1. To test this, we cultured *GRE1LacZ* limb buds in control media or media containing a WNT inhibitor, IWR1 (Chen et al., 2009). After 15 hours in culture, the mRNA level of the WNT target gene, *Axin2*, was downregulated in limbs cultured in IWR1 (Fig. 3.7C). However, the expression level of *LacZ* mRNA was not changed between control and IWR1 treated cultures. In addition, the β -galactosidase expression domain for GRE1LacZ did not change between control or IWR1 treated cultures (Fig. 3.7A,B). Under our experimental conditions, we conclude that WNT signaling does not regulate the activity of GRE1.

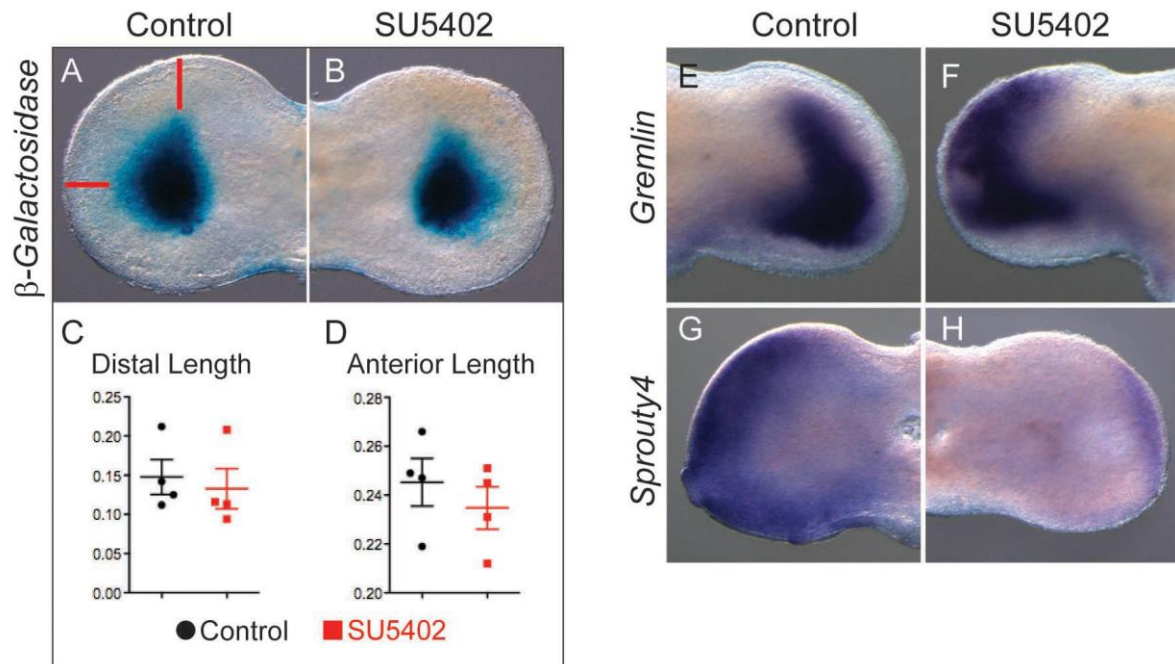


Figure 3.6: GRE1 enhancer activity is not negatively regulated by FGF. E11.5 GRE1LacZ^{+/-} forelimbs (45-48 somites) were cultured in vehicle-containing control media (0.1% DMSO) (A) while their contralateral forelimbs were cultured in 10 μ M SU5402 8 hours (B) and stained for β -galactosidase activity. The normalized distance of the β -galactosidase domain from the distal (C) and anterior (D) limb (schematized as red lines in (A)) is not significantly altered in SU5402-treated embryos (Mann Whitney U Test). Horizontal lines indicate the mean and standard error of mean. (E,F) Consistent with previous reports, inhibiting FGF signaling results in an increase in distal anterior Gremlin expression (n=2). (G,H) Contralateral hindlimbs from the same embryos shown in panels A and B show a reduction in the FGF target gene Sprouty4 in SU5402 cultured limb buds (H) compared to contralateral limb buds cultured in control media (G). Images A,B,G,H are from a 48 somite embryo. Images E,F are from a 45 somite embryo.

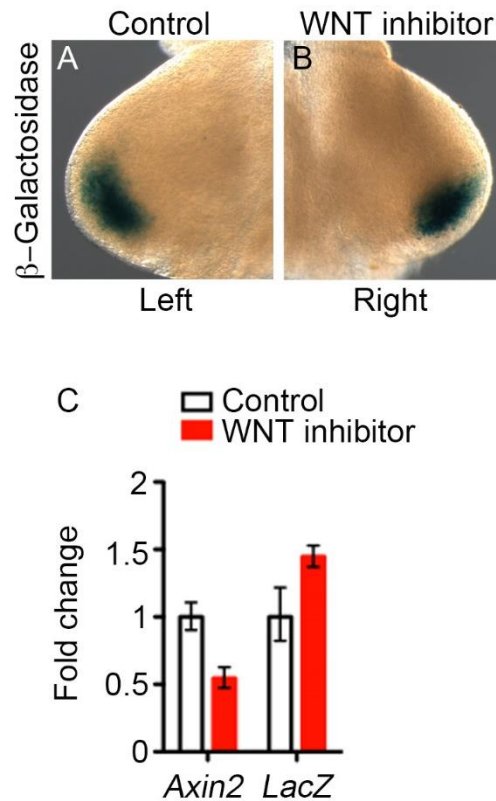


Figure 3.7: Inhibition of WNT signaling does not perturb GRE1 activity. E10.25 (32-34 somites) *GRE1LacZ*^{+/-} forelimbs were cultured in vehicle-containing control media (0.1% DMSO) (A) while their contralateral forelimbs were cultured in 1 μ M IWR1 (WNT inhibitor) for 15 hours (B) and stained for β -galactosidase activity. (C) qRT-qPCR for *Axin2* and *LacZ* expression. Gene expression normalized to *Gapdh* in the wild-type sample.

3.6: GRE1 FUNCTIONS AS A GLI-MEDIATED SILENCER

We generated mice containing a deletion of GRE1 (described in Appendix C). *Gremlin* ^{Δ GRE1/ Δ GRE1} forelimbs expressed *Gremlin* and *Formin* at levels that are indistinguishable from wild-type control forelimbs (Fig. 3.8A-C). *Gremlin* ^{Δ GRE1/ Δ GRE1} mice were viable and fertile with normal skeletal patterning (Fig. 3.8D-G). Embryos containing

one null allele of *Gremlin* (Khokha et al., 2003) and a second allele harboring the deletion of GRE1 also had normal skeletal patterning (Fig. 3.9A,B). These results indicate that GRE1 is not necessary for normal skeletal development. The *Gremlin* gene expression domain was nearly normal in *Gremlin*^{ΔGRE1/ΔGRE1} embryos at E11 (Fig. 3.8A,B) but at earlier stages, the distal anterior boundaries of expression were more diffuse (Fig. 3.10A,B). In light of these results, we hypothesized that redundant Gli-dependent CRMs might regulate *Gremlin*. Two additional Gli-binding regions are present within the *Gremlin* locus (Vokes et al., 2008). One of these regions was recently shown to have Shh-responsive enhancer activity and to be critical for mediating BAC reporter activity in transgenic embryos (Zuniga et al., 2012). We hypothesized that our Gli CRM might be redundant with other GREs under normal conditions but still required for robust regulation of *Gremlin*.

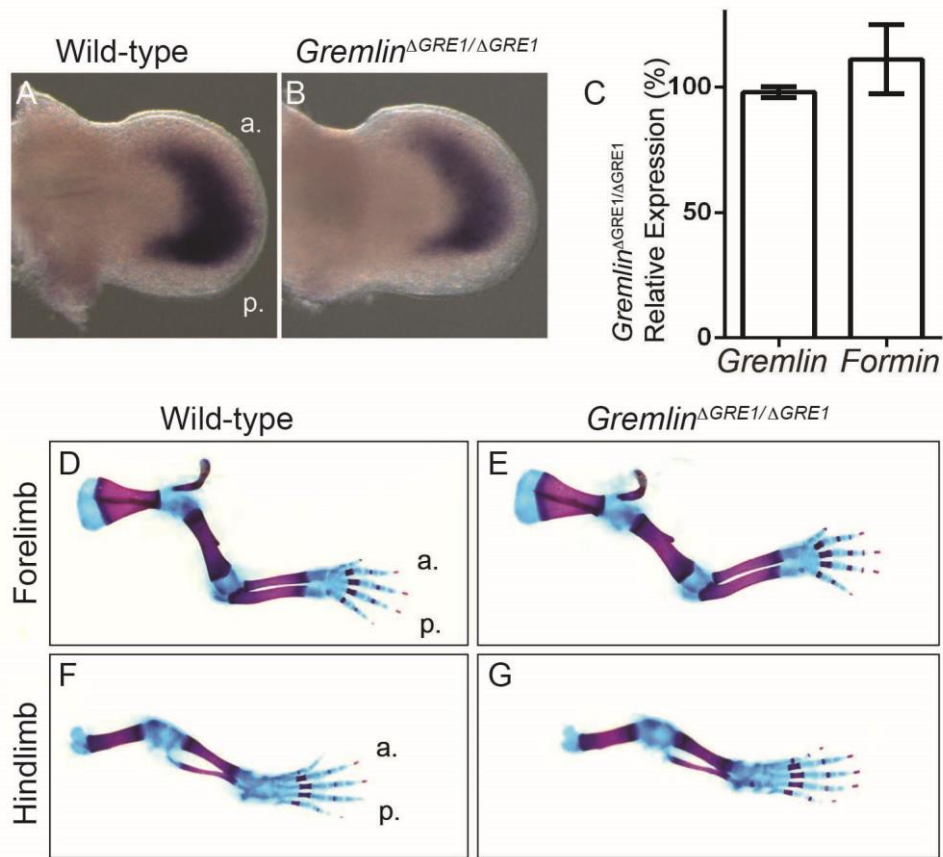


Figure 3.8: GRE1 is not essential for limb development. (A,B) *Gremlin* expression in forelimbs at E11 (41 somites). (C) *Gremlin*^{ΔGRE1/ΔGRE1} embryos express *Gremlin* and *Formin* at levels that are statistically indistinguishable from wild-type embryos (One Sample T-Test, Two Tails; *Gremlin* $p = 0.1172$; *Formin* $p = 0.4548$). Values are normalized to the distal marker *Jagged 1*. Error bars represent standard error of mean from four independent biological samples (E10.5, 34-37 somites). (D-G) E18.5 skeletal preparations showing forelimbs and hindlimbs of the indicated genotypes. ‘a.’, anterior; ‘p.’, posterior.

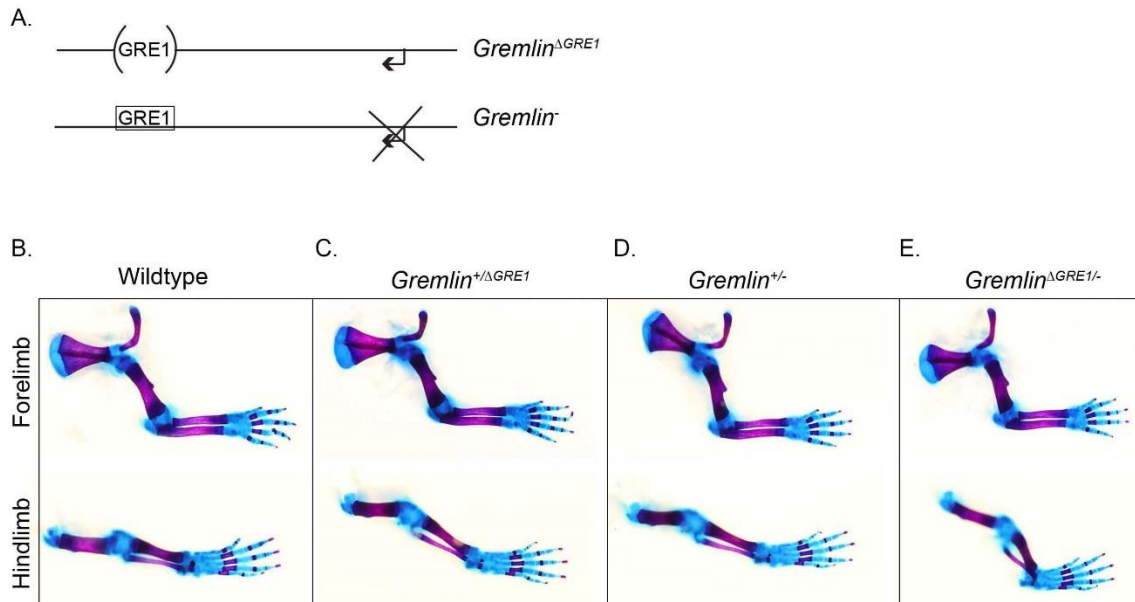


Figure 3.9: Gremlin and GRE1 transheterozygote displays normal limb patterning. (A) Embryos containing a null allele of Gremlin (*Greml^{tm1Rmh}*) and the other allele with a deletion of GRE1 have normal limb skeletal patterning. (B-E) Forelimbs and hindlimbs from the same embryo at E18.5 stained for bone (Alizarin Red) and cartilage (Alcian Blue). The numbers of skeletons that were analyzed for each genotype: (A) n=6, (B) n=3, (C) n=4, (D) n=4

Studies in *Drosophila* have tested the robustness of transcriptional responses to shadow enhancers by examining CRM deletion phenotypes at the outer ranges of permissive temperatures or by removing one copy of an upstream regulator (Frankel et al., 2010; Perry et al., 2010). We used the latter strategy to examine *Gremlin* expression in *Gremlin*^{ΔGRE1/ΔGRE1} embryos containing a single copy of *Gli3*, which is sufficient to prevent the distal-anterior expression of *Gremlin* seen in *Gli3*^{-/-} embryos (te Welscher et al., 2002). At E10.5, both wild-type and *Gli3*^{+/-} littermates have a sharp boundary of *Gremlin* expression that is restricted from the most distal-anterior mesoderm in the forelimbs (n=7;

brackets in Fig. 3.10A,C). *Gremlin*^{ΔGRE1/ΔGRE1} littermates have forelimbs with less pronounced distal-anterior borders of *Gremlin* and with weak ectopic expression in the anterior limb mesoderm directly adjacent to the apical ectodermal ridge (n=10; dashed arrow in Fig. 3.10B). In contrast, *Gremlin*^{ΔGRE1/ΔGRE1};*Gli3*^{+/-} littermates have forelimbs with ectopic distal-anterior *Gremlin* expression that is broader and stronger than in *Gremlin*^{ΔGRE1/ΔGRE1} forelimbs (n=8; Fig. 3.10D). This expression is significantly different from *Gli3*^{+/-} (p = 0.0002) or *Gremlin*^{ΔGRE1/ΔGRE1} forelimbs (p<0.0001), indicating a genetic interaction between *Gli3* and the *Gremlin*^{ΔGRE1} allele.

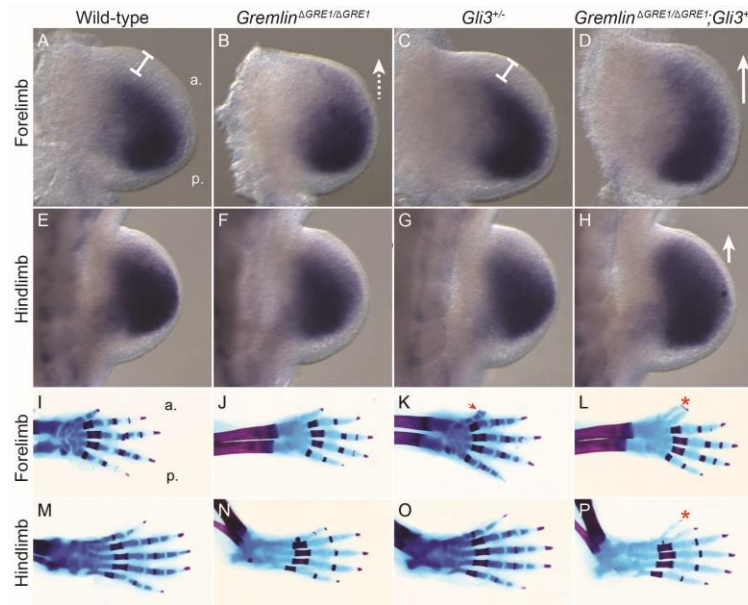


Figure 3.10: The GRE1 CRM interacts genetically with *Gli3* to repress *Greml1*. *Greml1* expression in various genetic backgrounds in the forelimbs of 35-36 somite embryos (A-D) and hindlimbs of 37-38 somite embryos (E-H). The white brackets in panels (A,C) indicate the *Gremlin* free domain in anterior limb buds. White arrows (B,D,H) indicate ectopic distal-anterior *Gremlin* expression in *Gremlin*^{ΔGRE1/ΔGRE1} backgrounds. (I-P) E18.5 skeletal preparations of the hand (J-L) or foot (M-P) in various genetic backgrounds. The arrowhead (K) highlights a bifurcated thumb; the asterisks (L,P) indicate polydactyly.

An expansion of Gremlin protein into the anterior distal mesenchyme would inhibit BMPs, causing an expansion in anterior growth (Lopez-Rios et al., 2012; Pizette and Niswander, 1999). This growth would likely result in anterior polydactyly, which is also seen in mice with reduced BMP activity (Dunn et al., 1997; Selever et al., 2004). In the mixed genetic background present in our colony, the presence of the *Gli3*^{+/-} ‘extra toes’ allele only rarely results in mice or embryos with fully polydactylous digits. In this study, all of the *Gli3*^{+/-} embryos had a single nub (a fleshy outgrowth that sometimes contains a single speck of cartilage) but none of them had distinct polydactylous digits (18/18 hindlimbs) (Fig. 3.10O). *Gremlin*^{ΔGRE1/ΔGRE1} littermates have normal digit patterning (14/14 hindlimbs) (Fig 3.10N). In contrast, *Gremlin*^{ΔGRE1/ΔGRE1};*Gli3*^{+/-} littermates have a distinct, polydactylous digit in 3/8 hindlimbs (Fig. 3.10P), a significant difference from *Gli3*^{+/-} embryos alone (p = 0.0215). *Gli3*^{+/-} forelimbs displayed a spectrum of phenotypes ranging from completely normal digits (7/17) to polysyndactyly (4/17). *Gremlin*^{ΔGRE1/ΔGRE1};*Gli3*^{+/-} forelimbs uniformly contained a polysyndactylous thumb (8/8), a significant increase in frequency compared to *Gli3*^{+/-} embryos (p = 0.0005; Figs. 4.10I-L). *Gremlin*^{ΔGRE1/+};*Gli3*^{+/-} embryos also contained a high proportion of polysyndactylous forelimbs (23/28). These results suggest that GRE1 has silencer activity that is required for robust anterior repression of *Gremlin*. Our result is consistent with previous studies showing a genetic interaction between *Gli3* and BMP4 (Dunn et al., 1997; Lopez-Rios et al., 2012). We concluded that silencer activity through GRE1 is required for robust, *Gli*-dependent repression of *Gremlin* in the anterior limb (schematized in Fig. 3.11A-D).

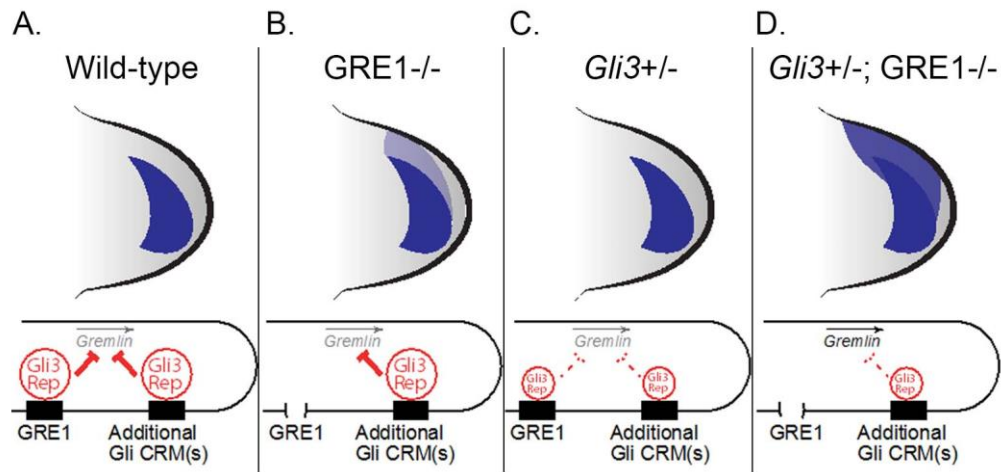


Figure 3.11: Schematic models showing how Gli3 repression of *Grem1* (blue crescent) might occur in various genetic backgrounds.

3.7: DISCUSSION

In this study we have performed the first genetic characterization of a vertebrate Gli CRM. Within the limb bud, most putative Gli target genes are associated with multiple Gli binding regions (Vokes et al., 2008). Our results, suggest that one role for multiple, distinct Gli binding regions around Gli target genes is to provide a robust silencing response that buffers against genetic perturbations. This contrasts with the *Fgf8* and *HoxD* loci where multiple enhancers with similar activity domains have been proposed to additively or synergistically amplify transcription (Marinic et al., 2013; Montavon et al., 2011). Our results further suggest that Gli silencers prevent transcriptional activity driven by additional, Gli-independent CRMs. We also show that GRE1 can act as a Gli-activator

dependent enhancer in the posterior limb although the biological role for this activity is unclear (see section on Gli enhancer activity).

We propose a model where Gli repressors bind to multiple Gli-dependent CRMs in the anterior limb, providing a robust silencing activity that prevents ectopic activation of *Gremlin* that would otherwise be driven by at least one additional Gli-independent CRM that is active throughout the distal limb (a pan-limb enhancer). Gli repressor-mediated silencing results in the anterior repression of *Gremlin* in the absence of threshold levels of Gli activator complexes. In the posterior limb, where Gli activator activity is high and Gli repressor activity is low, GRE1 silencing activity is lost and Gli-activator complexes provide enhancer activity. We have synthesized these results in a model for how *Gremlin* is regulated by Gli proteins within the limb (Fig. 3.11).

3.7.1: GRE1 enhancer activity

GRE1 enhancer activity is detected in the posterior limb in a spatial and temporal fashion that correlates with Shh signaling (Fig. 3.2). GRE1 requires Gli-activation for initiating and sustaining activity at E10.5 and ectopic Gli activator signaling is sufficient to drive GRE1 expression throughout the anterior-posterior axis (Fig. 3.3). These results suggest that GRE1 enhancer activity is primarily regulated by Shh signaling. GRE1 enhancer activity is transiently reduced in E10.5 *Gli3*^{-/-} limb buds (Fig. 3.3D). Our own results are consistent with several studies showing that *Gli3*^{-/-} limbs have reduced levels of

Gli activation caused by a combination of reduced levels of Gli proteins and a reduction in *Shh* (Bai et al., 2004; Bowers et al., 2012; Galli et al., 2010; Wang et al., 2007).

In marked contrast to *Gremlin* gene expression, the GRE1 enhancer domain does not expand in E10.5 *Gli3*^{-/-} limb buds (Fig. 3.3D,D’'). We rule out the trivial possibility that Gli repressors do not work through GRE1 because our subsequent experiments indicate that it does indeed mediate Gli repressor-mediated silencing of *Gremlin*, and it is bound by Gli3 repressor in chromatin immunoprecipitation assays (Vokes et al., 2008). The behavior of GRE1 contrasts with the behavior of a *Dpp* wing imaginal disc CRM in *Drosophila*, where both repressor and activator functions of Ci can be detected out in the same enhancer element (Muller and Basler, 2000). Within the mammalian neural tube, studies have reported conflicting conclusions regarding the role for Gli3 in restricting the boundaries of Gli activator enhancers or genes (Balaskas et al., 2012; Oosterveen et al., 2012; Peterson et al., 2012).

There are several possible explanations for the lack of anterior expansion of *GRE1lacZ* in E10.5 *Gli3*^{-/-} limb buds. The first is that Gli repressors might not compete with Gli activators to limit the anterior domain of enhancer activity. In this scenario, enhancer activity is driven solely by threshold-dependent Gli activation. The lack of baseline anterior activity would prevent visualization of the silencer activity in an enhancer reporter assay. A second possibility is that the *GRE1lacZ* transgenic construct is incapable of responding normally to Gli repressors because it is removed from its normal chromosomal environment. Indeed, our experiments suggest that Gli repressors do regulate the activity of additional CRMs in the *Gremlin* locus. Taken out of context, GRE1 could

also have altered affinities for Gli activator and repressor complexes that prevent its anterior expansion in *Gli3*^{-/-} embryos. A third possibility is that residual Gli repressor activity is sufficient to prevent anterior expansion of *GRE1LacZ* in *Gli3*^{-/-} limb buds. Consistent with this, recent work has indicated that there is a genetic role for Gli2 repressor in skeletal patterning in the absence of Gli3 (Bowers et al., 2012). However, *Gremlin* expression appears largely symmetrical along the anterior-posterior axis in *Gli3*^{-/-} limb buds, suggesting that the remaining Gli repressor activity mediated by Gli2 might not be sufficient to repress *Gremlin* (Fig. 3.3D') (Aoto et al., 2002; Litingtung et al., 2002; Welscher et al., 2002). Additional studies examining *GRE1LacZ* enhancer activity in *Gli2*^{-/-}; *Gli3*^{-/-} limb buds would be necessary to determine if GRE1 itself is more sensitive to Gli2 repression than the overall *Gremlin* gene expression pattern would suggest.

3.7.2: GRE1 and GLI repressors

Two models for Gli repression have been proposed (Wang et al., 2010). In one, Gli3 repressor acts as an inert decoy competing with Gli activator to regulate the transcription of target genes (Oosterveen et al., 2012; Wang et al., 2010). In the second, Gli repressor behaves like a conventional transcriptional repressor, recruiting transcriptional co-repressors that actively shut down transcription (Wang et al., 2010). While the first model would apply specifically to Gli activator target genes, the second model could in principle apply to both Gli activator target genes and to genes that only require Gli derepression. GRE1 displays properties that are associated with both classes of

Gli target genes. *Gremlin* is a Gli derepression gene and Gli3 works through GRE1 as a silencer, preventing transcription directed by additional CRMs that would otherwise lead to ectopic distal-anterior expression. This mechanism of repression is distinct from conventional CRMs where repressor activity is integrated at the CRM level with each CRM then acting as an autonomous module to regulate gene expression. In future studies, it will be interesting to determine the mechanism of repression, which could function as a basal regulator of transcriptional activity. Alternatively Gli3 might specifically inactivate one or more CRMs.

3.7.3: GLI proteins generate asymmetric gene expression

In the posterior limb bud, it is unclear whether Gli activators are simply indicative of a de-repressed environment that permits additional CRMs to drive expression or if they also provide a quantitative contribution as enhancers to increase *Gremlin* transcription. The only evidence suggesting GRE1 is an enhancer is the enhancer activity of the isolated element in transgenic limb buds (Fig. 3.2). While this fits the generally accepted criteria for an enhancer, there is no genetic evidence for reduced Gli activator responses in either *Gremlin*^{ΔGRE1/-} or *Gremlin*^{ΔGRE1/ΔGRE1}; *Shh*^{+/-} embryos (Fig. 3.9, data not shown).

The lack of any detectable phenotype suggests that in the context of the native genomic locus, the enhancer activity is absent, trivial or completely redundant with additional Gli-dependent CRMs. The ambiguity over the contribution of enhancer activity is represented in Fig. 3.12, suggesting that the major purpose of GRE1 enhancer activity

lies in counteracting Gli repression rather than providing quantitative levels of activation. In this way, GRE1 could act as a binary switch, causing transcription to be on or off in different domains (Fig. 3.12). This model provides a mechanism for how Shh signaling imposes asymmetric expression of ‘pre-patterned’ genes that would, in the absence of any Gli regulation, be symmetrically expressed throughout the limb bud. It also suggests that the inclusion of Gli-driven CRMs into the locus of pre-patterned limb might have provided an evolutionary mechanism for regulating asymmetric gene expression in a pre-existing pattern.

3.7.4: Multiple CRMs regulate *Grem1*

Within the context of this study, there appear to be at least three distinct CRMs regulating *Gremlin*. This is consistent with previous studies that describe a complex regulatory locus for *Gremlin* (Vokes et al., 2008; Wang et al., 1997; Zuniga et al., 2012; Zuniga et al., 2004). Several proteins have also been shown to regulate *Gremlin* at various developmental time points. In particular, BMPs and HoxA/D transcription factors both regulate *Gremlin* along the anterior-posterior axis. Their activity and expression domains make them excellent candidate regulators for the Gli-independent pan-limb enhancer (Fig. 3.12) (Benazet et al., 2009; Capdevila et al., 1999; Nissim et al., 2006; Sheth et al., 2013). Intriguingly, HoxA/D conditional mutants lack most *Gremlin* expression with the exception of a posterior domain that appears nearly identical to the Gli CRM enhancer domain (Fig. 3.1B) (Sheth et al., 2013). Although our model depicts pan-limb enhancer

activity with one CRM as the simplest possibility (Fig. 3.12), it is certainly possible that this activity integrates multiple Gli-independent enhancers active in distinct or overlapping domains.

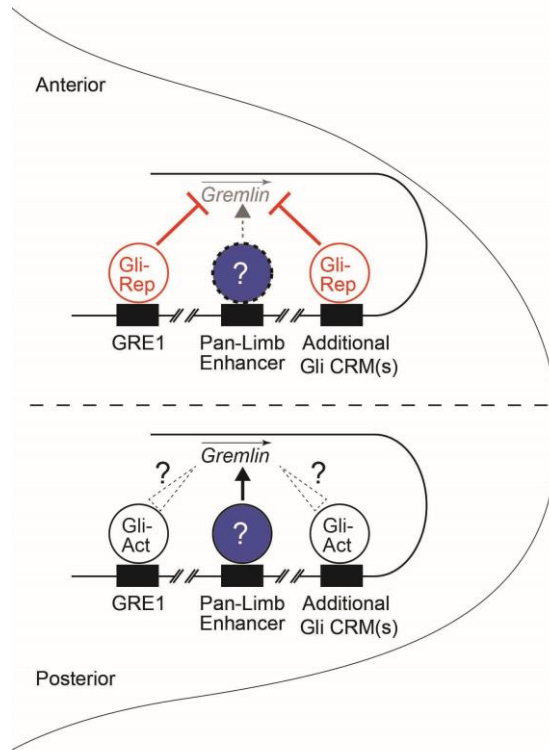


Figure 3.12: Gli proteins generate asymmetric expression of *Gremlin*. *Gremlin* is activated by a pan-limb enhancer (blue circle) that has activity throughout the distal limb. In genetic backgrounds where there is an absence of Gli regulation (no activation or repression, e.g. *Shh*^{-/-}; *Gli3*^{-/-}), the pan-limb enhancer drives symmetrical expression of *Gremlin* throughout the limb bud. In the posterior region, Gli-activators regulate redundant Gli-dependent CRMs, including GRE1, causing a loss of Gli-mediated silencing and possibly threshold-dependent enhancer activity (indicated by dashed arrows). In the anterior region, GRE1 acts as a silencer, preventing ectopic activation of *Gremlin* through a pan-limb enhancer. The additional Gli-dependent CRM(s) could be either directly or indirectly regulated by Gli signaling.

Recently, a second GRE that lies closer to the transcriptional start site has been characterized. While it does not contain a high affinity Gli motif within the core region, it is nonetheless bound by Gli3 in ChIP assays and requires Shh expression for enhancer activity in mutant embryos (Zuniga et al., 2012). Unlike GRE1, the more proximal GRE is essential for *Gremlin* transcriptional activity in the same BAC reporter used in this study (Zuniga et al., 2012). Notably, GRE1 is not sufficient to activate transcriptional activity in its absence. This more proximal GRE could integrate Gli signaling with additional, Shh-independent, facets of *Gremlin* or there could be additional, uncharacterized Gli-dependent element(s). Our study was limited to the contribution of a single CRM, and future studies will be required to determine if there are higher-order chromatin interactions among the individual CRMs regulating *Gremlin* as has been suggested for the *Fgf8* and *HoxD* loci (Marinic et al., 2013; Montavon et al., 2011). In *Drosophila*, Ci (Gli) repressors have been proposed to work cooperatively by binding to several distinct sites within a CRM regulating *Dpp* (Parker et al., 2011). The presence of an additional Gli CRM in the *Gremlin* locus raises the intriguing possibility that Gli proteins binding to distinct CRMs might nonetheless be able to cooperatively repress *Gremlin* in the context of a higher order chromatin structure.

3.7.5: GLI-bound CRMs confer robust transcriptional control

Embryos and mice lacking GRE1 have no detectable skeletal phenotype. Nonetheless, embryos do have subtle shifts in *Gremlin* expression (Fig. 3.10A,B), and

when one copy of *Gli3* is removed GRE1 is required for the repression of *Gremlin*. It is formally possible that the enhanced phenotype seen in Δ GRE1;*Gli3* compound heterozygous embryos (Fig. 3.10) is due to the presence of another allele co-segregating with GRE1. The primary support that this interaction occurs between GRE1 and *Gli3* is that is consistent with interactions observed between Gli3 and BMPs (which should have reduced anterior activity with ectopic *Gremlin* expression) (Dunn et al., 1997; Lopez-Rios et al., 2012).

Both the subtle changes in expression pattern and the requirement of the CRM as a mechanism for buffering genetic variation are analogous to the shadow enhancers described in *Drosophila* (Barolo, 2012; Frankel et al., 2010). Shadow elements are defined by the genetic interactions of two genetically defined CRMs (Frankel, 2012) and further genetic studies involving multiple Gli bound elements would be required to determine if the Gli CRM is functioning as a shadow repressor of *Gremlin*. Our study, focused exclusively on a single Gli CRM, is the first to address the potential genetic role that multiple Gli-bound CRMs play in regulating transcription. Multiple Gli binding sites are associated with many predicted Gli target genes (Peterson et al., 2012; Vokes et al., 2008) and we propose that they may act as a general mechanism for mediating robust transcriptional responses to Hh signaling.

Chapter 4: Manipulating gene expression in dissociated limb buds

Portions of this chapter are modified with permission from the authors. Lewandowski, J.P., Pursell, T. A., Rabinowitz, A. H., & Vokes, S. A. Manipulating gene expression and signaling activity in cultured mouse limb bud cells. Dev. Dyn. (2014) 243(7):928-936. J.P.L., T.P., conceived and performed experiments, and interpreted data; A.R., performed experiments.

4.1: INTRODUCTION

The developing vertebrate limbs provide a system to study cell differentiation, tissue morphogenesis, and the integration of signaling pathways. Decades of research have established a broad framework of the major pathways required during limb bud development, using a combination of genetic and embryological methods (Rabinowitz and Vokes, 2012). However, a major limitation of current genetic approaches is that testing gene function or DNA regulatory element activity is time consuming and resource-intensive, often requiring the generation of genetically modified embryos. Methods allowing a faster way to evaluate gene function and DNA regulatory elements would significantly improve the utility of the limb bud system.

Cell culture approaches are a way to fulfill this need; however, there are no broadly used cell lines that represent limb bud mesenchyme. A few immortalized limb bud mesenchyme cell lines have been generated (Trevino et al., 1993); these represent distinct types of mesenchyme but have not been extensively characterized. Cell lines derived from related lineages can differentiate into bone or cartilage (Denker et al., 1995; Long et al., 2004) but it is unclear to what extent they represent limb bud cells. Also, cultures of primary limb bud cells grown under standard conditions quickly differentiate into

chondrocytes, limiting their usefulness for studying limb bud development. In a significant advance two recent studies have shown that chicken limb bud cells, cultured in the presence of WNT3a and FGF8, express distal limb bud mesenchyme gene markers and remain undifferentiated (ten Berge et al., 2008; Cooper et al., 2011).

Using these studies as a foundation, we describe a method for culturing murine E10.5 limb bud cells in micromass-like conditions on a 96-well format. We then describe a method to deliver plasmids and siRNAs at high efficiency that result in quantifiable changes to endogenous gene expression. We specifically adapt these conditions to assay Hedgehog (Hh)-responsive gene expression. Furthermore, we show that this approach is readily amenable to study the response of other signaling pathways such as WNT and BMP that are also active in limb bud mesenchyme.

4.2: ASSESSMENT OF DIFFERENTIATION IN DISSOCIATED LIMB CELL CULTURES

Cultures of primary limb bud cells containing different signaling factors have successfully been used to prevent cell differentiation, allowing limb cells to be cultured as a progenitor population for several days (ten Berge et al., 2008; Cooper et al., 2011). Treatment with FGF8 alone can delay differentiation for 4 days while co-treatment with WNT3a essentially blocks further differentiation (ten Berge et al., 2008). Additional studies suggest that FGFs provide a distalizing influence on the limb (Rosello-Diez et al., 2011). We used these conditions as a foundation for culturing mouse forelimb cells. Limb buds from E10.5 (33-36 somites) mouse embryos were harvested and processed in

electroporation solution only, and post electroporation approximately 200,000 cells were plated per well on a 96-well half-area plate.

As an initial experiment, we cultured cells in media containing FGF8 and purmorphamine, a small molecule that constitutively activates the Hedgehog (Hh) pathway by binding to Smoothened (Sinha and Chen, 2006; Dessaud et al., 2007). We then stained cultures with Alcian blue to mark chondrocytes, and also examined genes expressed during chondrogenesis. As expected, at 72 hours Alcian blue staining was observed in cartilage forming nodules produced by limb cells cultured in control media (Fig. 4.1A). In contrast, little or no Alcian blue staining was observed in limb cells cultured in media containing FGF8, purmorphamine, or FGF8 and purmorphamine (Fig. 4.1B-D), suggesting that these conditions block cartilage formation.

While Alcian blue staining is indicative of cartilage formation, we also quantified differentiation by using quantitative reverse transcription PCR (qRT-PCR) to determine the expression of *Sox9*, an early marker of chondrocyte differentiation, as well as *Aggrecan 1* (*Agc1*), a chondrocyte-specific marker (Bi et al., 1999; Akiyama et al., 2002). We normalized gene expression to the 24 hour control sample in order to examine changes in gene expression over time. In addition, we compare these normalized data to the relative gene expression values from freshly isolated limb buds. When compared to control cultures, *Sox9* expression was moderately reduced at all time points in cells cultured in media containing FGF8, purmorphamine, and FGF8 and purmorphamine (Fig. 4.1E). The modest reduction in *Sox9* likely occurs because proximal expression has already initiated in E10.5 limb buds (Kawakami et al., 2005). *Agc1* is strongly activated in control cultures

while cells cultured in media containing FGF8 or purmorphamine had greatly reduced levels of *Agc1*, suggesting a delay in differentiation (Fig. 4.1F). Cells cultured in media containing both FGF8 and purmorphamine had essentially no *Agc1* expression (mean expression value = 0.333 at 72 hours) (Fig. 4.1F). To note, *Agc1* is not robustly detected in freshly isolated limb buds. Combined, our data indicate that limb bud cells cultured in media containing FGF8, purmorphamine, or the combination of FGF8 and purmorphamine prevent chondrogenic differentiation during the 3-day period of our assay.

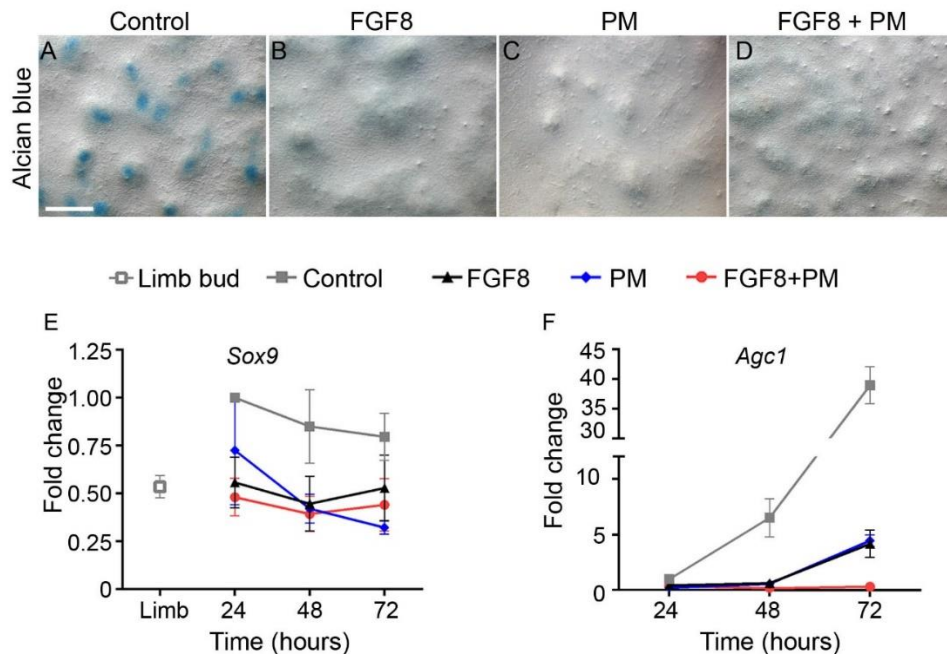


Figure 4.1: Limb bud cells cultured with FGF8 and purmorphamine do not differentiate. (A-D) Primary limb bud cell cultures at 72 hours stained with Alcian blue. Cells in control media (A) show nodules stained with Alcian blue, while cells cultured in 150 ng/mL FGF8-containing media (B), 5 μ M purmorphamine (PM) (C) or FGF8 and PM (D) have minimal or no Alcian blue staining. Cells are shown at the same magnification (10x), and the scale bar is 200 μ m. (E,F) qRT-PCR for chondrogenic markers in limb cell cultures at 24, 48, and 72 hours. Gene expression is normalized to *Gapdh* in the control sample at 24 hours, and comparison to freshly isolated limb cells is shown with a gray open square. Data points are the mean of 3 independent experiments and error bars represent the s.e.m.

4.3: PURMORPHAMINE PROMOTES AN INCREASE IN CELL NUMBER

Previous studies using WNT3a alone or in combination with FGF8 demonstrated that both are effective to promote an increase in cell number in chick limb bud cultures (ten Berge et al., 2008). We performed cell counts at 24, 48, and 72 hours to determine the individual and collective effect of FGF8 and purmorphamine on cell number during the 3-day culture period (Fig. 4.2A). Consistent with previous reports (ten Berge et al., 2008), FGF8 alone was not effective in promoting an increase in the number of cells over time. In contrast, cells cultured in purmorphamine alone or FGF8 and purmorphamine caused an increase in the number of cells, although not to the extent as WNT3a or the combination of WNT3a and FGF8 (Fig. 4.2A). In contrast, cells cultured in BMP4 had no increase in the number of cells. We conclude that treatment with purmorphamine or the combination of FGF8 and purmorphamine promotes an increase in cell number.

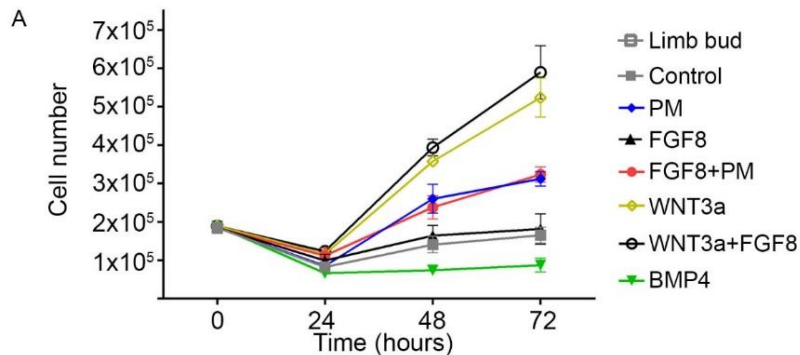


Figure 4.2: Individual and collective effects on cell number. (A) Effect of FGF8, purmorphamine (PM), both PM and FGF8, WNT3a (250 ng/mL), WNT3a and FGF8, and BMP4 (50 ng/mL) on limb cell number. PM alone and PM with FGF8 promote an increase in the number of limb mesenchyme cells in culture (red circle and blue diamond). Limb bud indicates number of cells initially plated. Data points are the mean of 5 independent samples and error bars indicate the s.e.m.

4.4: CULTURED LIMB CELLS ARE RESPONSIVE TO MULTIPLE SIGNALING PATHWAYS

Since the cells are cultured with FGF8 and FGF signaling in the AER maintains *Shh* expression in limb buds (Laufer et al., 1994; Niswander et al., 1994; Bastida et al., 2009), it was feasible that FGF8 could maintain endogenous *Shh* expression in our system. Compared to control cells, FGF8-treated cells have a mild upregulation of the FGF target gene *Dusp6* (Kawakami et al., 2003; Mariani et al., 2008) (Fig. 4.3C); however, *Shh* expression is rapidly lost in FGF8 treated cells (Fig. 4.3B). We conclude that under our experimental conditions, limb bud cells cultured in purmorphamine or FGF8 and purmorphamine do not enhance endogenous *Shh* expression.

Next, we next determined the ability of the cultured cells to respond to additional signaling pathways that are active in the limb mesenchyme. We treated cells with BMP4 or WNT3a and quantified induction by determining the gene expression levels for the target genes, *Msx2* (Pizette et al., 2001) and *Axin2* (ten Berge et al., 2008), respectively. At 24 hours BMP4 induced high levels of the *Msx2*, approximately 25 fold, and expression decreased to approximately 7 fold by 72 hours (Fig. 4.3D). WNT3a induced expression of the obligate target gene, *Axin2*, approximately 5 fold (Fig. 4.3E).

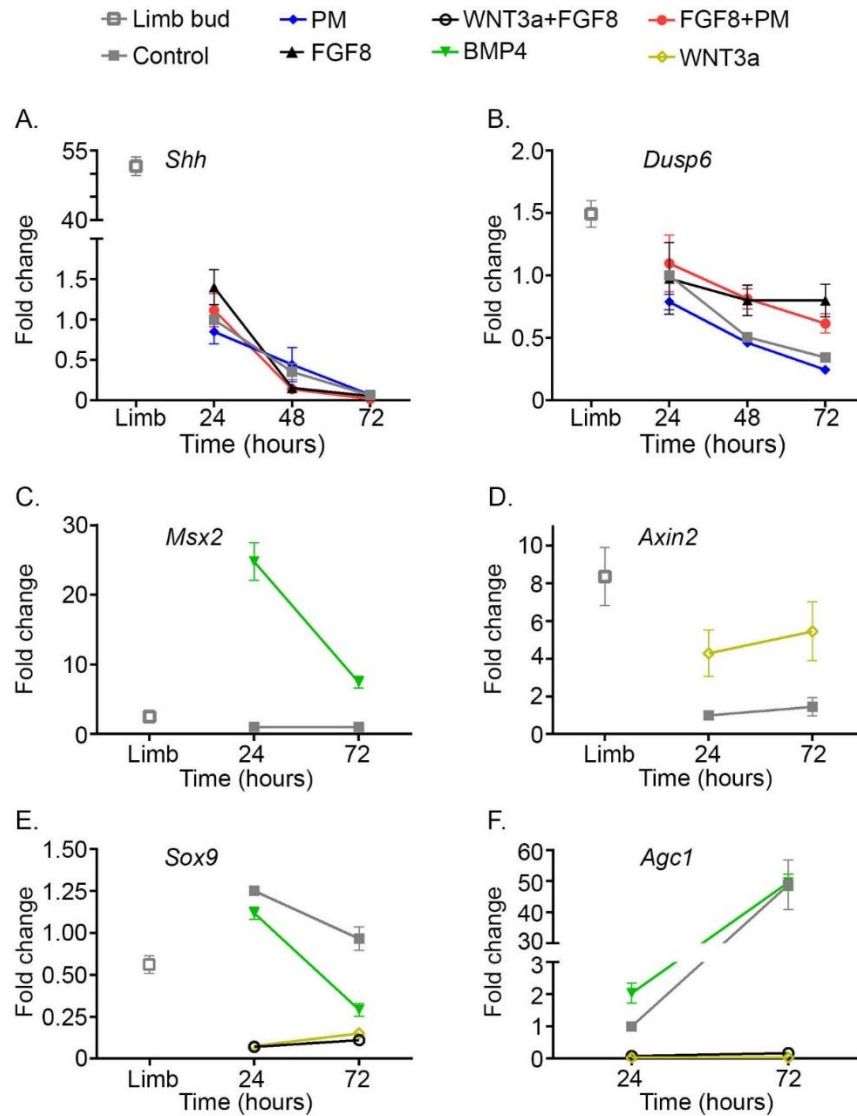


Figure 4.3: Cultured limb bud cells are responsive to multiple signaling pathways. (A-F) qRT-PCR for signaling pathway genes and chondrocyte differentiation markers. Note that *Shh* expression is highly downregulated in culture conditions (A). FGF8 signaling to cells shows a modest upregulation of *Dusp6* in FGF8, and PM with FGF8 cultures (B). Culturing cells in the presence of BMP4 (C) or WNT3a (D) upregulates obligate target genes, *Msx2* (C) and *Axin2* (D). WNT3a suppresses markers for chondrogenic differentiation, *Sox9* and *Agc1* (E,F). BMP4 treatment shows a downregulation of *Sox9* over time (E) and an upregulation of *Agc1* over time (F). Gene expression is normalized to *Gapdh* in the control sample at 24 hours, and comparison to freshly isolated limb cells is shown with a gray open square. Data points are the mean of 3 independent experiments and error bars represent the standard error of the mean.

We assessed the chondrogenic differentiation status of cells cultured in BMP4 and WNT3a by examining *Sox9* and *Agc1* expression. BMP4 treated cells at 24 hours showed similar levels of *Sox9* to the control culture; however, at 72 hours *Sox9* expression decreased (Fig. 4.3F). WNT3a alone or in combination with FGF8 treated cells showed a decrease in *Sox9* expression at all the time points (Fig. 4.3F), which is consistent with previous reports (ten Berge et al., 2008). The chondrocyte-specific marker, *Agc1*, was expressed in BMP4 treated cells to levels similar observed in the control cells. In contrast, cells cultured in WNT3a alone or with FGF8 had essentially no *Agc1* expression (mean expression value = 0.03 and 0.173, respectively) (Fig. 4.3G). The inhibition of *Agc1* is comparable to that observed in cells treated with both purmorphamine and FGF8 (Fig. 4.1F). Taken together, our data demonstrate that cells treated with both purmorphamine and FGF8 are maintained in an undifferentiated state similar to that previously reported for WNT3a alone and WNT3a and FGF8.

4.5: EXPRESSION OF GLI TARGET GENES IN DISSOCIATED LIMB CELL CULTURES

After adding purmorphamine, we sought to determine if limb bud cells were responsive to Hh signaling. We quantified the level of Hh-induced gene expression during the culture period using qRT-PCR. Expression of the obligate Hh target genes, *Gli1* and *Ptch1* (Marigo et al., 1996; Litingtung et al., 2002; te Welscher et al., 2002), were persistently upregulated at 24, 48, and 72 hours in limb cells cultured in media containing purmorphamine with or without FGF8 (Fig. 4.4A,B). In contrast, limb cells cultured in

media containing FGF8 alone did not show an induction of *Gli1* or *Ptch1* (Fig. 4.4A,B). We conclude that under our experimental conditions, limb bud cells cultured in purmorphamine either with or without FGF8 elicit similar activation of the Hh pathway.

We then examined the response of a broader group of Shh target genes: *HoxD13*, *Grem1*, *Jag1*, and *Hand2* (Chiang et al., 2001; Panman et al., 2006; Vokes et al., 2008; Benazet et al., 2009). Two genes, *Jag1* and *HoxD13*, were upregulated in response to Hh signaling while *Grem1* and *Hand2* did not show a strong upregulation in either cultures treated with purmorphamine or FGF8 and purmorphamine (Fig. 4.4C-F). A plausible explanation for the lack of Hh-responsiveness observed for *Grem1* is that in contrast to *HoxD13*, *Grem1* has an early and transient requirement for Shh signaling (Panman et al., 2006). *Shh* is expressed in E10.5 limb buds; therefore, this results in the prior activation of these genes before the limb cells are cultured. Taken together, our results suggest that determining the endogenous response of many Shh targets is limited in our current system using E10.5 limb buds (see Summary).

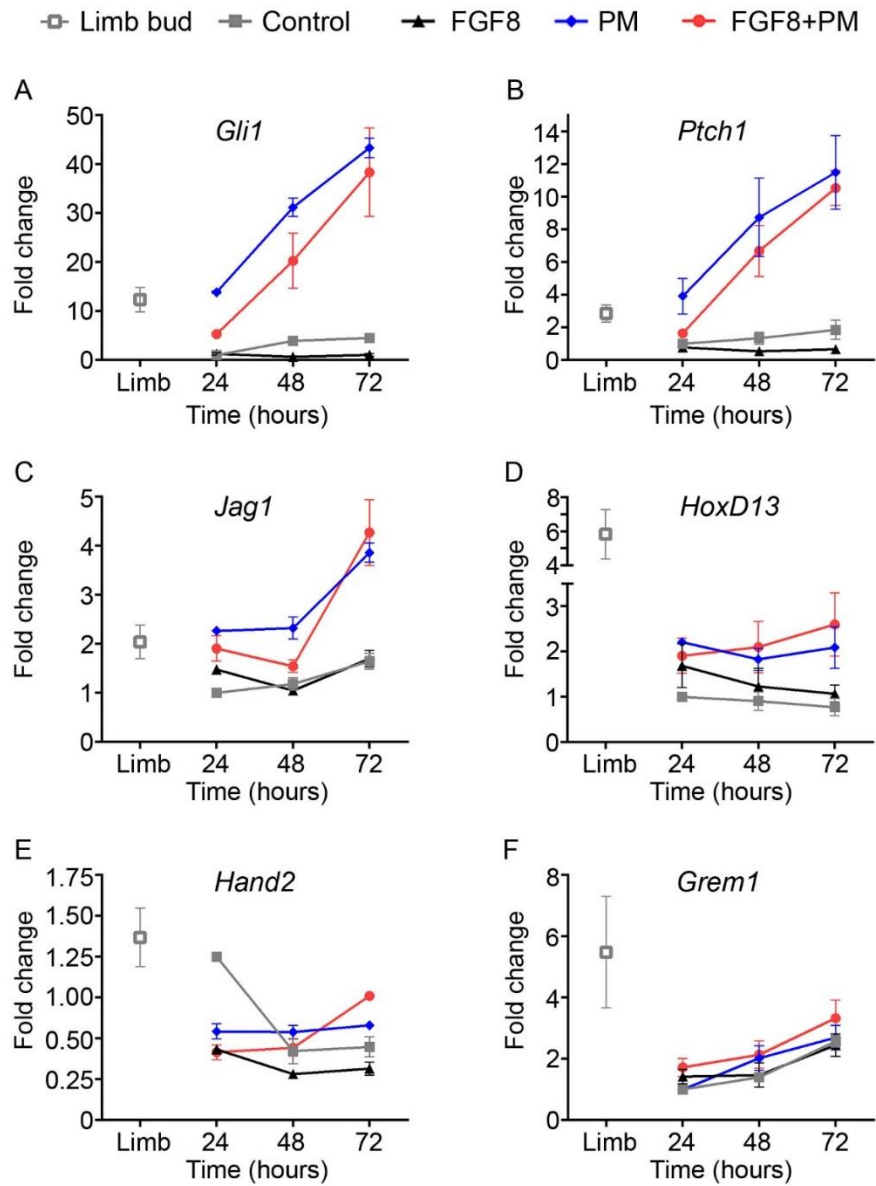


Figure 4.4: Regulation of Shh target genes in primary limb bud cultures. (A-F) qRT-PCR for Shh target genes at 24, 48, and 72 hours. Shh pathway target genes, *Gli1* (A) and *Ptch1* (B) are expressed at high levels in media containing purmorphamine (PM) and media containing both FGF8 and PM. Shh target genes, *Jag1* (C) and *HoxD13* (D), are upregulated in cultures with PM and both PM and FGF8. *Hand2* (E) and *Grem1* (F) do not show a strong upregulation with PM or both PM and FGF8. Gene expression is normalized to *Gapdh* in the control sample at 24 hours, and comparison to freshly isolated limb cells is shown with a gray open square. Data points are the mean of 3 independent experiments and error bars represent the standard error of the mean.

4.6: DELIVERING PLASMIDS AND siRNA INTO LIMB CELL CULTURES

Next, we sought to optimize conditions for delivering nucleic acids into cultured limb cells. Ideally, we wanted to deliver both plasmids and siRNA at high efficiency using low cell numbers, which would allow this system to be used in a medium-throughput format (Fig. 4.5A). We utilized a 96-well electroporation device (Lonza) and optimized conditions, determining the electroporation efficiency by flow cytometry. Under our standard conditions, greater than 90% of cells were successfully electroporated with plasmids or siRNAs (Fig. 4.5B).

After establishing conditions for DNA and RNA delivery, we attempted to manipulate gene expression in limb cells cultured in media containing FGF8 and purmorphamine. We first tested a *Gapdh* siRNA and quantified the level of mRNA knockdown at 24, 48, and 72 hours. Compared to cells electroporated with control siRNA, *Gapdh* was reduced 66% at 24 hours, 54% at 48 hours, and 56% at 72 hours at all time points (Fig. 4.5C). We then attempted to knockdown *HoxD13* and *Cdk6*. We chose these genes because they are regulated by Shh signaling, and are expressed in the posterior distal limb (te Welscher et al., 2002; Panman et al., 2006; Lopez-Rios et al., 2012). Compared to cells electroporated with control siRNA, *HoxD13* was reduced 64%, and *Cdk6* was reduced 80% (Figs. 4.5D,E). The expression of additional genes such as *Tbp*, *Hoxa13*, and *Jag1* were unchanged in *HoxD13* and *Cdk6* siRNA cultures (data not shown). We conclude that, in this system, both plasmids and siRNAs can be delivered in a highly efficient manner. Because the electroporation is performed in a 96-well format, this method can easily be scaled to accommodate higher-throughput assays.

After modulating gene expression levels, we sought to determine if this culture system could be used to assay the activity of DNA regulatory elements (promoters or enhancers). To test this, we utilized a well-established Hh responsive promoter for the *Patched* gene in *Drosophila melanogaster*. This element has been used to measure Hh responsiveness in both *Drosophila* and mammalian cells when placed upstream of a firefly luciferase reporter gene (Nybakken et al., 2005; Yuen et al., 2006; Vokes et al., 2007). We modified this construct by placing the promoter element upstream of a codon-optimized *Gaussia* luciferase gene (dPtc-GLuc). We used this reporter because it is more sensitive than firefly luciferase, and because it is secreted into the media, allowing the same sample to be assayed at multiple time points (Tannous et al., 2005). The dPtc-GLuc construct was electroporated into limb cells and half of the cells were cultured in control media (FGF8 alone), and the other half were cultured in media containing FGF8 and purmorphamine. dPtc-GLuc stimulated a 6.9 fold increase in reporter activity in limb cells cultured in FGF8 and purmorphamine media compared to cells cultured in control media (FGF8 alone) (Fig. 4.5F). We conclude that this limb cell culture method can be used to test DNA regulatory element activity mediated by the Hh signaling pathway. With minor adaptations, this system should be applicable to test the activity of DNA regulatory elements in a variety of different contexts.

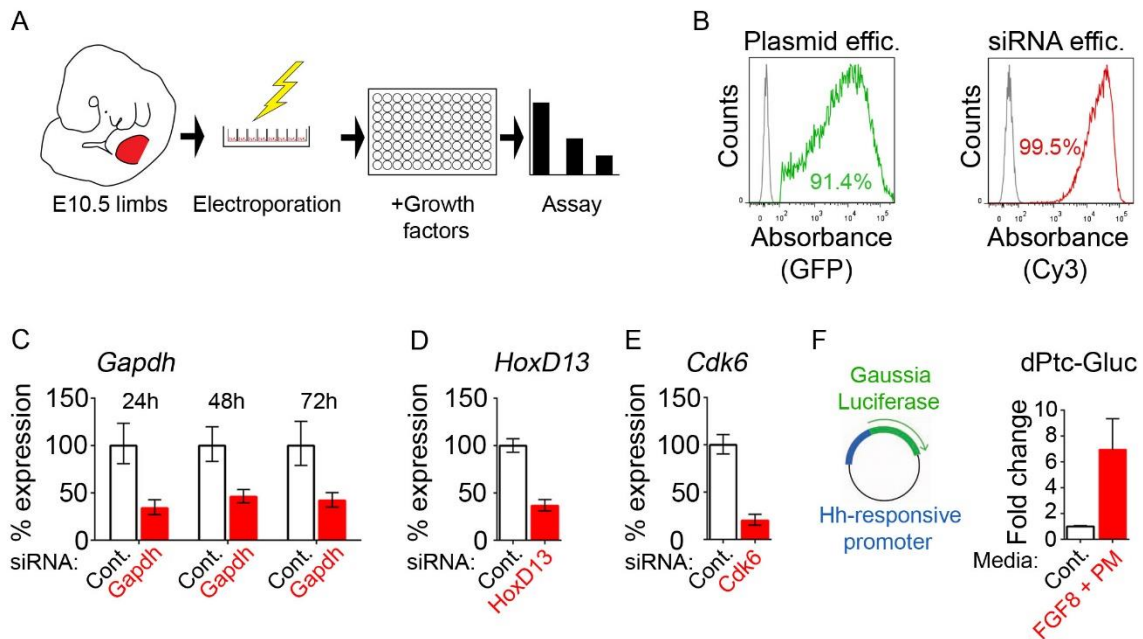


Figure 4.5: Method to efficiently deliver plasmids and siRNAs into primary limb bud cells in culture. (A) Illustration of delivering DNA/siRNA into cultured limb bud cells. E10.5 mouse forelimbs (red) are dissected, and limb cells are electroporated with plasmids or siRNA. Limb cells are then plated on a 96-well half area plate, cultured, and assayed (qRT-PCR or *Gaussia* luciferase). (B) Flow cytometry histograms showing a 91.4% efficiency of electroporating plasmids (green) and 99.5% efficiency for siRNA (red) relative to the control (gray). (C-E) qRT-PCR showing gene expression in cultures electroporated with either a gene-specific siRNA or control siRNA. Gene expression is normalized to *Gapdh* in the control sample for each time point. Limb bud cells electroporated with *Gapdh* siRNA show *Gapdh* knockdown at 24, 48, and 72 hours post-electroporation (C). *HoxD13* and *Cdk6* siRNA knockdown shown at 24 post-electroporation (D,E). Normalized *Gaussia* luciferase expression of a Hh responsive element (dPtc-GLuc) in media containing FGF8 only (control) or FGF8 and purmorphamine (PM) (F). Data points are the mean of 3 independent experiments and error bars represent the standard error of the mean.

4.7: DISCUSSION

This report provides methods for culturing relatively low numbers of mouse limb bud cells and electroporating plasmids and siRNAs. In an average experiment, we obtain

approximately 4.45 million forelimb cells per litter of mice, producing approximately 10 wells of cells (from 5 electroporations). We routinely pool several litters, providing material for dozens of potential parameters in a single experiment. Therefore, this method should enable medium-throughput assays involving DNA regulatory elements and gene manipulation that were not previously feasible. Furthermore, the ability to manipulate Shh-target genes suggests that it is possible to use this system to investigate Shh-mediated gene regulatory networks, and that this method could be adapted to investigate responses of other signaling networks present in the limb bud.

Despite these advances, there are a number of limitations to this *in vitro* system. In cultured limb cells, the multiple cross-regulatory interactions that occur between limb ectoderm and mesenchyme are no longer maintained. In their absence, there is a rapid downregulation of Shh activity (Honig, 1983; Anderson et al., 1993; Laufer et al., 1994; Niswander et al., 1994). By adding purmorphamine (Hh pathway activator) and FGF8, we short-circuit this loop but lose the information conferred by spatially and temporally regulated signaling. A second limitation is that many Shh-responsive genes could have inputs from additional signaling pathways that are not present in our culture conditions. For instance, WNT3a synergizes with FGF8 to maintain limb bud cells in a proliferative, undifferentiated state (ten Berge et al., 2008). However, we did not add WNT3a to the culture media when assaying for Hh-responsiveness because we were concerned about potential cross-talk between the Hh and Wnt pathways. Ectodermally secreted WNTs are important for several facets of limb development (reviewed in (Rabinowitz and Vokes,

2012)), and in future experiments it would be interesting to determine their effects on this culture system.

A caveat of using E10.5 limb buds in this culture system is that they have undergone some degree of specification. Previous work in chick has indicated that similar culture conditions are insufficient to reverse the specification of distal cells already committed to a distal fate (Cooper et al., 2011). These results provide a possible explanation for the presence of the chondrogenic marker, *Sox9*, because it is already expressed in the limb bud when the tissue is harvested (Fig. 4.1E). However, the lack of further differentiation is indicated by the near absence of Alcian blue or *Agc1* (Fig. 4.1C,D,F). In addition, many Shh target genes are only responsive to Shh during a transient time period (Panman et al., 2006; Zhu et al., 2008). This provides a potential explanation for why we detect a modest induction of *HoxD13* and *Jag1*, distal markers that remain Shh-responsive until at least E10.75 (Panman et al., 2006) but do not detect Hh-mediated upregulation of *Grem1* and *Hand2* (Fig 4.4).

These caveats would likely be circumvented using limb bud cells obtained from earlier stage embryos or from *Shh*^{-/-} embryos. Both of these are straightforward to implement, but would result in a large reduction in experimental material, limiting the utility for higher-throughput approaches. In future studies, we can imagine variations on this technique that utilize limb bud cells obtained from multiple genetic backgrounds. These methods could also be adapted to microfluidic-based approaches, allowing for reductions in required cell number while increasing the number of experimental parameters.

Chapter 5: Future directions and concluding remarks

In this work, the previous chapters present evidence that GLI-target genes cluster into three distinct domains within the SHH responsive region in the developing mouse limb. In addition, GLI-target genes have distinct requirements for SHH signaling, and SP1 acts as a factor to maintain gene expression for a cohort of GLI target genes (Chapter 2). Also shown, a GLI-bound CRM functions as a silencer in the anterior limb to robustly repress *Grem1* (Chapter 3). And lastly, I demonstrate a medium-throughput platform to culture mouse limb bud cells in order to manipulate gene expression and test the activity of DNA regulatory elements (Chapter 4).

5.1: MECHANISMS MEDIATING A TEMPORAL HEDGEHOG RESPONSE

The data presented in Chapter 2 show that GLI target genes have different temporal requirements for SHH signaling. Interestingly, the expression pattern of GLI target genes correlate with the different temporal activities. Genes that require only an initial SHH signaling input are found in the central (category 2) and posterior-proximal (category 3) domains in the limb. Subsequently, we demonstrate that SP1 acts to maintain gene expression for a subset of GLI target genes. While this work begins to explore how GLI target genes are maintained, several outstanding questions remain: Does SP1 maintain GLI target genes in other HH regulated tissues? What molecular mechanisms are employed to maintain GLI target genes? Are there additional factors involved in mediating GLI target gene expression?

HH signaling regulates the development of several embryonic tissues. Another well-established system used to study HH signaling is the developing neural tube. Since

Sp1 is expressed in essentially all cell types, albeit at variable levels, it would be interesting to determine if SP1 maintains the expression of GLI target genes in the neural tube (Saffer et al., 1991). Interestingly, previous work identified a GC-rich Sp1 motif in neural GLI-bound cis-regulatory modules (Vokes et al., 2007). Further testing this hypothesis could be approached *in vivo* using a Sp1 conditional knockout allele; this approach could be applied to the mouse limb bud as well.

The molecular mechanisms utilized to maintain transcription of GLI target genes are not well understood. Since Sp1 has been previously shown to mediate the interaction between distal regulatory elements with proximal promoters (Deshane et al., 2010; Su et al., 1991), it is worth investigating if such a mechanism is utilized to maintain the expression of GLI target genes. As proposed in the model in Chapter 2, SP1 maintains chromatin interactions for a cohort of GLI-target genes. Further studies using 4C or Hi-C techniques to uncover the chromatin interactions around GLI target genes under wild-type, Shh-deficient, and Sp1-deficient conditions would clarify the functions for these factors.

Lastly, much work in the neural tube has uncovered roles for several additional factors (SoxB1, Sox2, and Nkx2.2) that are involved in mediating a HH transcriptional response (Oosterveen et al., 2012; Oosterveen et al., 2013; Peterson et al., 2012; Lek et al., 2010). It is interesting to speculate that there are additional factors involved in mediating a HH response in the developing limb. In this work (Chapter 2), DNA motif analysis for GLI-bound regions uncovered several novel sequences which do not correspond to a known transcription factor. Future studies using a DNA mutational approach are necessary to determine their contribution, if any, to regulate the activity of GLI-bound CRMs. Furthermore, determining the factors that bind to the novel DNA motifs would likely lead to the identification of domain specific co-factors for GLI-bound CRMs.

5.2: HOW DOES FGF INTEGRATE WITH SHH TO REGULATE GLI-TARGETS?

The SHH-GREM1-FGF signaling loop is critical to drive limb outgrowth and patterning during development (Fig. 1.2) (Khokha et al., 2003; Litingtung et al., 2002; Michos et al., 2004; te Welscher et al., 2002; Zuniga et al., 1999). The integration of the SHH and FGF signaling pathways to co-regulate a group of GLI-target genes is poorly understood. In this work (Chapter 2), the expression of a subset of GLI target genes was determined after inhibition of FGF signaling. While the majority of GLI target genes were unchanged, interestingly, a group of GLI target genes were also downregulated or upregulated (Fig. 2.6). The data indicate that a cohort of GLI target genes are reciprocally regulated by FGF signaling.

Several genes including: *Grem1*, *Osr2*, *Rasgef1b*, *Smoc1*, *Fam181b* showed an increase in expression after FGF inhibition (Fig. 2.11). Interestingly, in wild-type limbs, these genes show expression patterns that are mostly restricted from the distal mesenchyme (Fig 2.2). Previous studies (and this work) demonstrate that inhibiting FGF signaling causes *Grem1* to expand into the anterior-distal mesenchyme (Fig 3.6) (Verheyden and Sun, 2008). This raises the possibility that FGF signaling represses a larger cohort of GLI target genes from the distal mesenchyme. Further studies require determining how the gene expression domain changes after FGF inhibition.

Moreover, the molecular mechanisms mediating distal repression of GLI-target genes are unknown. Evidence from this work demonstrate that FGF signaling does not repress *Grem1* expression through the GLI-bound CRM, GRE1 (Fig. 3.6), suggesting that FGF mediates repression through distinct CRMs. Further studies to determine the CRMs which integrate FGF signaling to mediate repression of GLI target genes in the distal mesenchyme will highlight the integration of the SHH and FGF signaling pathways to sculpt gene expression domains.

5.3: DUAL FUNCTIONING GLI-BOUND CRMS

Digit asymmetry in the developing limb is regulated by polarized gene expression. Recent work in the bovine limb demonstrates that the loss of polarized gene expression leads to a loss of digit asymmetry (Lopez-Rios et al., 2014). For mammals, including mouse and human, the asymmetric pentadactylous hand/foot is a key feature. As mentioned throughout this work, HH signaling drives asymmetric gene expression in the limb. In Chapter 3, the GLI-bound CRM, GRE1, was shown to robustly repress *Grem1* in the anterior-distal limb. In separate experiments using a mouse transgenic enhancer assay, GRE1 activated reporter expression, indicating that the element has enhancer activity. Taken together, GRE1 mainly functions as an anterior silencer element for *Grem1*, and GRE1's role as a bonafide enhancer needs clarification.

However, an outstanding question remains: Is it a general property of GLI-bound CRMs to function as dual silencers and enhancers? Many GLI target genes are associated with multiple GLI-bound CRMs. How these CRMs individually or collectively regulate the expression of a particular GLI target gene is not known. Several GLI target genes including *Hoxd13*, *Hoxd12*, and *Cdk6* have been shown to expand into the anterior limb (similar to *Grem1*) in Gli3-deficient limbs (Lopez-Rios et al., 2012). In this work (Chapter 2), an *in situ* hybridization screen identified a cohort of GLI target genes that are predominately expressed in the Shh responsive region in the limb. It would be interesting to determine if the gene expression boundaries for this group of GLI target genes are changed in Gli3-deficient limbs. Furthermore, additional studies determining the ability of the associated GLI-bound CRMs to enhance and/or silence gene expression would be required.

5.4: CONCLUDING REMARKS

The developing mouse limb bud is an excellent system to study a variety of biological processes including, signal transduction, transcriptional control, and cell dynamics. We are at the beginning stages of applying system-level experimental techniques in order to study these processes. Such approaches will provide much insight into how this multifaceted tissue grows and organizes during development.

Appendix A: GLI target gene expression patterns

This appendix contains data pertaining to the spatial distribution of GLI target genes discussed in Chapter 2.

A.1: SPATIAL DISTRIBUTION OF GLI TARGET GENES

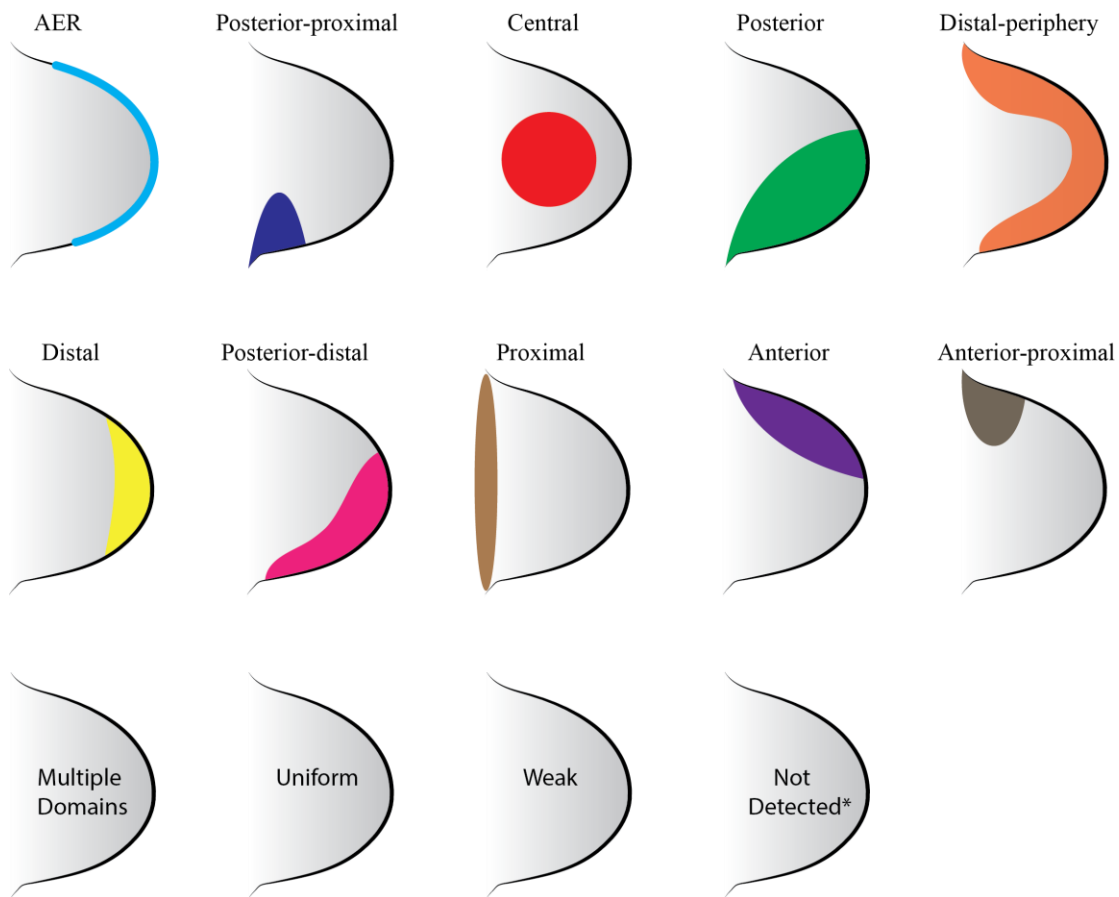


Figure A1: Schematized spatial distributions of GLI target genes in E10.5 mouse limb buds. Colored regions indicate areas where gene expression was observed. Multiple domains indicates at least 2 spatially unique expression domains; not detected indicates no expression detected and the asterisk indicates that expression was detected only later in E11.5 limbs for a subset of GLI target genes.

Gene name	Distribution
Cited4	AER
Dlx5	AER
Enpp1	AER
Fzd7	AER
Zic3	Anterior
Epha3	Anterior
Fam181b	Central
Ndnf	Central
Fam69c	Central
Cldn11	Central
Cldn9	Central
Fbxo41	Central
Fbxo8	Central
Hhip	Central
Osr2	Central
Smoc1	Central
Whrn	Central
Rspo3	Central
Clstn2	Distal
Arl6	Distal
Baz2b	Distal
Mpnd	Distal
Hoxd10	Distal
Igf1r	Distal
Lrrc20	Distal
Zfp933	Distal
Mnd1	Distal
Mrpl23	Distal
Olf91	Distal
Punc	Distal
Rgs19	Distal
Rspo4	Distal
Sall4	Distal
Shcbp1	Distal

Table A1: Classification of the spatial expression of GLI target genes in E10.5 mouse limb buds. Spatial categories indicated in the distribution column are schematized in Fig. A.1. Multiple domains indicates at least 2 spatially unique expression domains; not detected indicates no expression detected and the asterisk indicates that expression was detected only later in E11.5 limbs for a subset of GLI target genes.

Slc2a1	Distal
Smad7	Distal
Sp1	Distal
Srp19	Distal
Thap11	Distal
Trim62	Distal
Zfp64	Distal
Trp53rk	Distal
Pdpf	Distal-periphery
Aprt	Distal-periphery
Asf1a	Distal-periphery
Bmp4	Distal-periphery
Fndc3c1	Distal-periphery
Gpsn2	Distal-periphery
Grcc10	Distal-periphery
Id3	Distal-periphery
Ier5	Distal-periphery
Klf3	Distal-periphery
Med30	Distal-periphery
Arhgef3	Multi-domain
Bmp2	Multi-domain
Ebf3	Multi-domain
Efna1	Multi-domain
Kit	Multi-domain
Scube1	Multi-domain
Sfrp2	Multi-domain
Sulf1	Multi-domain
Tbx2	Multi-domain
Tbx3	Multi-domain
Tmem30b	Multi-domain
Ust	Multi-domain
Wnt11	Multi-domain
Hoxa7	Multi-domain
Galp	No probe
Ppnr	No probe
Nrarp	No probe
Tas2r119	No probe
Ube2v1	No probe
Zfp353	No probe

Table A1, cont.

Depdc7	Not detected embryo
9830107B12Rik	Not detected embryo
Ap1s2	Not detected embryo
Hccs	Not detected embryo
Jazf1	Not detected embryo
Popdc3	Not detected embryo
Prkce	Not detected embryo
Npvf	Not detected embryo
5430416O09Rik	Not detected limb
Apoa2	Not detected limb
Dcn	Not detected limb
Isl1	Not detected limb
Pqlc2	Not detected limb
Drd3	Not detected limb
Aldh1a2	Not detected limb*
Ednrb	Not detected limb*
Eomes	Not detected limb*
Igfbp7	Not detected limb*
Lum	Not detected limb*
Myl4	Not detected limb*
Pdlim	Not detected limb*
A130014H13Rik	Not detected limb*
A530021J07Rik	Not detected limb*
Atp6v1g3	Not detected limb*
Avpr2	Not detected limb*
Pax9	Not detected limb*
Gata5	Not detected limb*
Gli1	Posterior
Hand2	Posterior
Ptch1	Posterior
Ptch2	Posterior
Dock6	Posterior-distal
Calml4	Posterior-distal
Cdk6	Posterior-distal
Grem1	Posterior-distal
Hoxd11	Posterior-distal
Hoxd13	Posterior-distal
Ier2	Posterior-distal
Jag1	Posterior-distal

Table A1, cont.

Klf9	Posterior-distal
Msi2	Posterior-distal
Pam	Posterior-distal
Ralgps2	Posterior-distal
Rasgef1b	Posterior-distal
Sall1	Posterior-distal
Sall3	Posterior-distal
Sap30	Posterior-distal
Shroom3	Posterior-distal
Sox4	Posterior-distal
Tpd5211	Posterior-distal
Runx3	Posterior-distal
Adamts19	Posterior-proximal
Cntfr	Posterior-proximal
Col23a1	Posterior-proximal
Dlk1	Posterior-proximal
Ltbp1	Posterior-proximal
Lypd6	Posterior-proximal
Osr1	Posterior-proximal
Prdm1	Posterior-proximal
Svep1	Posterior-proximal
Pkdcc	Proximal
Bmpr1b	Proximal
Meis1	Proximal
Meis2	Proximal
Alx4	Proximal-anterior
Hoxb4	Proximal-anterior
Hoxc4	Proximal-anterior
Irx3	Proximal-anterior
Pax1	Proximal-anterior
Pbx1	Proximal-anterior
Ppp1r2	Uniform
Cdc42ep4	Uniform
Cobll1	Uniform
Creb5	Uniform
D16Ertd472e	Uniform
Efcab2	Uniform
Haghl	Uniform
Hmga1	Uniform
Kbtbd8	Uniform

Table A1, cont.

Ncor2	Uniform
Nfe2l3	Uniform
Ppp2r4	Uniform
Slc26a11	Uniform
Slc35c1	Uniform
Sparcl1	Uniform
Tbx4	Uniform
Tmem48	Uniform
Trim59	Uniform
Tct36	Uniform
Tmtc1	Uniform
Alg13	Uniform
Zmiz1	Uniform
Cyrr1	Weak
Foxf1a	Weak
Foxf2	Weak
Kcne3	Weak
Tcte3	Weak
2410187C16Rik	Weak
2610306H15Rik	Weak
3110043J09Rik	Weak
4921524J17Rik	Weak
4930525K10Rik	Weak
Cd302	Weak
Cxxc4	Weak
E130309F12Rik	Weak
Hook1	Weak
Inha	Weak
Maml3	Weak
Mgmt	Weak
Pmch	Weak
Polr2k	Weak
Prokr2	Weak
Pus7l	Weak
Ramp2	Weak
Sdk2	Weak
Slc24a6	Weak
Smo	Weak
Stxbp6	Weak

Table A1, cont.

Tank	Weak
Thap1	Weak
Tmem5	Weak
Tmepai	Weak
Ube2t	Weak
Xpnpep2	Weak
Zfp281	Weak
Zfp704	Weak
Tctex1d2	Weak
Frmd8	Weak
Trmt10c	Weak
Smug1	Weak
Tpcn1	Weak
Xpa	Weak

Table A1, cont.

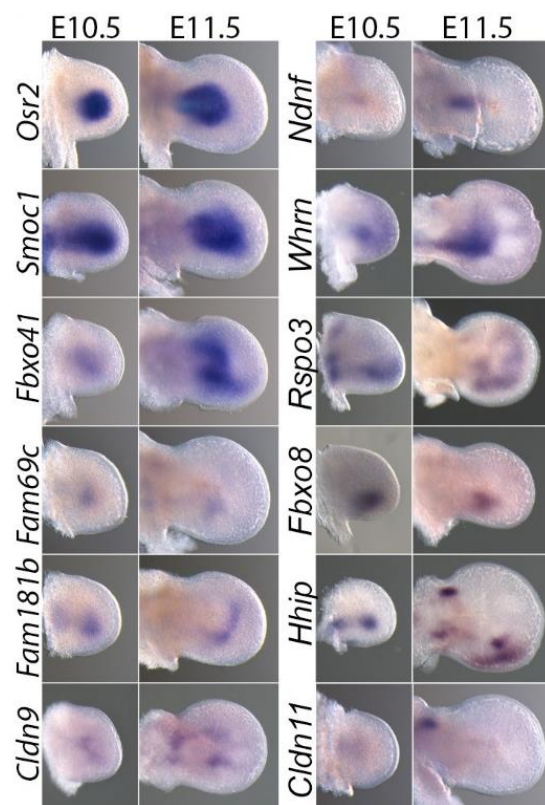


Figure A3: Category 2 (central) gene expression patterns in E10.5 and E11.5 mouse forelimbs.

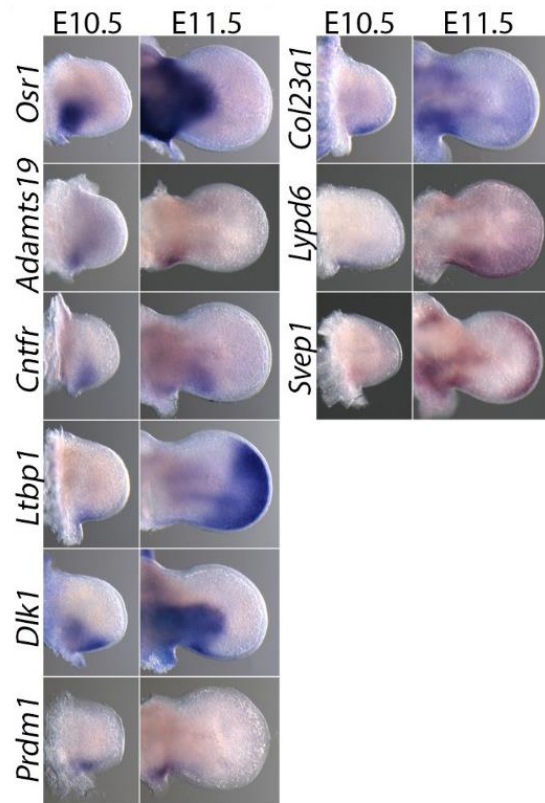


Figure A4: Category 3 (posterior-proximal) gene expression patterns in E10.5 and E11.5 mouse forelimbs.

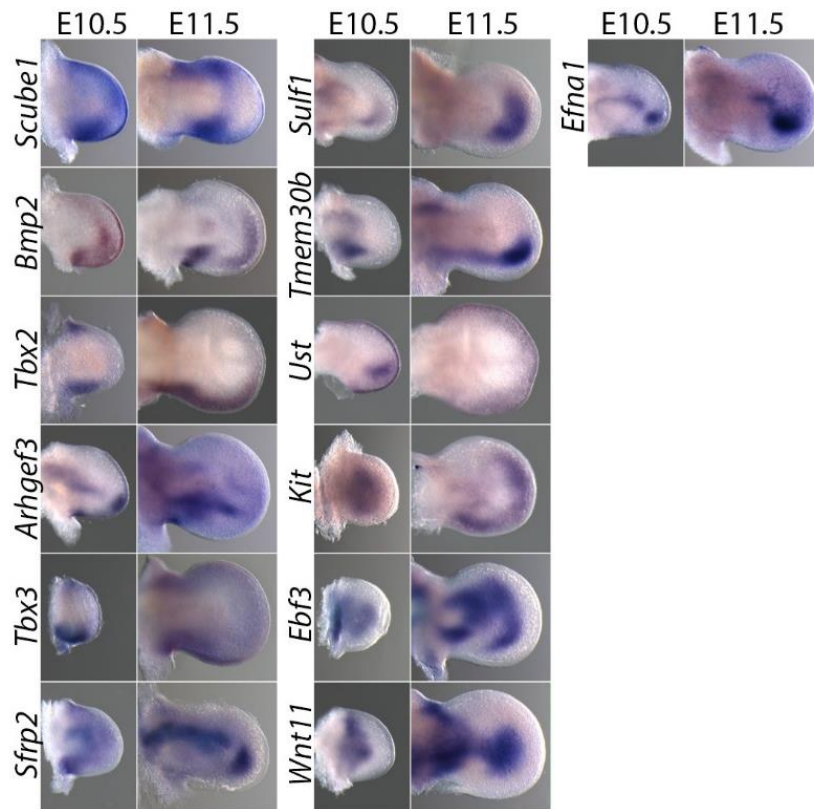


Figure A5: Multiple domain gene expression group in E10.5 and E11.5 mouse forelimbs

Appendix B: RNAseq

This appendix contains gene expression data generated from the RNAseq experiments discussed in Chapter 1. The methods used to analyze this data can be found in Appendix C.

B.1: DIFFERENTIALLY EXPRESSED GENES IN CYCLOPAMINE TREATED LIMBS

Gene Symbol	FC log2	PValue	FDR
Gli1	-3.1436	1.14E-35	2.00E-31
Ptch2	-3.5246	1.86E-18	1.09E-14
Fgf4	-4.2379	3.53E-14	1.24E-10
Sall1	-1.2629	5.16E-14	1.51E-10
Fgf8	-1.6897	7.48E-13	1.88E-09
Mamdc2	-2.6636	1.19E-11	2.32E-08
Ptch1	-1.4175	6.48E-11	1.14E-07
Hoxd12	-1.3554	5.21E-10	8.32E-07
Ina	-8.1995	8.78E-10	1.29E-06
A930011O12Rik	-5.4016	9.10E-09	1.23E-05
Elavl3	-2.7694	4.29E-08	4.73E-05
Stmn2	-2.2772	4.31E-08	4.73E-05
Tubb3	-1.909	4.26E-08	4.73E-05
Myt1	-4.2316	5.08E-08	5.25E-05
Thy1	-2.8683	8.10E-08	7.49E-05
Ano1	-1.3849	7.96E-08	7.49E-05
Hsd11b2	-1.1627	1.09E-07	9.11E-05
Greb1	-0.9356	1.40E-07	0.00011
Nhlh2	-3.2223	3.09E-07	0.00023

Table B1: Cyclopamine RNAseq. Genes downregulated ($\geq 25\%$, 0.1% FDR) in E10.25 mouse forelimbs cultured in the presence of cyclopamine, a Hh pathway inhibitor. Log2 expression is shown. Genes sorted by the false discovery rate (FDR).

Hoxd13	-1.0851	2.97E-07	0.00023
Sall3	-0.947	3.27E-07	0.00023
Rfx4	-4.5236	3.51E-07	0.00024
Nhlh1	-5.1715	5.99E-07	0.00039
Msi2	-0.8364	6.52E-07	0.00041
Msx3	-4.3918	7.76E-07	0.00047
Frem1	-0.9955	8.53E-07	0.0005
Robo3	-4.4424	1.10E-06	0.00062
Cntn2	-1.5186	1.90E-06	0.00104
Aox3	-2.0027	2.04E-06	0.00105
Mtus1	-1.1243	2.14E-06	0.00107
Pou3f2	-3.1676	2.25E-06	0.0011
Fabp7	-3.6102	2.47E-06	0.00117
Neurod4	-7.0957	2.97E-06	0.00137
Enpp2	-1.1723	3.78E-06	0.0017
Grem1	-0.891	4.28E-06	0.00188
Miat	-1.8729	4.45E-06	0.00191
Car12	-0.8459	6.17E-06	0.00252
Slc17a6	-6.7562	1.19E-05	0.00426
Scrt2	-4.1805	1.22E-05	0.00426
Sox2	-3.3159	1.12E-05	0.00426
Sost	-1.5847	1.18E-05	0.00426
Hoxd11	-0.9075	1.21E-05	0.00426
Kdm5d	-0.9009	1.19E-05	0.00426
Chrna3	-3.7603	1.60E-05	0.00542
Chl1	-2.1129	1.81E-05	0.00599
Akap6	-2.013	1.87E-05	0.0061
Slc1a2	-1.8176	2.22E-05	0.00697
Srrm4	-2.6922	2.42E-05	0.00745
Cdk6	-0.9908	2.86E-05	0.00837
Tfap2c	-0.8318	3.42E-05	0.00969
Scg3	-4.6185	3.92E-05	0.01076
Zic1	-3.4593	4.49E-05	0.01212
Ccnd1	-0.7107	6.10E-05	0.01599
Ppp2r2c	-2.6222	6.22E-05	0.01608
Pappa2	-1.4931	6.70E-05	0.01706
Apcdd1	-0.6731	7.20E-05	0.01808
Olig3	-6.5397	7.91E-05	0.01957

Table B1, cont.

Dock6	-0.6647	0.00012	0.02918
Lmo2	-0.8597	0.00015	0.03615
Elavl4	-1.4405	0.00017	0.03893
Gja8	-3.5064	0.00018	0.04081
Zic4	-4.0419	0.00024	0.05122
Neurog2	-6.5028	0.00027	0.05692
Sst	-3.5554	0.00029	0.06
Cln6	-0.7028	0.00029	0.06
Spry4	-0.62	0.00031	0.06432
Wnt10b	-1.9916	0.00037	0.07401
Uty	-0.8006	0.00038	0.07401
Has2	-0.719	0.00042	0.08114
Slc4a4	-0.7958	0.00044	0.08181
Prtg	-0.6674	0.00044	0.08181
Lhx1	-2.839	0.00049	0.08947
Pax6	-2.5219	0.0005	0.09009
Gsx1	-6.1242	0.00054	0.09632
Stac	-2.6579	0.00057	0.09928

Table B1, cont.

B.2: DIFFERENTIALLY EXPRESSED GENES IN SHH-DEFICIENT LIMBS

Gene name	logFC	PValue	FDR
Hoxd13	-6.009669587	2.52E-108	4.46E-104
Hoxd12	-6.554686341	1.77E-104	1.57E-100
Gli1	-5.714119311	5.46E-71	2.42E-67
Hist1h2ab	-2.522446436	1.32E-60	4.66E-57
Fgf4	-6.905818531	1.11E-56	3.29E-53
Hoxd11	-2.509735373	1.53E-52	3.86E-49
Grem1	-2.626013966	5.69E-45	1.26E-41
Ptch1	-2.367971302	5.43E-37	1.07E-33
Ptch2	-4.409820957	6.34E-37	1.12E-33
Frem1	-1.813423967	3.50E-35	5.64E-32
Hand2	-2.155543855	3.16E-33	4.67E-30
Sall1	-1.904572443	3.95E-30	5.38E-27
Osr2	-4.00904607	5.02E-30	6.35E-27
Mamdc2	-3.736843977	3.48E-28	4.11E-25
Hoxa13	-4.641746714	1.97E-26	2.18E-23
Ddx3y	-1.471171848	2.59E-26	2.70E-23
Eif2s3y	-1.52010606	2.48E-23	2.44E-20
AI506816	-1.725998004	3.81E-23	3.55E-20
Rasgef1b	-1.444915572	3.08E-19	2.48E-16
Ccnd1	-1.180154143	1.30E-18	1.00E-15
Aox3	-3.356518399	2.49E-18	1.76E-15
Cbln1	-1.686346572	2.93E-18	2.00E-15
Hey1	-1.317992716	4.73E-18	3.11E-15
Kdm5d	-1.375969559	1.53E-16	9.36E-14
Sall3	-1.787394806	4.93E-16	2.91E-13
Uty	-1.497976371	1.41E-15	8.07E-13
Hhip	-2.995924586	2.71E-15	1.46E-12
Cdk6	-1.612728183	2.82E-15	1.47E-12
Scn11a	-5.742201227	2.67E-14	1.28E-11
Rspo3	-1.285191713	2.68E-14	1.28E-11
Tpd52l1	-1.55839175	8.20E-14	3.63E-11
Cpa2	-1.346326115	5.43E-13	2.29E-10
5730457N03Rik	-3.016163876	9.06E-13	3.70E-10

Table B2: Genes downregulated ($\geq 25\%$, 0.1% FDR) in *Shh*^{-/-} E10.25 mouse forelimbs. Log₂ expression is shown. Gene expression sorted by false discovery rate (FDR).

Msi2	-0.947297051	1.05E-12	4.12E-10
Pam	-1.014214849	1.31E-12	5.04E-10
Socs2	-1.105952356	1.39E-12	5.25E-10
Nid1	-0.972989446	1.99E-12	7.33E-10
1300002K09Rik	-3.801442176	2.34E-12	8.47E-10
Itga8	-1.168491418	5.24E-12	1.82E-09
Mid1ip1	-1.542303715	1.01E-11	3.44E-09
Hoxa11as	-1.118485568	1.44E-11	4.72E-09
Cyp26b1	-0.952961447	1.57E-11	5.06E-09
Gpt2	-0.888039192	2.45E-11	7.76E-09
Cyp1b1	-1.347183489	3.23E-11	9.69E-09
Sgms2	-2.052733554	5.40E-11	1.57E-08
Shh	-1.790774934	6.58E-11	1.88E-08
Gbx2	-2.118878938	1.16E-10	3.22E-08
Ppp2r2c	-2.985081511	1.36E-10	3.70E-08
Hoxd10	-0.904859269	1.58E-10	4.23E-08
Eogt	-0.897337773	1.66E-10	4.39E-08
Rnd3	-0.835057295	2.11E-10	5.42E-08
Cpm	-1.003094513	2.40E-10	5.98E-08
Gpx2	-2.624989208	3.29E-10	8.03E-08
Enpp2	-1.163546063	4.27E-10	1.02E-07
Bcat1	-0.851042728	5.37E-10	1.27E-07
Frzb	-0.810370728	1.16E-09	2.63E-07
Fgf8	-1.731682449	1.55E-09	3.43E-07
Ntm	-2.280540742	2.24E-09	4.83E-07
Hsd11b2	-1.242478795	3.34E-09	7.05E-07
Smoc1	-1.432903526	4.59E-09	9.46E-07
Emb	-0.791508169	5.25E-09	1.07E-06
Cmah	-0.917201795	6.48E-09	1.30E-06
Wnt5a	-0.743973753	1.34E-08	2.55E-06
Pou4f1	-3.21530322	1.59E-08	2.99E-06
Fgf9	-1.85862692	2.75E-08	4.87E-06
Naaa	-1.278812552	3.08E-08	5.30E-06
Calml4	-2.224692749	3.69E-08	6.23E-06
Adamtsl2	-1.675004396	5.29E-08	8.39E-06
Spry4	-0.951162092	5.30E-08	8.39E-06
Sall4	-1.17052878	8.36E-08	1.28E-05
Osr1	-1.390562319	1.09E-07	1.60E-05

Table B2, cont.

Fgf10	-0.931807163	1.15E-07	1.69E-05
Dusp4	-0.778148895	1.68E-07	2.39E-05
Has2	-0.816115205	1.97E-07	2.70E-05
Gldc	-0.987696501	2.18E-07	2.93E-05
Jag1	-0.860090694	2.81E-07	3.68E-05
Kbtbd8	-0.779968648	4.01E-07	5.11E-05
Tmem173	-0.859456044	4.21E-07	5.33E-05
Prdm1	-1.147649933	4.29E-07	5.39E-05
D7Ert715e	-0.898788472	4.63E-07	5.73E-05
Pdlim3	-2.370038864	4.78E-07	5.88E-05
Gucy2c	-3.13947821	5.08E-07	6.21E-05
Mtus1	-0.918797186	5.46E-07	6.58E-05
Evx1	-2.452171405	5.81E-07	6.96E-05
Fst	-1.744048492	6.68E-07	7.84E-05
Shisa2	-0.984808516	7.43E-07	8.54E-05
Gcnt4	-1.936118071	8.66E-07	9.90E-05
Mthfd2	-0.686460798	9.48E-07	0.000106916
Olfm1	-0.723972274	1.25E-06	0.000136226
Dkk4	-4.6027019	1.59E-06	0.000169152
Cxxc4	-1.106765871	1.73E-06	0.000182901
Lmo2	-0.92726587	1.77E-06	0.00018599
Chl1	-1.323889863	1.87E-06	0.000192371
Slc1a4	-0.749582312	2.02E-06	0.000207
Megf10	-1.853046266	2.04E-06	0.00020731
Evx2	-7.150867391	2.39E-06	0.000241658
Serinc5	-0.741506458	2.67E-06	0.000264634
Pmaip1	-0.623152515	2.74E-06	0.000270038
Lmo1	-0.816799218	3.37E-06	0.00032092
C1galt1	-0.685904459	3.57E-06	0.000338131
Arid3a	-0.67980241	3.59E-06	0.000338458
Sost	-1.042115707	3.96E-06	0.000368009
Hoxa10	-0.625854558	3.98E-06	0.000368009
Map1b	-0.748357994	4.43E-06	0.000402801
Lypd6	-1.266670047	5.10E-06	0.00044728
Lin28b	-0.686086908	5.48E-06	0.000475927
Tubb6	-0.761249881	5.96E-06	0.000506487
Cirh1a	-0.590270957	6.56E-06	0.000553117
Bcl2	-0.802325613	6.59E-06	0.000553221

Table B2, cont.

Cd24a	-0.625899016	6.71E-06	0.000560408
Scd1	-0.57749676	1.02E-05	0.000809596
Slc8a3	-1.344553435	1.07E-05	0.000838903
Phlda1	-1.238688622	1.08E-05	0.00084851
Chrna1	-1.298865837	1.20E-05	0.00092947
Kcne3	-0.942221043	1.22E-05	0.00093485
Taf4b	-0.752382738	1.30E-05	0.000985419
Chrdl1	-0.802811101	1.33E-05	0.001003821
Rcsd1	-0.880169045	1.55E-05	0.001143453
Slc1a5	-0.655696176	1.54E-05	0.001143453
Fam46a	-1.233790281	1.88E-05	0.001358131
Rragd	-0.595782288	2.08E-05	0.001472679
Gad1	-2.992703067	2.40E-05	0.00165534
Gnai1	-0.658257815	2.41E-05	0.001656504
Hprt	-0.557934392	3.17E-05	0.002125197
Gnb4	-0.696119345	3.38E-05	0.002247442
Shisa3	-1.140989621	3.64E-05	0.002395829
Trim71	-0.674894981	3.85E-05	0.002526494
Syndig1	-1.951813826	4.06E-05	0.002632976
Rprml	-3.988427265	4.10E-05	0.002653198
Nlrp1a	-0.809881116	4.18E-05	0.002692624
Tagln2	-0.622920319	5.22E-05	0.003278901
Rab34	-0.59094049	5.27E-05	0.003297158
Slc35d3	-1.706511645	6.01E-05	0.003719237
Srms	-1.626142155	6.30E-05	0.003871492
Calm1	-0.568741463	6.37E-05	0.00388916
Fbxo8	-0.684093415	6.54E-05	0.003967622
Nrp2	-0.512300244	6.59E-05	0.00398594
Gpd1l	-0.591423816	6.73E-05	0.00404333
Ets2	-0.527706077	6.93E-05	0.004119801
Vwde	-1.123167311	7.27E-05	0.004276961
Sv2b	-2.277281716	8.69E-05	0.004859928
Atp1a2	-1.234979022	8.75E-05	0.004859928
Krt23	-2.114121661	9.35E-05	0.005124856
Mir17hg	-0.502319928	9.32E-05	0.005124856
Alg13	-0.589952744	9.51E-05	0.005188183
Fdps	-0.516132208	0.000101431	0.005477264
Mycn	-0.666281579	0.000110351	0.0058695

Table B2, cont.

Fam19a4	-2.283954704	0.000115718	0.006079054
Timm23	-0.547997657	0.000119462	0.00620501
Prdx6	-0.48649853	0.000119125	0.00620501
Padi3	-0.977858633	0.000121517	0.006274264
Irs1	-0.577999103	0.000121858	0.006274264
Galnt11	-0.54667955	0.000127502	0.006508124
Acsl4	-0.56455966	0.000137118	0.006958829
Rgag1	-2.561093987	0.000147703	0.007321847
Eda2r	-1.043021118	0.000161221	0.007886451
Cdc6	-0.488957959	0.000163623	0.007961801
Hs3st6	-1.892636241	0.000167334	0.008072866
Lbh	-0.498016106	0.000167971	0.008072866
Dusp6	-0.481423932	0.000172756	0.00826986
Rasl11a	-0.674872162	0.000188063	0.008930202
Larp4	-0.494060794	0.000187863	0.008930202
Cxcl12	-0.579187695	0.000191837	0.009085076
Ddx39	-0.473808082	0.000203044	0.009564647
Mfsd2a	-0.707926058	0.000210512	0.009863982
Tmem256	-0.699658621	0.000214984	0.009968031
Vcan	-0.499029708	0.000223718	0.010290244
Nop2	-0.473140404	0.000228933	0.010450666
Gja3	-0.986530151	0.000232246	0.010574655
Rbm20	-1.271339359	0.000244245	0.011065397
Ctps	-0.472975647	0.000248862	0.011215871
Esm1	-1.00359957	0.000250078	0.011242085
Heatr1	-0.488002295	0.000254202	0.0113856
Itm2a	-0.469152123	0.000263475	0.011666655
Sc4mol	-0.535578084	0.000269397	0.011899146
Sdad1	-0.518043637	0.000278058	0.012190484
Fam64a	-0.642172209	0.00028394	0.012326326
Dusp9	-0.488070508	0.000283795	0.012326326
Itgav	-0.472228843	0.00028383	0.012326326
Hoxa11	-0.700269146	0.000291642	0.012598952
Hgf	-0.538773484	0.000293937	0.012667174
Cited1	-1.164737383	0.000298448	0.012799098
Abcc4	-0.92034169	0.000299166	0.012799098
Cnr1	-0.742910238	0.000307804	0.013105341
Sel1l3	-0.945135823	0.000322742	0.013578164

Table B2, cont.

Atp10d	-0.554395585	0.000365982	0.015075044
Gcat	-0.568564352	0.000378713	0.015527246
Dmrta1	-1.382612379	0.000385598	0.015773012
Ttn	-0.887027783	0.000392748	0.015883046
Hus1	-0.461410429	0.000391623	0.015883046
6030408B16Rik	-1.119576697	0.000400318	0.016145292
Hist1h3h	-0.713220512	0.00041708	0.016649876
Rpf2	-0.484962252	0.000417375	0.016649876
Tgm3	-2.10482046	0.000429102	0.016852005
Greb1	-0.598670964	0.000441152	0.017172948
T	-1.829507614	0.000446138	0.017328942
Otud4	-0.453523716	0.000453084	0.017407849
Edar	-0.775071378	0.000458027	0.017528292
Apln	-0.785434811	0.000472629	0.017982622
Col19a1	-1.278599372	0.000501282	0.018810804
Lama1	-0.518378013	0.000500824	0.018810804
Krt17	-1.27229783	0.000502463	0.018815258
Ccne1	-0.466893294	0.000507336	0.018917761
Hist1h2ag	-0.909862301	0.000516397	0.019110293
Lgalsl	-0.563555511	0.000521704	0.019227483
Ddx21	-0.464807776	0.000524327	0.019227483
Naf1	-0.63449942	0.000550961	0.020038224
Slc25a15	-0.514504009	0.000584293	0.021077388
Asns	-0.487096182	0.000597151	0.021453836
D16Ertd472e	-0.518056782	0.000603927	0.021566038
Mthfd1l	-0.496958233	0.000603166	0.021566038
Mthfd1	-0.457432829	0.000626285	0.022229968
Uroc1	-2.843087171	0.000665265	0.023300226
Pitrm1	-0.451410616	0.000666961	0.023300226
Nsmaf	-0.449564493	0.000673856	0.023448588
Prss12	-0.813978447	0.000679554	0.023529129
Sms	-0.435748316	0.000680156	0.023529129
Ppat	-0.452925956	0.000685728	0.023675671
Prss50	-2.433845106	0.000693845	0.023909307
Psat1	-0.473983579	0.00069846	0.024021608
Aimp2	-0.530540393	0.000704027	0.024166121
Pvt1	-0.80212056	0.000719171	0.024628091
Abce1	-0.477785812	0.000720266	0.024628091

Table B2, cont.

Cdk2ap1	-0.436609305	0.000725552	0.024761019
Polr1b	-0.454739707	0.000727678	0.024785834
Bhlha9	-0.740781135	0.000755278	0.025446434
Shmt1	-0.449163998	0.000752982	0.025446434
Zfp280c	-0.447474603	0.000761397	0.025541408
Nhp2	-0.524563465	0.00076825	0.025722589
Dhcr24	-0.475866043	0.000776327	0.025934798
Pdzd2	-0.84947475	0.000831249	0.027481521
Dleu7	-5.781440428	0.000851989	0.027997087
Prkg2	-1.098773242	0.000860304	0.028062838
Dctpp1	-0.535208265	0.000861912	0.028062838
Foxd2	-2.148944337	0.000868727	0.028204665
Tfap2c	-0.588590703	0.000879513	0.028204665
Arid3b	-0.510488492	0.000878588	0.028204665
lfrd1	-0.470317273	0.000877924	0.028204665
Fam60a	-0.452189062	0.000882192	0.028204665
Saa2	-3.239346694	0.000891591	0.028453799
Nolc1	-0.436447594	0.000893264	0.028455919
Insig1	-0.448413565	0.000924511	0.029136901
Slc7a6	-0.425431306	0.000953997	0.029853701
Cntfr	-0.79963146	0.00099514	0.030977027
Ppp6c	-0.443234178	0.001021541	0.03168744
Plcg2	-0.788930156	0.00104449	0.032118065
Mif	-0.449104377	0.001053285	0.032276452
8430423G03Rik	-3.690091251	0.001071025	0.032760177
Man2a1	-0.480470247	0.001075368	0.032760177
Aprt	-0.426320586	0.001076469	0.032760177
Npm3-ps1	-1.69729813	0.001080649	0.03283098
Gm5127	-1.559048951	0.001082938	0.032844178
Slc25a5	-0.531334719	0.001106769	0.033225592
Cck	-5.775406112	0.001125706	0.033566513
Gas5	-0.420033368	0.001150671	0.033986277
Mat2a	-0.432102783	0.001157516	0.034056345
Ddx18	-0.431943577	0.001179532	0.034532027
N4bp3	-0.609363387	0.001185084	0.034580244
Rrp12	-0.451951484	0.001220714	0.035228459
Snhg5	-0.440929994	0.001221221	0.035228459
Aen	-0.497835672	0.001229179	0.035400341

Table B2, cont.

Polr1e	-0.472644258	0.001266411	0.036004297
Cihc1	-0.721209108	0.001324112	0.037290827
Hes1	-0.439783798	0.001339429	0.037597414
Mical2	-1.291151148	0.001361055	0.038058394
Tagap1	-0.517996634	0.001362298	0.038058394
Cpne5	-1.214374473	0.001380447	0.038444139
Mycl1	-0.466820303	0.001403697	0.038726283
Naa25	-0.420543655	0.00143587	0.03930778
Nmd3	-0.456529414	0.001473248	0.040144872
Hccs	-0.475402088	0.001505701	0.040840701
Tkt	-0.429831669	0.001515169	0.041034682
Rtn4r1	-2.331254283	0.001532827	0.041386319
Galk1	-0.429430331	0.001543113	0.041600622
Tbrg4	-0.474525449	0.001552456	0.041788908
Ydjc	-0.974584329	0.001570396	0.042143728
Dnmt3b	-0.432011938	0.001607018	0.042866724
1700001O22Rik	-1.383906148	0.001645593	0.043437789
Zfp275	-0.429627583	0.001648046	0.043437789
Tuba1c	-0.419003051	0.001646413	0.043437789
Smyd2	-0.48092095	0.001671988	0.044003344
Rsl1d1	-0.476731065	0.001697421	0.044540328
Exosc9	-0.414572526	0.001741067	0.045416462
Tmem215	-5.74214984	0.00175654	0.045618541
Ldlr	-0.426870439	0.001756199	0.045618541
Cse1l	-0.454902893	0.001759348	0.045624544
Phf16	-0.455924935	0.001768813	0.0456694
Wdr18	-0.422401306	0.001805706	0.046249859
Rnf125	-0.747080628	0.001811351	0.046295301
Lrrtm4	-1.206453138	0.001851683	0.047125144
Rbpms2	-0.634380927	0.001854462	0.047125144
2310061I04Rik	-0.740372385	0.001903675	0.048031177
Zfp9	-0.503664374	0.001916404	0.048283567
5830417I10Rik	-0.482706779	0.001926998	0.04848153
Gnl3	-0.455290441	0.001943954	0.048769559
Tle4	-0.4284246	0.001977683	0.049336216
Nap1l5	-0.963340222	0.002113883	0.05178576
Fat3	-0.456850102	0.002121115	0.051891155
Fstl5	-2.294954733	0.002125481	0.051926229

Table B2, cont.

Usp14	-0.418626548	0.002131568	0.052003222
Thbs1	-0.440280643	0.002149132	0.052286325
Eef1e1	-0.47358928	0.002239476	0.053966809
Tmc7	-0.626172455	0.002290632	0.05504977
Klf9	-1.025909613	0.00233232	0.055824394
Ptpmt1	-0.502692201	0.00233598	0.055836549
Ipo11	-0.429131615	0.002384273	0.056533127
Dock6	-0.491159627	0.002427961	0.057492046
Slc25a33	-0.58766669	0.00247459	0.058129898
Akr1c19	-1.777488984	0.002492666	0.058262071
Slc14a2	-2.126337298	0.002514992	0.058535521
Pknox2	-1.032693774	0.002561955	0.059255055
Slco4a1	-1.664291252	0.002568217	0.059298346
Pus7	-0.426346983	0.002638778	0.060698756
Nme1	-0.425773284	0.002672066	0.061146807
Dars	-0.426980901	0.002681619	0.061286237
Pear1	-0.581442316	0.002744452	0.062320173
Bche	-0.612526536	0.00276711	0.062754235
Lrig1	-0.459735521	0.002840325	0.063923559
Zfp961	-0.426368319	0.00287511	0.064542383
E2f5	-0.510974996	0.002902843	0.065082477
Jazf1	-0.800963135	0.00292374	0.065385462
Zfp948	-0.46403483	0.002977493	0.066402108
Tma16	-0.448422541	0.002983609	0.066402108
Plscr1	-0.436362662	0.002988566	0.06641592
Sf3b4	-0.453845802	0.003021627	0.066898816
Pde3b	-0.422904441	0.003036777	0.067066585
Nsdhl	-0.52054298	0.003074128	0.067387331
Xpo4	-0.465833857	0.003088285	0.067613978
Cdr2	-0.439292737	0.003174266	0.06889706
Gm3086	-1.747414069	0.003235885	0.069809972
D19Bwg1357e	-0.411027768	0.003268275	0.070422986
Timm8a1	-0.486430934	0.00328497	0.070525325
Pgf	-0.743315132	0.00334414	0.070935816
Rangrf	-0.437021479	0.003348517	0.070943704
Calcr1	-0.464390382	0.003448486	0.072428559
Etv4	-0.435165865	0.003531112	0.073580074
2310069G16Rik	-2.961188768	0.003576594	0.073919051

Table B2, cont.

Cdc42ep3	-0.653376922	0.003588983	0.074088659
Litaf	-0.438546965	0.003649674	0.075113439
Thy1	-5.591871524	0.003703956	0.075755732
Creg2	-2.296767733	0.003734941	0.076125756
Pycr2	-0.433809349	0.003746208	0.076267625
Maff	-0.780358304	0.003896216	0.0784202
Mars2	-0.545258407	0.003924277	0.078716648
Chchd4	-0.458997895	0.003939317	0.078858833
Kctd1	-0.451579716	0.003968371	0.078858833
Leprotil1	-0.433340412	0.00398784	0.0790074
Haus2	-0.422937624	0.004073148	0.080517415
Cdh19	-5.349440061	0.004347769	0.08416141
Dppa4	-5.349437968	0.004343636	0.08416141
Fcrl6	-5.349436145	0.00434004	0.08416141
Acat3	-1.06397713	0.004389923	0.084884621
Ppa1	-0.412412039	0.004458063	0.0859208
Hist4h4	-0.455470379	0.004463183	0.085925967
Gm21057	-5.599481858	0.004501228	0.086470454
Slc6a2	-5.456366843	0.004603105	0.087623081
Saa1	-5.370059736	0.004612308	0.087623081
Siglecg	-5.370046797	0.004609588	0.087623081
Gar1	-0.617503795	0.004630019	0.087623081
Snord35a	-1.349074372	0.004709493	0.087903195
Mir20a	-0.835471977	0.004687954	0.087903195
Arhgap9	-0.710624113	0.004709809	0.087903195
Hk2	-0.461828149	0.004744513	0.08827187
Pla2g12a	-0.484262385	0.004784374	0.08864104
Pgbd5	-0.93301453	0.004802712	0.088702431
Slc41a1	-0.447124251	0.004792953	0.088702431
Usp9y	-3.725807611	0.004885925	0.090051505
Ndufaf4	-0.476016987	0.00493185	0.090803454
Sema5b	-1.552956892	0.004964244	0.090964926
Cth	-0.410976376	0.005020121	0.091477755
Tcf15	-0.890647148	0.005203563	0.093785338
Tfr3	-0.518363325	0.005333813	0.095042761
Svep1	-0.631830061	0.005342614	0.095103902
Hesx1	-1.607223291	0.005366467	0.095241341
Plaur	-1.725144745	0.005490781	0.096685827

Table B2, cont.

Dclre1b	-0.462318762	0.005491528	0.096685827
Gfra3	-1.181803164	0.005587637	0.097891424
Ablim2	-1.816307587	0.00572804	0.099389682
Fam199x	-0.410845221	0.00573817	0.099446644

Table B2, cont.

Appendix C

C.1: MICE AND ETHICS STATEMENT

Experiments involving mice were approved by the Institutional Animal Care and Use Committee at the University of Texas at Austin. E10.5 embryos (33-36 somites) were obtained from Swiss Webster crosses.

C.2: WHOLE-MOUNT IN SITU HYBRIDIZATION

Whole-mount *in situ* hybridization was performed on a minimum of two Swiss-Webster embryos per stage at E10.5 and E11.5. Antisense probes were generated from plasmids as described previously (Yu et al., 2012). *in situ* hybridization was performed on an *in situ* hybridization robot (Intavis) as described previously (Yu et al., 2012).

C.3: RIBOPROBES

Gene name	Forward primer	Reverse primer	RIKEN ID
0610012D17Rik	ccgaccacacttccttcta	tgaatttccccttttctc	0610012D17
1200004M23Rik	caagttcagtgttgccttc	gtgaggtcagcctttcttt	E430022B16
1600014K23Rik	ccacagccacactctacttc	agagcaggaaggaataatg	2510019J21

Table C1: Generating riboprobes against GLI target genes. DNA template used to generate a riboprobes are from the RIKEN Fantom2 collection. Forward and reverse primers used to amplify regions are indicated. Riboprobes generated by other methods such as linearization of plasmid, generated from other non-RIKEN plasmids, or mouse limb cDNA are indicated.

2410187C16Rik	ctgttgctctctcctcctg	gtgtcttccctggtagctct	2410187C16
2610306H15Rik	ttgtcaacttctggaatgg	tctggacagtaggctcaaaa	2610306H15
2700038C09Rik	gggtcctaaagtgggtttc	tcaggaaagttcagtgtgt	2700038C09
2810408P10Rik	Linearized plasmid	Linearized plasmid	2810408P10
3110043J09Rik	cagtcacaagttggaaaa	ccagatcaagttcaatccaa	E030002L15
4921524J17Rik	cttcaactctgttggtgc	tgatacagcctcaaatgctt	4921524J17
4930525K10Rik	Linearized plasmid	Linearized plasmid	4930525K10
5430416O09Rik	ctggactgtgtgtgaggtt	gaaacaccttgtgctctctg	5430416O09
9430076C15Rik	cattcagaagccaaatgag	ctttctgcatggctgttate	D430026C09
9830107B12Rik	gaggatccacaggaccttac	tcagctcctctttgacata	9830107B12
A130014H13Rik	taccgttatgatgtgcttcc	agaacaagcacgcagaaata	A130014H13
A530021J07Rik	aagcgtagacatctggttca	ttctggctggagacataaaa	A530021J07
A830059I20Rik	ctgctcttttcgactctctg	gcgctgtaatcataggacac	A830059I20
A930038C07Rik	gctgttctactggtgtttgc	gcattcatctttgtttctgc	4831422J22
Adamts19	agaagaatctttgccaggac	tcaccaacaggatcaaagtc	D030062M24
Aldh1a2	cacaggctctactgaggttg	cgcatttaaggcattgtaac	6820449I02
Alg13	aggaagctgtttggagagtc	aatgctgattttctcacca	E430039H24
Alx4	ggggattcccaggaggcgac	gcaaggagacatacctgggcg	limb cDNA
Ap1s2	ctaccctcgcagcctaag	gaggcagtgaccatctacag	B230210K03
Apoa2	aaggactgcagcacagaat	gtttaactccttccgcattt	I530003A11
Aprt	tcgactacatgcaggtcta	caaaacggttattgatctcc	0610008N13
Arhgef3	agaccttcgatgtgtgtgc	ggaaaacatggagtttcaca	1200004I24
Arl6	cagacttcaggtttgcttg	aaaacgttctccagagtcc	1110018H24
Asf1a	gaaaaccaccagtaaaacc	aaacctgggtggcatataat	E430021K15
Atp6v1g3	gaggcaagctaaggaagaag	ttaggcagggataactgtga	6720467K22
Avpr2	ggaaccaagaaataggcagt	acgttgagcaaagatgaaga	D630034C19
AW548124	ctacactgttccgaagtgg	gagcactctgagactggttg	5730519I16
B230399E16Rik	gttctctcaacacacagga	cacacaatcccatgcttatt	B230399E16
Baz2b	acgatctggaagaggaagag	tcttgaatgacgctttgaat	5830435C13
Bmp2	Linearized plasmid	Linearized plasmid	Lab plasmid
Bmp4	Linearized plasmid	Linearized plasmid	Lab plasmid
Bmpr1b	tctttagcactcaaggcaag	atgatgaatccgtgtttctg	D930007I02
C330023D02Rik	cagaggactgggtcattgta	atcacagccagggaatatct	A530078P09
Calml4	gagaaccaaactcagttcca	gcagtggtgtgtcactctct	2010002G05
Cd302	cctgctaggcatgttctatg	gttagatccaggatggttcc	0610038N09

Table C1, cont.

Cdc42ep4	gagggctgtgtaggaaaagt	ggtgtgtgtgtgtgtgtgt	1500041M20
Cdk6	atcacccgtactccaagat	tccattgtgaatcaccttc	9130423C03
Cited4	ggctgtctgtttcttttc	tctgagaagcaatcgaactc	2610524B15
Cldn11	actggtctctaccactgcaa	aatcaacaacaatggaatgc	1500001D22
Cldn9	ccgcagctgtgaggtctggc	cgcggggacgctcaaagtgt	Limb cDNA
Clstn2	gtcctgtagccctcacttct	ccttgaagagtgctgtatg	C130053D20
Cntfr	cccgcagccgactagttag	tattttattaacaacttaa	4930502A07
Cobll1	gactttgagctcaccaactg	tgatgttcctgactaccag	D430044D16
Col23a1	tcaaaattcaggtgtggttc	tgtgagcctcagatttcta	6820412L02
Cxxc4	aggcccactcacaagtagt	gtttgtacatgcccataa	A830026K07
Cyyr1	accggtctctgtcctaaaga	tctccacctatctctgagca	6330416N05
D16Ertd472e	tcagtgagaggccataaaga	tagaggatgaaagcaggaca	A930031E11
Dcn	tgggctgcatagttagtgtt	caccctcacctcatagttaa	9530076L14
Depdc7	gatagcagttgcagccttta	cgtctaaactcctccctgtt	6330584N14
Dlk1	gtgtcaatggagctctgcaag	ctccttgttgaagtggtca	1600023D19
Dlx5	tggaggacttttgaagaggt	gcagccttattaatgtgtcg	F930032M16
Drd3	ggtgagcctggctgtggcag	tggccaggagagaggggctg	Limb cDNA
E130307M08Rik	aggaggaggaagaagatgtg	tatcttggacatacggccatc	2610511M14
E130309F12Rik	ccgtgggtggttaattgtaa	ctgagaagcacagactcc	E130309F12
Ebf3	tctgatgccttaaaagtgga	aatcgaggcaatttagttcc	3110018A08
Ednrb	gacagatcagctgttgc	agttgtcatatccgtgatcg	D030003K13
Efcab2	agcagaatatggaggagag	tcttttgcacacctcagt	4931421D06
Efna1	gtgactgtcaatggcaaat	gaaatcttgagagatgctg	2310004J15
Enpp1	tgggtcagtagcatttgaag	gggatcaaacccagtaagtc	E430029D02
Eomes	acaatgtttctgtggaagtg	cgatgtctagctgttggtc	F830028H02
Epha3	aaacacagtgcagaggagaa	caatcccgaactccataca	B130048J04
Fbxo41	gctgtcagtgctggatactc	gaaaccacaacttgagaca	9630017H13
Fbxo8	agaacttggccttagtctg	ggtcagatccaactttgaca	6330500C02
Foxf1	tcagcaagtgaaaagggata	tccctcatctcagtggttc	E030047N19
Foxf2	gcattgtcttctactcgttg	gctttcttgaattgtgtgc	4022445M22
Fzd7	ctgctagagcttagcgtga	caggtggatgtctgtgagtt	2310081G03
Gata5	cagtcactactggctggag	gaatttcaactccaacaca	9130423G08
Gli1	Linearized plasmid	Linearized plasmid	Lab plasmid
Gm784	gagagatcccagatgtttcc	aattcaggttgggagat	D130058O17
Grcc10	ctctcttccaaggacagtt	gcacacatacagagaaccaat	3010025G03

Table C1, cont.

Grem1	Linearized plasmid	Linearized plasmid	Lab plasmid
Haghl	gaccatgaagggtcaaagtca	tcgaaggcacagtaggaata	B930082I15
Hand2	Linearized plasmid	Linearized plasmid	Lab plasmid
Hccs	tccattgcagatgataggtc	aaccagttttcaacagcaaa	5730448P21
Hhip	acctagcacttccactcctc	ccaatgtgatcataccatcc	6330416O15
Hmga1	gacaaggctaacttcccatt	caaattcaggaggatgaaca	2410030H14
Hook1	atgacctggaagaatctgt	gccttcttcagctcttcttc	A830044F05
Hoxa7	gaaggaattccatttcaacc	atcatggtttgcaggattg	9030406A02
Hoxb4	acagcctggatttttcttc	accaacaaaaggttctaggc	5730551B08
Hoxc4	ttactgtctcgcaaatgaat	agctagcgacctgtaaagt	D030011O04
Hoxd10	aattacaccgggaatgtttt	ctctccacttgggagacttt	6030426C21
Hoxd11	taatttccctcccaacattt	cctcttgcaataaaggttt	E230017H14
Hoxd13	Linearized plasmid	Linearized plasmid	Lab plasmid
Id3	tgtctcttttctccctctc	attctcgaaaagccagtc	0610039A06
Ier5	caaacctcatcagcatcttc	ccagacgaactccctctagt	I830008A05
Igflr	aattgtggttcacctcttt	acaccacaagaaactgaaa	A330103N21
Igfbp7	ttctgttctctctctctcc	gtggcactcactctctccag	0610007D03
Inha	ctcccaggctatccttttcc	gaaactgggagggtgtacga	Limb cDNA
Irx3	ggagatcgatttggaaaact	caaggcactacagcgatatt	E030042N12
Isl1	ttctgaatggtgctgtttct	tctacatatggcgctttgat	G630030I18
Jag1	ggcagccttaggatcatagt	agcaggaaaagaaagaggaaa	6230411J17
Jazf1	cagcgagtatgatgaggaag	tgtgagtcgatgtttgaaa	C820002C15
Kbtbd8	tccatgcttgcagtattctt	gcaaaactgaggaggaatftt	D230024C02
Kcne3	accagtgtttctgtctgtgc	atatgtgttcatgggctctg	2210017H05
Kit	cttgattaagtcggatgctg	ggaccagacatcacttcaa	B830009P17
Klf3	ggttctccttctctctgaa	tttgatcccagtgtgtttc	1810073A04
Klf9	cgtttgcagtcgaataaact	agatgggaggattttccata	4632425M20
ler2	gtctacctctcagccaaggt	gagagttcgacctgagatt	6720401C09
Lrrc20	ggtcaatgagactgtggaaa	ctaggctctagcctcacctc	A830036L06
Ltbp1	tggcaaagacagagacaact	gttatgaggaaggggacaac	C730041O04
Lum	cttggcattagtcggtagtg	gataaacgcaggtattgcag	1500035A23
Lypd6	aatcgtcttgcattctctca	ttgctgtgattgtgtgtgt	E130115E03
Maml3	tttattgatccagagccaga	gtgtcttagggcaggtcttt	C230025H14
Med30	acttaccagaccggctaac	gcctttgaaaagggtaacag	I730042E14
Meis1	tgcaaaactgacctgtttct	accaccctaactccaata	6720477P20

Table C1, cont.

Mgmt	cataaacctcaggcctttct	agcctggatctatttgaag	G630095K06
Mnd1	gcatgtcaaagaaaagagga	catattcacaagctcccaga	2610034E18
Mrg1	agcaaatcacatggctcac	gccattgcacatattcatct	B130038I01
Mrpl23	Linearized plasmid	Linearized plasmid	E030002D02
Msi2	cctcaccagatagccttagag	aggggaacagacaggtacag	6030413L18
Myl4	gagcctaagaaggagactgc	gaagccatgtgagtccaata	2810417B17
Ncor2	ctcaccaagtgtcctctctg	tggggtcttcttattcttc	F630016H22
Nfe2l3	ctcacgattctgttgagctt	agagaatgttcaggctgtga	5430406J03
Npvf	ggtagcggaaaatactcccagctg	accacaggtcacggctccgta	Limb cDNA
Olfr91	tgcttcaccacaacctgtgt	tcaaagcctttttccatgct	Limb cDNA
Osr1	acagcaacaaaatcccttg	ataaagtgccagtcgcaata	1110067L16
Osr2	ctgcagctcaccaattactc	acagaatcctttcccacact	D230050P11
Pam	tcatcactgggagttactg	gccacattctgtgtacaggt	D130061M01
Pax1	acattcagtcagcaacatcc	ccgaactaggaaggtagga	5830427P13
Pax9	actcatatcccagtcctc	tcttgaaaagggaggttac	9430070E09
Pbx1	atgctttaaactgccacaga	aaaatttaaagcctcctg	B130052B10
Pdlim3	tgaaccacaggaattcaaac	tgttctgtctgcaaaggat	6720456D19
Pmch	catccaatgcactctgttt	taatgcacacgtcaagcata	A230109K23
Polr2k	Linearized plasmid	Linearized plasmid	2010016L13
Popdc3	atcagagtgacagtcgatgg	tgtggaccataatagcaacc	D330028H18
Ppp1r2	tgaatcagtgagacctgtc	gagagaggccaatttcagat	E130119E11
Ppp2r4	caaaactgatcaggaagcag	acagcctctcatcaaacaga	6030457C15
Prdm1	cctgcagaacactacttgg	taccctaagaagcaacacga	5031440G22
Prkce	cgaccatggtagtgttcaat	ccaactgtaaggctgttttg	A730046G04
Prokr2	catccatccaggtcactaga	atcacatccacacctgact	B830005M06
Ptch1	Linearized plasmid	Linearized plasmid	Lab plasmid
Ptch2	cacacttgaccagctaaag	tccttgataacctgcaccac	A730013M03
Punc	tgatcacatgggagaagaac	agaaatgctcagtgctgtg	D030056K15
Pus7I	gttgtaaaaccaaaccgtga	gcctccaaaattctctctgt	4732482O11
Ralgps2	ggcttttgaaggaacagat	catctcactcattccctga	9930012L10
Ramp2	Linearized plasmid	Linearized plasmid	1110019C20
Rasgef1b	gaagcccttatccaacactt	gagatgattgcatcaaga	4732452O09
Rg9mtd1	ttggcaaagaagtaccagaa	gaaggcactctgttctatg	1300018J16
Rgs19	agaaggcgcgacttatctat	tgcacactgtaggtgtgta	A730001O09

Table C1, cont.

Rspo3	gcatgaagcagataggagtg	tctggttgagatagcagcat	4732402G11
Rspo4	cagaggctcttctcttcat	gaaaagggagacggataaaa	A930029K19
Runx3	aacccaaatcaatgtcctct	ttggtcaaagttgtctgct	E130320J01
Sall1	cttcacttttccgacacttg	aacagaacctggagagaagg	G630023L11
Sall3	cctcagctcccagtaagtct	tgttgttaccgcgataatc	B130022O04
Sall4	accagtccaagaaaggaaag	ccgatgacaaatgagacact	C330011P20
Sap30	actgctgaagtctccatgtg	tggtacaaatcaacctctgg	E430025B08
Scube1	tccaatgagggtatgaactg	tcatctccacacagtccttc	A630023E24
Sdk2	tgccttctgcaaagttagaa	tacctgtactccagcgagaa	5330435L01
Sfrp2	tatctggtcatgggacagaa	gagcaacgaaatgtttgaag	I920164A09
Shcbp1	ccacgaattatccaaacaaa	ggatatgtggctcagtggta	D930001E18
Shroom3	cttggtctgtgtctctcac	tgaggagtgtggacttcac	1110002N03
Slc24a6	ggagatgccttctcagattt	gtcaactcactcttctct	4632424F05
Slc26a11	ggtgtccttctacacctcc	ttagcatcaatgcggtagtt	F630021I08
Slc2a1	cttatgggcttctccaaact	gctcgtctacaacaaacag	F730013E15
Slc35c1	cctcaatgccatctatacca	gtagggcttcccaagacta	E430007K15
Smad7	gaagagagtctccgaggaag	gagtagactcaccctcgt	2810433N14
Smo	caagaagagcaagatgatcg	agcctccattaggttagtgc	B930075H04
Smoc1	ctgtgttgtcccagagtgt	attccatcttctccctca	A530047A09
Smug1	tccctataaggcctttgaac	ccaccaatgaagtgtaggaa	1200013B09
Sox4	ctgcaggcttctaaagtga	ttttgtggccttgaatttta	D130055G04
Sp1	gtaggcagcagcttccagta	aacctatcccaacctaaaca	E430018D04
Sparc11	accactcaaccaactact	attgctctctgttctctcc	6330500I21
Srp19	cgaccaggacaggtttattt	ttcaagtaactcatgggaca	1110036A13
Stxbp6	cacataatgctttcgctac	aaacctccaaaaccagata	K430308H17
Sulf1	aattcaagctcccagaactc	gcctatggggatacattctc	B130018L10
Svep1	tcctgtatcccagttgtttg	gacagacacctccattctga	4833413O10
Tank	caggctgaaatcacagctac	gaagttatgggtcaattcc	E430026L09
Tbx2	aacatttctgacaagcatgg	tgaacaaaacggaagaaga	A930005K01
Tbx3	ttaaagtgaggtgctctgga	cacagatctttgaggttggga	D430026F23
Tbx4	tatcatctcaactccatgc	acgtccacatgttacagctc	3930401C23
Tcte3	aaaggaagcctagcatgttc	ctggtcctgagctattcaca	1700026A18
Thap1	aacggacagggtagtctactc	cgacgtccttctctctctg	4833431A01
Thap11	ctgcacttctacagtttcc	tcatcttcaactccatcagg	G730039J03
Tmem30b	gtgacacatcttgccatttt	cccactaagatcatttgcag	9130011B11

Table C1, cont.

Tmem48	gcactggaactgagagctta	aaactcctcctcgaatagc	2810475A17
Tmem5	gaacgcattacagcttcac	gtaactgcagaggagcactg	6330415D21
Tmepai	tggtgatggtggttatgatt	tctccttctccttgttctcc	2210418I02
Tmtc1	cttcaatgtatggcttctgc	tgaataggcatcagcaaaat	B230379O03
Tpcn1	tcaggagaagatggctgtaa	taaagaagagcagcaacagg	5730403B01
Tpd5211	gaatcgctaccatctgctg	agtgggattttggtcttcat	1810073J04
Trim59	tcaggagattgacagaccag	ttcattccttgaatctgtgg	4933403N21
Trim62	gggacagaggtcctacaatc	atggacatgctcactgaatc	1110038I18
Trp53rk	tcttttggtgactatgctct	ggatgttgccataaattcaa	C330019P15
Ube2t	cttgagatcatgcagagagc	caaaagagaccaccttgaca	C330020M11
Ust	gagacatgtccacttctca	cattttcgtcatcttctc	D930010O20
Whrn	gtactacctggcccagtacc	tcagaggacaactgcaact	F930011M09
Wnt11	ctgcatgaagaatgagaagg	aaagagggttgaagtgagc	5930404H12
Xpa	gaggaaaagcagacgtcac	cccctctccttacctacaga	2210417B19
Xpnpep2	aacagatggagacctggaat	aggctaaagcactcttgtt	9030008G12
Zfp281	ttactaccaccttcacgtc	ttatacatggaagcctgtgg	9330157H23
Zfp64	gtggaaggagacacctttc	atgaaacctggcttttgtt	2700078A12
Zfp704	cttgtgccaaaacagacact	ttggctaagctgctacagaa	6820415O14
Zic3	aacaaccacgtctgctattg	accagcatcttcccatttat	9430037B07
Zmiz1	agtacaggctgtgtgcagg	gactgtgttctgggagtgaa	E330020C23
Ube2v1	Linearized plasmid	Linearized plasmid	Lab plasmid

Table C1, cont.

C.4: QUANTITATIVE REVERSE-TRANSCRIPTASE PCR

RNA was extracted using TRIzol (Invitrogen). 300ng of DNase I treated RNA was used to synthesize cDNA using random hexamers and SuperScript II (Invitrogen). qRT-PCR experiments were performed using SensiFast SYBR lo-rox (Bioline) on a ViiA7 platform (Applied Biosystems).

C.5: SHH^{-/-} FORELIMB RNASEQ

To generate *Shh*^{-/-} embryos, heterozygous *Shh*^{tm1Amc} mice (in previous generations mated to a Cre deleter strain to generate a null allele) (Dassule et al., 2000) were crossed, and E10.25 (33 to 35 somites) embryos were collected and genotyped for the wild-type and null allele. Forelimbs were collected and combined from three embryos of the same genotype, and RNA was isolated using TRIzol (Invitrogen) and treated with DNase I. Two biological replicates for each genotype were sequenced. The average *Shh*^{-/-} somite number for replicate one was 34, and replicate two was 33.3. The average wild-type somite number for replicate one was 34, and replicate two was 33.7. Library construction was performed following Illumina manufacturer suggestions, and libraries were sequenced on the Illumina HiSeq platform using paired-end sequencing. Reads were aligned to the mouse reference genome mm10 using TopHat 2.0.9 (Trapnell et al., 2009) with default parameters and the option to incorporate genome annotation (parameter “-G”). Aligned reads were assigned to genes by HTSeq-count (Anders et al., 2010) using the default unioncounting mode. Following HTSeq-count, edgeR 3.4.2 was used to conduct differential expression analysis (‘classic’ edgeR) (Robinson et al., 2010). Differentially expressed genes were identified based on an FDR of 0.05 and a mean fold change of 25% (supplementary material Table S3). The data discussed in this publication have been deposited in NCBI’s Gene Expression Omnibus and are accessible through GEO Series accession number GSE58222.

C.6: CYCLOPAMINE TREATED WILD-TYPE FORELIMB RNASEQ

Wild-type E10.25 (31-34 somites) forelimbs were cultured as described in (Panman et al., 2006; Zúñiga et al., 1999). For each culture condition, forelimb pairs from seven wild-type embryos were cultured for 15 hours in 10 μ M cyclopamine (Toronto Research) or in 0.125% ethanol for controls. Immediately after the incubation period, limb buds were separated from the adjacent tissue and RNA was isolated using TRIzol (Invitrogen) and treated with DNase I. Two biological replicates for each culture condition were sequenced. The average somite number for wild-type controls was 32 for replicate one, and 32.6 for replicate two. The average somite number for wild-type samples treated with cyclopamine was 32 for replicate one, and 32.8 for replicate two. Library preparations were generated following ABI manufacturer suggestions, and libraries were sequenced on an ABI SOLiD platform using paired-end sequencing. Reads were aligned to the mouse reference genome mm10 using TopHat 2.0.9 (Trapnell et al., 2009) with default parameters and the option to incorporate genome annotation (parameter “-G”). Aligned reads were assigned to genes by HTSeq-count (Anders et al., 2010) using the default union-counting mode. Following HTSeq-count, edgeR 3.4.2 was used to conduct differential expression analysis (‘classic’ edgeR) (Robinson et al., 2010). Differentially expressed genes were identified based on an FDR of 0.05 and a mean fold change of 25% (supplementary material Table S4). The data discussed in this publication have been deposited in NCBI’s Gene Expression Omnibus and are accessible through GEO series accession number GSE58222.

C.7: DE NOVO MOTIF DISCOVERY AND GLI MOTIF QUALITY ANALYSIS

De novo motif discovery was performed DNA motifs in GLI-bound CRMs were discovered by de novo motif discovery method. We mapped motif PWMs to GLI-bound CRMs in each category, background sequences were modeled as a third-order Markov chain (Ji et al. 2006). Then, we compared relative enrichment levels (r_1) of the discovered motifs in high-quality binding regions versus matched control genomic regions. We chose a motif selection procedure to select enriched motifs by simultaneously requiring $r_1 \geq 2$, number of motif sites (n_{1B}) $\geq \max(1/5 * (\text{number of genes}), 5)$, motif score ≥ 1 . We used TOMTOM motif comparison tool to visualize their sequence logos with their PWMs as input. The quality of Gli motifs was assessed by using a Gli motif with the highest score, and then mapped the PWM of the Gli motif to GLI-bound CRMs within each category. The Gli matrix was compared to a third-order background Markov model. A log-likelihood ratio for Gli motif quality was determined as described previously (Vokes et al., 2007). With the Gli consensus-binding pattern from each binding region, we calculated probability for each motif site in each category using a Welch's t-test.

C.8: SP1 MOTIF META-ANALYSIS

The peak lists were from hmChIP publically available mouse TF ChIP datasets and analyzed using CisGenome software. Here we had two controls for each peak list: matched genomic controls and random controls. For each control, we compared relative enrichment (r_1) of Sp1 motif. $r_1 > 2$ means Sp1 is enriched, while $r_1 < 1$ means sp1 is not enriched.

Additional ChIP datasets were obtained from (Cotney et al., 2012; DeMare et al., 2013; Infante et al., 2013; Peterson et al., 2012; Visel et al., 2009). For each peak list from the papers, we overlapped the GLI3 peaks with all the peaks in the limb bud and divided it into two datasets: regions containing Gli3 and regions without Gli3. The Sp1 enrichment analyses were the same as peak lists from hmChIP.

C.9: CO-IMMUNOPRECIPITATION

Female RosaGli1-Flag^{c/c} (Vokes et al., 2007) were mated to male Prx1Cre mice (Logan et al., 2002), and embryo forelimbs were collected at E10.5. Protein lysate was run on a 10% SDS-PAGE gel, and assayed for SP1 (Millipore 07645, 1:1000) and M2 anti-FLAG (Sigma, 1:2000).

C.10: MOUSE FORELIMB TRUNK CULTURES

Embryo trunks containing forelimbs were cultured as previously described (Panman et al., 2006; Aimee Zuniga et al., 1999). To inhibit HH signaling, limb buds were cultured for 15 hours in 10 μ M cyclopamine (Toronto Research) or in 0.125% ethanol for controls. To inhibit SP-mediated transcription, contralateral forelimbs were cultured for 15 h in 300 nM mithramycin A (Sigma) or 0.03% DMSO for controls. To inhibit FGF signaling, contralateral forelimbs were cultured for 4, 8, and 15 hours in media containing 10 μ M SU5402 (Tocris) or 0.125% DMSO for controls. To activate the SHH pathway,

contralateral forelimbs were cultured for 15 hours in 10 μ M purmorphamine (Stemgent) or 0.125% DMSO. Immediately after incubation, limb buds were processed for *in situ* hybridization, β -galactosidase staining (Whiting et al., 1991), or separated from the adjacent tissue and processed for qRT-PCR.

C11: DISSECTING, DISSOCIATING, AND NUCLEOFECTING MOUSE LIMB CELLS

1. Dissect forelimbs at the proximal base, excluding the adjacent mesoderm from E10.25-E10.5 (33-36 somites) mouse embryos. Note that the ectoderm is not specifically removed. Place dissected forelimbs in a petri dish containing PBS and keep on ice. Limb buds from multiple litters can be pooled.
2. Transfer limb buds to a 15ml tube and pulse centrifuge, and remove the PBS supernatant.
3. Add 1 mL of 0.25% Trypsin/EDTA to the 15mL tube, and incubate at 37°C for 10 min.
4. Gently pipette the limb buds with a P1000 tip to further dissociated until there are minimal clumps of tissue.
5. Inactivate the Trypsin by adding 9mL of limb bud culture media (10% calf serum) to the 15 mL tube.
6. Remove the remaining tissue aggregates with a 40 μ m cell strainer. Place the nylon filter on top of a 50 mL tube and apply the 10 mL cell mixture. Save the cell flow-through.

7. Determine the concentration of cells in the flow-through using a hemocytometer.
8. Determine the number of electroporations and transfer the appropriate volume of cells to a single 15 mL tube and centrifuge at 200 x g for 5 min. One electroporation requires 7.5×10^5 cells.
9. While the cells are centrifuging, prepare the complete electroporation solution by combining the appropriate volume of SF solution and Supplemental 1 solution into a 1.5 mL tube, and incubate at 37°C. A single electroporation requires 18 µL SF solution and 4 µL Supplemental 1 solution (complete electroporation solution).
10. Remove all of the cell culture media and add the total volume of the complete electroporation solution to a 15 mL conical tube. Using a P1000 pipette, gently suspend the cells in the solution, and transfer to a new 1.5 mL tube.
11. For each electroporation transfer 20 µL of cells into a new 1.5 mL tube, and add 1-4 µL of prepared DNA / RNA.
12. Pipette mixture 1-2 times and transfer the entire mixture to an electroporation cuvette.
13. Electroporate the sample(s) using the 96-well Shuttle System (Lonza AAM-1001S) set to program DS113.
14. After electroporation, add 80 µL of pre-warmed (37°C) limb cell culture media (high serum) to each electroporation cuvette, and incubate at 37°C for 10 min.
15. While the cells are recovering prepare the 96-well half area plate with the appropriate cell culture media. Add 20 µL of either FGF8 concentrate media

- (750 ng/mL) or FGF8 (750 ng/mL) and purmorphamine (25 μ M) concentrate media to each well.
16. Remove the electroporation cuvette plate from the 37°C incubator and transfer (~100 μ l) of the electroporated cells to a new 1.5 mL tube. Wash each cuvette with 100 μ l of limb cell culture media (high serum) to each well and transfer the wash media to the corresponding 1.5 mL tube. The total volume of the 1.5 mL tube is ~200 μ l.
 17. Add 80 μ l of electroporated cells to each well containing 20 μ L of concentrated media on the 96-well half-area plate. The final volume in each well is 100 μ L; the final concentrations of FGF8 and purmorphamine are 150 ng/mL and 5 μ M, respectively.
 18. Every 24 hours change the media or perform assay (luciferase, qRT-PCR).
 19. For qRT-PCR experiments, carefully remove the media, and add 100 μ L of Trypsin/EDTA, and incubate at 37°C for 5 min. Transfer the cells into a 1.5 mL tube and wash the well out with 100 μ L PBS and add to the same tube. Centrifuge the 1.5 mL tubes containing the cells at 350 x g, remove the supernatant and proceed to RNA isolation (see RNA isolation and qRT-PCR section for the complete methods).
 20. For *Gaussia* luciferase experiments, replace the media with limb bud cell media containing 0.5% serum 24 hours post electroporation.

C12: GAUSSIA LUCIFERASE ASSAY

To determine if this method could be used to assay the activity of DNA regulatory elements, we electroporated 300ng of a Hh responsive element, the *Drosophila Patched* promoter, upstream of the *Gaussia* luciferase reporter gene (Pastrana et al., 2009), and 100ng of a LacZ plasmid (pSV40LacZ). *Gaussia* luciferase values were normalized to β -Galactosidase levels using the BetaFluor β -Galactosidase Assay Kit (Novagen, #70979).

C13: FLOW CYTOMETRY ANALYSIS

Limb bud cells were electroporated with 1 μ g of GFPmax plasmid (Lonza) or 10 picomoles of Cy3-labeled *Gapdh* siRNA, and cultured for 24 hours. To determine the electroporation efficiencies flow cytometry analysis was performed using a LSR Fortessa (BD Biosciences), and the primary data were processed using FlowJo software (Tree Star).

C14: ALCIAN BLUE STAINING AND IMAGING

To determine if cells were adopting a chondrogenic fate, limb cells in culture were stained with Alcian blue at 72 hours as previously described (Paulsen and Solursh, 1988). Briefly, cells were washed 2x with 150 μ L PBS, and then cells were fixed with 150 μ L of acidified alcohol for 15 min. Cells were rehydrated sequentially in 150 μ L 95%, 80%, 70%, 50%, 25% ethanol for 5 min. Ethanol was removed and 150 μ L of Alcian blue stain was added and incubated at 4°C for 16 hours. Cells were washed 8x with 150 μ L 0.1N

HCl with agitation, and washed 1x with 150 μ L H₂O. All liquid was removed, and cells were imaged on a Leica M165 FC stereomicroscope.

C15: GRE1 MOUSE TRANSGENICS

The *GRE1LacZ* transgenic line, officially named Tg(Rr26-lacZ)438Svok (MGI:5052053), was generated by pronuclear injection using the previously described enhancer reporter construct containing the 438-bp Gli binding region (chr2:113640843-113641280) (Vokes et al., 2008). The BAC transgenic constructs were generated using the Quick&Easy BAC Modification Kit (Gene Bridges) to modify a previously generated BAC containing *LacZ* within the *Gremlin* transcript (Zuniga et al., 2004). The homology arms for both targeting vectors were chr2:113,640,295-113,640,842 and chr2:113,641,281-113,641,757. After targeting, the FRT-flanked neomycin-resistance cassette was removed with a heat shock inducible FlpE construct (Gene Bridges), leaving a 69-bp FRT site and linker sequence precisely in place of the Gli CRM (chr2:113640843-113641280). The official name for the *Gremlin*^{GRE1} allele is Rr26<tm1Svok> (MGI:5486166). This allele results in the replacement of the 438-bp CRM sequence with an 89-bp sequence containing a single LoxP scar. Further details on the generation of this allele are provided in the supplemental information (Fig. S4).

C16: PRIMERS

Gene name	Forward Primer	Reverse Primer
Adams19	aagccggcacatagcttctt	cagccagactgaatgctcca
Agc1	ggcactgttaccgccactt	cccctcgatagtcctgtca
Axin2	gaggagatcgaggcagaagc	cacctctgctgccacaaaac
B-Actin	gctgtattccctccatcgtg	cacggtggccttagggtcag
Calml4	ttctggtgtccatgaggtgc	gaagtcagctctccgttct
Cdk6	tcccaggagaggaagactgg	gccgtaggcggatataccttt
Cntfr	tgttccaccgtgactcctg	agctgcagtagaagcccttg
Dock6	cagccccgagaatgccggac	ggaggtgaggcctttctgcc
Dusp6	cggaaatggcgatctgcaag	gacgactcgtacagctcctg
Fam181b	tcggaagtctggacaaaggc	acgccgagtctatgaagctg
Fbxo41	atgtgggctcccgaactact	gaggatttctgggctgatga
Fbxo8	tccggcaacaataggaacgctc	ttcgcgctggagaacacgat
Fgf8	ccggacctaccagctctaca	ggcaattagctcccctct
Fmn1	gacccgcaccaactttatg	ggcctctgacaggggtttt
Gapdh	gggaaggtcgggtgtaacg	ctcgtcctggaagatggtg
Gli1	cccagctcgtccgcaaaaca	ctgctgcggcatggcactct
Grem1	actcgtccacagcgaagaac	tcattgtgctgagccttgc
Hand2	ccataatgggagtggccag	cgaggagaacccctactcc
Hhip	gtccctgctccccgattc	acctggaatatggcctcggca
HoxD13	tgtccacttttgatccgg	ttctcctccccgtcggta
Ier2	aagaggaagtgtgcgagtc	tagacgggcttcttgcctg
Jag1	gtgctacaatcgtgccagtg	ggggaccacagacgttagaa
Klf9	tctggagagtcccgatgagg	gaaagggcgttcacctga
LacZ	gggccgcaagaaaactatcc	tctgacaatggcagatccca
Ltbp1	agctttgccagatccctgtc	ctttgacccctgctggcta
Msi2	acgattgacccaaaagtgc	catcagcatcgcactccta
Msx2	caagtgaagggggaggtgta	cagggacctgacatggagtt
Ndnf	agcgcacactccttgcc	gtggcgggaggatactgaac
Osr1	gaggggcttccggatcttc	ttggccaagtttagccgc
Osr2	cctccagccctacacaagg	gcttgctcaggtcctccatt
Pam	gggactgtgtacattggcga	aactgcctcggcttcttga

Table C2: Primers used in qRT-PCR experiments.

Prdm1	atccagettccctaccgagt	gggggactactctcgtcctt
Ptch1	gaccggccttgctcaacc	cagggcgtgagcgtgacaa
Ralgps2	aggctcaggggctgatgagga	cgcgtattcttctggcgtaacct
Rasgef1b	gcagcagtgaccaaatagcaa	caacatggctggaacttggc
Rps3	atggggtgctcctagccc	taccgcagccatggtaag
Sall1	gcctaccattgctccaact	cgccacttgggttcttctgtg
Sall3	catgtggaacaatgacccc	atgcctccgttctggatgac
Sap30	ttcaagctccaaccagacc	gccttgagatccgatttgtt
Shh	tctcgagaccaactccgat	gacttctcctccatccccac
Smoc1	tgctcacgccccacttctgtg	agggctgggtctcggcactt
Sox4	ggagatgtgctgggagtagc	ctggtagcctcacctctct
Sox9	taagttccccgtgtcatcc	ttgccagagtcttctgtgag
Sp1	tgctgcttcgagtctgagaa	agcgaccaagatcactccat
Sp3	ctcgctctgctggcctctac	cccacgggttgggtctctctcc
Spry4	gaccactcgggttcgggga	ggggcgtctgctgtcaagg
Svep1	tgtctgacgtaagccacac	ggcggcattgaagtggtttt
Tbp	ggcctctcagaagcatcacta	gccaaagcctgagcataa
Tpd5211	aatcgctaccatctgctget	cttcctgtagcggttccgt

Table C2, cont.

Commonly used abbreviations

Shh	Sonic hedgehog
Hh	Hedgehog
Fgf	Fibroblast Growth Factor
GRE1	Gremlin regulatory element 1
CRM	Cis-regulatory module
KD	Knockdown
siRNA	Small interfering RNA
PM	Purmorphamine
MitA	Mithramycin A
Cyc	Cyclopamine
FDR	False Discovery Rate
FC	Fold change
qRT-PCR	Quantitative Reverse Transcriptase PCR

References

- Ahn, S. and Joyner, A. L. (2004). Dynamic changes in the response of cells to positive hedgehog signaling during mouse limb patterning. *Cell* 118, 505-516.
- Akiyama H, Chaboissier MC, Martin JF, Schedl A, de Crombrughe B. 2002. The transcription factor Sox9 has essential roles in successive steps of the chondrocyte differentiation pathway and is required for expression of Sox5 and Sox6. *Genes Dev* 16:2813-2828.
- Allen, B. L., Song, J. Y., Izzi, L., Althaus, I. W., Kang, J. S., Charron, F., Krauss, R. S. and McMahon, A. P. (2011). Overlapping roles and collective requirement for the coreceptors GAS1, CDO, and BOC in SHH pathway function. *Dev Cell* 20, 775-787.
- Anderson R, Landry M, Muneoka K. 1993. Maintenance of ZPA signaling in cultured mouse limb bud cells. *Development* 117:1421-1433.
- Aoto, K., Nishimura, T., Eto, K. and Motoyama, J. (2002). Mouse GLI3 regulates Fgf8 expression and apoptosis in the developing neural tube, face, and limb bud. *Dev Biol* 251, 320-332.
- Aza-blanc, P., Laget, M., Schwartz, C. and Kornberg, T. B. (1997). Proteolysis That Is Inhibited by Hedgehog Targets Cubitus interruptus Protein to the Nucleus and Converts It to a Repressor. *Cell* 89, 1043–1053.
- Bai, C. B., Stephen, D. and Joyner, A. L. (2004). All mouse ventral spinal cord patterning by hedgehog is Gli dependent and involves an activator function of Gli3. *Dev Cell* 6, 103-115.
- Balaskas, N., Ribeiro, A., Panovska, J., Dessaud, E., Sasai, N., Page, K. M., Briscoe, J. and Ribes, V. (2012). Gene regulatory logic for reading the Sonic Hedgehog signaling gradient in the vertebrate neural tube. *Cell* 148, 273-284.
- Barolo, S. (2012). Shadow enhancers: frequently asked questions about distributed cis-regulatory information and enhancer redundancy. *Bioessays* 34, 135-141.
- Bangs, F., Welten, M., Davey, M. G., Fisher, M., Yin, Y., Downie, H., Paton, B., Baldock, R., Burt, D. W. and Tickle, C. (2010). Identification of genes downstream of the Shh signalling in the developing chick wing and syn-expressed with Hoxd13 using microarray and 3D computational analysis. *Mech. Dev.* 127, 428–41.
- Bastida MF, Sheth R, Ros MA. 2009. A BMP-Shh negative-feedback loop restricts Shh expression during limb development. *Development* 136:3779-3789.
- Baur, F., Nau, K., Sadic, D., Allweiss, L., Elsässer, H.-P., Gillemans, N., de Wit, T., Krüger, I., Vollmer, M., Philipsen, S., et al. (2010). Specificity protein 2 (Sp2) is essential for mouse development and autonomous proliferation of mouse embryonic fibroblasts. *PLoS One* 5, e9587.
- Bell, S. M., Schreiner, C. M., Waclaw, R. R., Campbell, K., Potter, S. S. and Scott, W. J. (2003). Sp8 is crucial for limb outgrowth and neuropore closure. *PNAS* 100, 12195–12200.

- Benazet, J. D., Bischofberger, M., Tiecke, E., Goncalves, A., Martin, J. F., Zuniga, A., Naef, F. and Zeller, R. (2009). A self-regulatory system of interlinked signaling feedback loops controls mouse limb patterning. *Science* 323, 1050-1053.
- Bi W, Deng JM, Zhang Z, Behringer RR, de Crombrughe B. 1999. Sox9 is required for cartilage formation. *Nat Genet* 22:85-89.
- Biehs, B., Kechris, K., Liu, S. and Kornberg, T. B. (2010). Hedgehog targets in the *Drosophila* embryo and the mechanisms that generate tissue-specific outputs of Hedgehog signaling. *Development* 137, 3887-3898.
- Blume, S. W., Snyder, R. C., Ray, R., Thomas, S., Koller, C. a and Miller, D. M. (1991). Mithramycin inhibits SP1 binding and selectively inhibits transcriptional activity of the dihydrofolate reductase gene in vitro and in vivo. *J. Clin. Invest.* 88, 1613–21.
- Bowers, M., Eng, L., Lao, Z., Turnbull, R. K., Bao, X., Riedel, E., Mackem, S. and Joyner, A. L. (2012). Limb anterior-posterior polarity integrates activator and repressor functions of GLI2 as well as GLI3. *Dev Biol* 370, 110-124.
- Butterfield, N. C., Metzis, V., McGlinn, E., Bruce, S. J., Wainwright, B. J. and Wicking, C. (2009). Patched 1 is a crucial determinant of asymmetry and digit number in the vertebrate limb. *Development* 136, 3515-3524.
- Capdevila, J., Tsukui, T., Rodriguez Esteban, C., Zappavigna, V. and Izpisua Belmonte, J. C. (1999). Control of vertebrate limb outgrowth by the proximal factor Meis2 and distal antagonism of BMPs by Gremlin. *Mol Cell* 4, 839-849.
- Chamberlain, C. E., Jeong, J., Guo, C., Allen, B. L. and McMahon, A. P. (2008). Notochord-derived Shh concentrates in close association with the apically positioned basal body in neural target cells and forms a dynamic gradient during neural patterning. *Development* 135, 1097–106.
- Chang, D. T., López, A., Kessler, D. P. Von, Chiang, C., Simandl, B. K., Zhao, R., ... Beachy, P. A. (1994). Products , genetic linkage and limb patterning activity of a murine hedgehog gene. *Development*, 3353, 3339–3353.
- Charité, J., McFadden, D. G. and Olson, E. N. (2000). The bHLH transcription factor dHAND controls Sonic hedgehog expression and establishment of the zone of polarizing activity during limb development. *Development* 127, 2461-2470.
- Chen, J. K., Taipale, J., Young, K. E., Maiti, T. and Beachy, P. (2002). Small molecule modulation of Smoothed activity. *Proc. Natl. Acad. Sci. U. S. A.* 99, 14071–6.
- Chiang, C., Litingtung, Y., Lee, E., Young, K., Corden, J., Westphal, H. and Beachy, P. (1996). Cyclopia and defective axial patterning in mice lacking Sonic hedgehog gene function. 407–413.
- Chiang, C., Litingtung, Y., Harris, M. P., Simandl, B. K., Li, Y., Beachy, P. a and Fallon, J. F. (2001). Manifestation of the limb prepattern: limb development in the absence of sonic hedgehog function. *Dev. Biol.* 236, 421–35.
- Cooper KL, Hu JK, ten Berge D, Fernandez-Teran M, Ros MA, Tabin CJ. 2011. Initiation of proximal-distal patterning in the vertebrate limb by signals and growth. *Science* 332:1083-1086.

- Dai, P., Akimaru, H., Tanaka, Y., Maekawa, T., Nakafuku, M. and Ishii, S. (1999). Sonic Hedgehog-induced activation of the Gli1 promoter is mediated by GLI3. *J Biol Chem* 274, 8143-8152.
- Denker AE, Nicoll SB, Tuan RS. 1995. Formation of cartilage-like spheroids by micromass cultures of murine C3H10T1/2 cells upon treatment with transforming growth factor-beta 1. *Differentiation* 59:25-34.
- Deshane, J., Kim, J., Bolisetty, S., Hock, T. D., Hill-Kapturczak, N. and Agarwal, A. (2010). Sp1 regulates chromatin looping between an intronic enhancer and distal promoter of the human heme oxygenase-1 gene in renal cells. *J. Biol. Chem.* 285, 16476–86.
- Dessaud E, Yang LL, Hill K, Cox B, Ulloa F, Ribeiro A, Mynett A, Novitch BG, Briscoe J. 2007. Interpretation of the sonic hedgehog morphogen gradient by a temporal adaptation mechanism. *Nature* 450:717-720.
- Drossopoulou, G., Lewis, K. E., Sanz-Ezquerro, J. J., Nikbakht, N., McMahon, a P., Hofmann, C. and Tickle, C. (2000). A model for anteroposterior patterning of the vertebrate limb based on sequential long- and short-range Shh signalling and Bmp signalling. *Development* 127, 1337–48.
- Dunn, N. R., Winnier, G. E., Hargett, L. K., Schrick, J. J., Fogo, A. B. and Hogan, B. L. (1997). Haploinsufficient phenotypes in Bmp4 heterozygous null mice and modification by mutations in Gli3 and Alx4. *Dev Biol* 188, 235-247.
- Echelard, Y., Epstein, D. J., St-Jacques, B., Shen, L., Mohler, J., McMahon, J. A. and McMahon, A. P. (1993). Sonic hedgehog, a member of a family of putative signaling molecules, is implicated in the regulation of CNS polarity. *Cell* 75, 1417-1430.
- Estella, C. and Mann, R. S. (2010). Non-Redundant Selector and Growth-Promoting Functions of Two Sister Genes , buttonhead and Sp1 , in Drosophila Leg Development. *PLoS Genet.* 6,.
- Estella, C., Rieckhof, G., Calleja, M. and Morata, G. (2003). The role of buttonhead and Sp1 in the development of the ventral imaginal discs of Drosophila. *Development* 130, 5929–41.
- Falkenstein, K. N. and Vokes, S. a. (2014). Transcriptional Regulation of Graded Hedgehog Signaling. *Semin. Cell Dev. Biol.*
- Fan, H., Oro, A., Scott, M. P., & Khavari, P. A. (1997). Induction of basal cell carcinoma features in transgenic human skin expressing Sonic Hedgehog. *Nature Medicine*, 3, 788–792.
- Frankel, N. (2012). Multiple layers of complexity in cis-regulatory regions of developmental genes. *Dev Dyn* 241, 1857-1866.
- Frankel, N., Davis, G. K., Vargas, D., Wang, S., Payre, F. and Stern, D. L. (2010). Phenotypic robustness conferred by apparently redundant transcriptional enhancers. *Nature* 466, 490-493.
- Gailani, M. R., Stahle-Backdahl, M., Leffel, D. J., Glynn, M., Zaphiropoulos, P. G., Pressman, C., Uden, AB., Dean, M., Brash, DE., Bale, A., Toftgard, R. (1996).

- The role of the human homologue of *Drosophila* patched in sporadic basal cell carcinomas. *Nature*, *14*, 78–81.
- Galli, A., Robay, D., Osterwalder, M., Bao, X., Benazet, J. D., Tariq, M., Paro, R., Mackem, S. and Zeller, R. (2010). Distinct roles of Hand2 in initiating polarity and posterior Shh expression during the onset of mouse limb bud development. *PLoS Genet* *6*, e1000901.
- García-Huerta, P., Díaz-Hernandez, M., Delicado, E. G., Pimentel-Santillana, M., Miras-Portugal, M. T. and Gómez-Villafuertes, R. (2012). The specificity protein factor Sp1 mediates transcriptional regulation of P2X7 receptors in the nervous system. *J. Biol. Chem.* *287*, 44628–44.
- Gawantka, V., Pollet, N., Delius, H., Vingron, M. and Pfister, R. (1998). Gene expression screening in *Xenopus* identifies molecular pathways, predicts gene function and provides a global view of embryonic patterning. *Mech. Dev.* *77*, 95–141.
- Gene, C., Osteoblastic, C. S., Goto, T., Matsui, Y., Fernandes, R. J., Hanson, D. A., Kubo, T., Yukata, K., Michigami, T., Komori, T., et al. (2006). Sp1 Family of Transcription Factors Regulates the Human alpha2 (XI) Collagen Gene (COL11A2) in Saos-2 Osteoblastic Cells. *J. Bone Miner. Res.* *21*, 661–673.
- Gidoni, D., Dynan, W. and Tjian, R. (1984). Multiple specific contacts between a mammalian transcription factor and its cognate promoters. *Nature* *312*,.
- Gilmour, J., Assi, S. a, Jaegle, U., Kulu, D., van de Werken, H., Clarke, D., Westhead, D. R., Philipsen, S. and Bonifer, C. (2014). A crucial role for the ubiquitously expressed transcription factor Sp1 at early stages of hematopoietic specification. *Development* *141*, 1–11.
- Guo, G., Rödelberger, C., Digweed, M. and Robinson, P. N. (2013). Regulation of fibrillin-1 gene expression by Sp1. *Gene* *527*, 448–55.
- Hagen, G., Muller, S., Beato, M., Suske, G. and Marburg, P. (1992). Cloning by recognition site screening of two novel GT box binding proteins: a family of Sp1 related genes. *Nucleic Acids Res.* *20*, 5519–5525.
- Hallikas, O., Palin, K., Sinjushina, N., Rautiainen, R., Partanen, J., Ukkonen, E. and Taipale, J. (2006). Genome-wide prediction of mammalian enhancers based on analysis of transcription-factor binding affinity. *Cell* *124*, 47-59.
- Harfe, B. D., Scherz, P. J., Nissim, S., Tian, H., McMahon, A. P. and Tabin, C. J. (2004). Evidence for an expansion-based temporal Shh gradient in specifying vertebrate digit identities. *Cell* *118*, 517-528.
- Honig L, S. 1983. Polarizing activity of the avian limb examined on a cellular basis. New York: A.R. Liss. v. p.
- Hsu, D. R., Economides, A. N., Wang, X., Eimon, P. M. and Harland, R. M. (1998). Identifies a Novel Family of Secreted Proteins that Antagonize BMP Activities. *Mol. Cell* *1*, 673–683.
- Hu, J. K.-H., McGlenn, E., Harfe, B. D., Kardon, G. and Tabin, C. J. (2012). Autonomous and nonautonomous roles of Hedgehog signaling in regulating limb muscle formation. *Genes Dev.* *26*, 2088–102.

- Ingham, P. W., Nakano, Y. and Seger, C. (2011). Mechanisms and functions of Hedgehog signalling across the metazoa. *Nat Rev Genet* 12, 393-406.
- Jacob, J. and Briscoe, J. (2003). Gli proteins and the control of spinal-cord patterning. *EMBO Rep* 4, 761-765.
- Jeong, J., Mao, J., Tenzen, T., Kottmann, A. H. and McMahon, A. P. (2004). Hedgehog signaling in the neural crest cells regulates the patterning and growth of facial primordia. *Genes Dev* 18, 937-951.
- Jeong, J. H., Hines-Boykin, R., Ash, J. D. and Dittmer, D. P. (2002). Tissue specificity of the Kaposi's sarcoma-associated herpesvirus latent nuclear antigen (LANA/orf73) promoter in transgenic mice. *J Virol* 76, 11024-11032.
- Jiang, J., & Hui, C.-C. (2008). Hedgehog signaling in development and cancer. *Developmental Cell*, 15(6), 801–12. doi:10.1016/j.devcel.2008.11.010
- Ji, H., Vokes, S. A. and Wong, W. H. (2006). A comparative analysis of genome-wide chromatin immunoprecipitation data for mammalian transcription factors. *Nucleic Acids Res.* 34, e146.
- Ji, H., Jiang, H., Ma, W., Johnson, D. S., Myers, R. M. and Wong, W. H. (2008). An integrated software system for analyzing ChIP-chip and ChIP-seq data. *Nat. Biotechnol.* 26, 1293–300.
- Johnson, RL., Rothman, AL., Xie, J., Goodrich, LV., Bare, JW., Bonifas, JM., Quinn, AG., Myers, RM., Cox, DR., Epstein, EH., Scott, MP. (1996) Human homolog of patched, a candidate gene for the basal cell nevus syndrome. *Science*. 272:1668-1671.
- Kasaai, B., Gaumond, M.-H. and Moffatt, P. (2013). Regulation of the bone-restricted IFITM-like (Bril) gene transcription by Sp and Gli family members and CpG methylation. *J. Biol. Chem.* 288, 13278–94.
- Kawakami, Y., Esteban, C. R., Matsui, T., Rodríguez-León, J., Kato, S. and Izpisua Belmonte, J. C. (2004). Sp8 and Sp9, two closely related buttonhead-like transcription factors, regulate Fgf8 expression and limb outgrowth in vertebrate embryos. *Development* 131, 4763–74.
- Kawakami Y, Tsuda M, Takahashi S, Taniguchi N, Esteban CR, Zemmyo M, Furumatsu T, Lotz M, Izpisua Belmonte JC, Asahara H. 2005. Transcriptional coactivator PGC-1alpha regulates chondrogenesis via association with Sox9. *Proc Natl Acad Sci U S A* 102:2414-2419.
- Khokha, M. K., Hsu, D., Brunet, L. J., Dionne, M. S. and Harland, R. M. (2003). Gremlin is the BMP antagonist required for maintenance of Shh and Fgf signals during limb patterning. *Nat. Genet.* 34, 303–307.
- Khokha, M. K., Hsu, D., Brunet, L. J., Dionne, M. S. and Harland, R. M. (2003). Gremlin is the BMP antagonist required for maintenance of Shh and Fgf signals during limb patterning. *Nat Genet* 34, 303-307.
- Laufer, E., Nelson, Craig, Johnson, R., Morgan, B. and Tabin, C. (1994). Sonic hedgehog and Fgf-4 Act through a Signaling Cascade and Feedback Loop To Integrate Growth and Patterning of the Developing Limb Bud. *Cell* 79, 993–1003.
- Lek, M., Dias, J. M., Marklund, U., Uhde, C. W., Kurdija, S., Lei, Q., ... Ericson, J. (2010).

- A homeodomain feedback circuit underlies step-function interpretation of a Shh morphogen gradient during ventral neural patterning. *Development*, 137(23), 4051–60. doi:10.1242/dev.054288
- Lewandowski, J. P., Pursell, T. A., Rabinowitz, A. H. and Vokes, S. A. (2014). Manipulating Gene Expression and Signaling Activity in Cultured Mouse Limb Bud Cells. *Dev. Dyn.*
- Li, Y., Zhang, H., Litingtung, Y. and Chiang, C. (2006). Cholesterol modification restricts the spread of Shh gradient in the limb bud. *Proc. Natl. Acad. Sci. U. S. A.* 103, 6548–53.
- Li, D., Sakuma, R., Vakili, N. a, Mo, R., Puvindran, V., Deimling, S., Zhang, X., Hopyan, S. and Hui, C.-C. (2014a). Formation of proximal and anterior limb skeleton requires early function of *irx3* and *irx5* and is negatively regulated by *shh* signaling. *Dev. Cell* 29, 233–40.
- Li, Q., Lewandowski, J. P., Powell, M. B., Norrie, J. L., Cho, S. H. and Vokes, S. a (2014b). A Gli silencer is required for robust repression of *gremlin* in the vertebrate limb bud. *Development* 141, 1906–14.
- Litingtung, Y., Dahn, R. D., Li, Y., Fallon, J. F. and Chiang, C. (2002). Shh and Gli3 are dispensable for limb skeleton formation but regulate digit number and identity. *Nature* 418, 979-983.
- Livak KJ, Schmittgen TD. 2001. Analysis of relative gene expression data using real-time quantitative PCR and the 2(-Delta Delta C(T)) Method. *Methods* 25:402-408.
- Logan, M., Martin, J. F., Nagy, A., Lobe, C., Olson, E. N. and Tabin, C. J. (2002). Expression of Cre Recombinase in the developing mouse limb bud driven by a *Prxl* enhancer. *Genesis* 33, 77-80.
- Long F, Chung UI, Ohba S, McMahon J, Kronenberg HM, McMahon AP. 2004. *Ihh* signaling is directly required for the osteoblast lineage in the endochondral skeleton. *Development* 131:1309-1318.
- Lopez-Rios, J., Speziale, D., Robay, D., Scotti, M., Osterwalder, M., Nusspaumer, G., Galli, A., Hollander, G. A., Kmita, M. and Zeller, R. (2012). GLI3 constrains digit number by controlling both progenitor proliferation and BMP-dependent exit to chondrogenesis. *Dev Cell* 22, 837-848.
- Lopez-Rios, J., Duchesne, A., Speziale, D., Andrey, G., Peterson, K. a, Germann, P., ... Zeller, R. (2014). Attenuated sensing of SHH by *Ptch1* underlies evolution of bovine limbs. *Nature*, 511(7507), 46–51. doi:10.1038/nature13289
- Mariani FV, Ahn CP, Martin GR. 2008. Genetic evidence that FGFs have an instructive role in limb proximal-distal patterning. *Nature* 453:401-405.
- Marigo, V., Scott, M. P., Johnson, R. L., Goodrich, L. V and Tabin, C. J. (1996). Conservation in hedgehog signaling: induction of a chicken patched homolog by Sonic hedgehog in the developing limb. *Development* 122, 1225–33.
- Marinic, M., Aktas, T., Ruf, S. and Spitz, F. (2013). An integrated holo-enhancer unit defines tissue and gene specificity of the *Fgf8* regulatory landscape. *Dev Cell* 24, 530-542.

- Matise, M. P., Epstein, D. J., Park, H. L., Platt, K. A. and Joyner, A. L. (1998). Gli2 is required for induction of floor plate and adjacent cells, but not most ventral neurons in the mouse central nervous system. *Development* 125, 2759-2770.
- McGlinn, E., van Bueren, K. L., Fiorenza, S., Mo, R., Poh, A. M., Forrest, A., Soares, M. B., Bonaldo, M. D. F., Grimmond, S., Hui, C.-C., et al. (2005). Pax9 and Jagged1 act downstream of Gli3 in vertebrate limb development. *Mech. Dev.* 122, 1218–33.
- McKay, D. J., Estella, C. and Mann, R. S. (2009). The origins of the *Drosophila* leg revealed by the cis-regulatory architecture of the *Distalless* gene. *Development* 136, 61–71.
- Méthot, N. and Basler, K. (1999). Hedgehog controls limb development by regulating the activities of distinct transcriptional activator and repressor forms of *Cubitus interruptus*. *Cell* 96, 819–31.
- Michos, O., Panman, L., Vintersten, K., Beier, K., Zeller, R. and Zuniga, A. (2004). Gremlin-mediated BMP antagonism induces the epithelial-mesenchymal feedback signaling controlling metanephric kidney and limb organogenesis. *Development* 131, 3401–10.
- Minowada, G., Jarvis, L. a, Chi, C. L., Neubüser, a, Sun, X., Hacoheh, N., Krasnow, M. a and Martin, G. R. (1999). Vertebrate *Sprouty* genes are induced by FGF signaling and can cause chondrodysplasia when overexpressed. *Development* 126, 4465–75.
- Mohammadi, M., McMahon, G., Sun, L., Tang, C., Hirth, P., Yeh, B. K., Hubbard, S. R. and Schlessinger, J. (1997). Structures of the tyrosine kinase domain of fibroblast growth factor receptor in complex with inhibitors. *Science* 276, 955-960.
- Montavon, T., Soshnikova, N., Mascrez, B., Joye, E., Thevenet, L., Splinter, E., de Laat, W., Spitz, F. and Duboule, D. (2011). A regulatory archipelago controls Hox genes transcription in digits. *Cell* 147, 1132-1145.
- Motoyama, J. (1998). *Ptch2*, a second mouse *Patched* gene is co-expressed with *Sonic hedgehog*. *Nat. Genet.* 18, 104–106.
- Muller, B. and Basler, K. (2000). The repressor and activator forms of *Cubitus interruptus* control Hedgehog target genes through common generic gli-binding sites. *Development* 127, 2999-3007.
- Nahmad, M. and Stathopoulos, A. (2009). Dynamic interpretation of hedgehog signaling in the *Drosophila* wing disc. *PLoS Biol.* 7,.
- Niswander, L., Jeffrey, S., Martin, G. and Tickle, C. (1994). A positive feedback loop coordinates growth and patterning in the vertebrate limb. 609–612.
- Nissim, S., Hasso, S. M., Fallon, J. F. and Tabin, C. J. (2006). Regulation of Gremlin expression in the posterior limb bud. *Dev Biol* 299, 12-21.
- Niswander L, Jeffrey S, Martin GR, Tickle C. 1994. A positive feedback loop coordinates growth and patterning in the vertebrate limb. *Nature* 371:609-612.
- Nybakken K, Vokes SA, Lin TY, McMahon AP, Perrimon N. 2005. A genome-wide RNA interference screen in *Drosophila melanogaster* cells for new components of the Hh signaling pathway. *Nat Genet* 37:1323-1332.
- Oosterveen, T., Kurdija, S., Alekseenko, Z., Uhde, C. W., Bergsland, M., Sandberg, M., Andersson, E., Dias, J. M., Muhr, J. and Ericson, J. (2012). Mechanistic differences

- in the transcriptional interpretation of local and long-range shh morphogen signaling. *Dev Cell* 23, 1006-1019.
- Pan, Y., Bai, C. B., Joyner, A. L. and Wang, B. (2006). Sonic hedgehog signaling regulates Gli2 transcriptional activity by suppressing its processing and degradation. *Mol Cell Biol* 26, 3365-3377.
- Panman, L., Galli, A., Lagarde, N., Michos, O., Soete, G., Zuniga, A. and Zeller, R. (2006). Differential regulation of gene expression in the digit forming area of the mouse limb bud by SHH and gremlin 1/FGF-mediated epithelial-mesenchymal signalling. *Development* 133, 3419-3428.
- Parker, D. S., White, M. A., Ramos, A. I., Cohen, B. A. and Barolo, S. (2011). The cis-regulatory logic of Hedgehog gradient responses: key roles for gli binding affinity, competition, and cooperativity. *Sci Signal* 4, ra38.
- Pastrana DV, Tolstov YL, Becker JC, Moore PS, Chang Y, Buck CB. 2009. Quantitation of human seroresponsiveness to Merkel cell polyomavirus. *PLoS Pathog* 5:e1000578.
- Paulsen DF, Solorsh M. 1988. Microtiter micromass cultures of limb-bud mesenchymal cells. *In Vitro Cell Dev Biol* 24:138-147.
- Perry, M. W., Boettiger, A. N., Bothma, J. P. and Levine, M. (2010). Shadow enhancers foster robustness of Drosophila gastrulation. *Curr Biol* 20, 1562-1567.
- Persson, M., Stamatakis, D., te Welscher, P., Andersson, E., Bose, J., Ruther, U., Ericson, J. and Briscoe, J. (2002). Dorsal-ventral patterning of the spinal cord requires Gli3 transcriptional repressor activity. *Genes Dev* 16, 2865-2878.
- Peterson, K. A., Nishi, Y., Ma, W., Vedenko, A., Shokri, L., Zhang, X., McFarlane, M., Baizabal, J. M., Junker, J. P., van Oudenaarden, A., et al. (2012). Neural-specific Sox2 input and differential Gli-binding affinity provide context and positional information in Shh-directed neural patterning. *Genes Dev* 26, 2802-2816.
- Pietsch, T., Waha, A., Koch, A., Pietsch, T., Waha, A., Koch, A., ... Wicking, C. (1997). Medulloblastomas of the Desmoplastic Variant Carry Mutations of the Human Homologue of Drosophila patched. *Cancer Research*, (57), 2085–2088.
- Pizette, S. and Niswander, L. (1999). BMPs negatively regulate structure and function of the limb apical ectodermal ridge. *Development* 126, 883-894.
- Probst, S., Kraemer, C., Demougin, P., Sheth, R., Martin, G. R., Shiratori, H., Hamada, H., Iber, D., Zeller, R. and Zuniga, A. (2011). SHH propagates distal limb bud development by enhancing CYP26B1-mediated retinoic acid clearance via AER-FGF signalling. *Development* 138, 1913–23.
- Rabinowitz, A. H. and Vokes, S. A. (2012). Integration of the transcriptional networks regulating limb morphogenesis. *Dev Biol* 368, 165-180.
- Rainger, J., van Beusekom, E., Ramsay, J. K., McKie, L., Al-Gazali, L., Pallotta, R., Saponari, A., Branney, P., Fisher, M., Morrison, H., et al. (2011). Loss of the BMP antagonist, SMOC-1, causes Ophthalmo-acromelic (Waardenburg Anophthalmia) syndrome in humans and mice. *PLoS Genet.* 7, e1002114.
- Ramialison, M., Reinhardt, R., Henrich, T., Wittbrodt, B., Kellner, T., Lowy, C. M.

- and Wittbrodt, J. (2012). Cis-regulatory properties of medaka synexpression groups. *Development* 139, 917–28.
- Riddle, R. D., Johnson, R. L., Tabin, C., & Laufer, E. (1993). Sonic hedgehog Mediates the Polarizing Activity of the ZPA. *Cell*, 75, 1401–1416.
- Roselló-Díez, A., Arques, C. G., Delgado, I., Giovinazzo, G. and Torres, M. (2014). Diffusible signals and epigenetic timing cooperate in late proximo-distal limb patterning. *Development* 141, 1534–43.
- Ruiz i Altaba, A. (1997). Catching a Gli-mouse of Hedgehog. *Cell* 90, 193-196.
- Saffer, J. D., Jackson, S. P. and Annarella, M. B. (1991). Developmental Expression of Spl in the Mouse. *Mol. Cell. Biol.* 11,.
- Sahara, S., Kawakami, Y., Izpisua Belmonte, J. C. and O’Leary, D. D. M. (2007). Sp8 exhibits reciprocal induction with Fgf8 but has an opposing effect on anterior-posterior cortical area patterning. *Neural Dev.* 2, 10.
- Sanders, T. a, Llagostera, E. and Barna, M. (2013). Specialized filopodia direct long-range transport of SHH during vertebrate tissue patterning. *Nature* 497, 628–32.
- Sasaki, H., Nishizaki, Y., Hui, C., Nakafuku, M. and Kondoh, H. (1999). Regulation of Gli2 and Gli3 activities by an amino-terminal repression domain: implication of Gli2 and Gli3 as primary mediators of Shh signaling. *Development* 126, 3915-3924.
- Saunders, JW Jr., Gasseling, MT., (1968) Ectodermal-mesodermal interactions in the origin of limb symmetry. *Epithelial-Mesenchymal Interactions.* 78-97.
- Scherz, P. J., McGlinn, E., Nissim, S. and Tabin, C. J. (2007). Extended exposure to Sonic hedgehog is required for patterning the posterior digits of the vertebrate limb. *Dev. Biol.* 308, 343–54.
- Selever, J., Liu, W., Lu, M. F., Behringer, R. R. and Martin, J. F. (2004). Bmp4 in limb bud mesoderm regulates digit pattern by controlling AER development. *Dev Biol* 276, 268-279.
- Shah, A., Tenzen, T., McMahon, A. P. and Woolf, P. J. (2009). Using mechanistic Bayesian networks to identify downstream targets of the sonic hedgehog pathway. *BMC Bioinformatics* 10, 433.
- Sheth, R., Gregoire, D., Dumouchel, A., Scotti, M., Pham, J. M., Nemeč, S., Bastida, M. F., Ros, M. A. and Kmita, M. (2013). Decoupling the function of Hox and Shh in developing limb reveals multiple inputs of Hox genes on limb growth. *Development* 140, 2130-2138.
- Shlyueva, D., Stampfel, G. and Stark, A. (2014). Transcriptional enhancers: from properties to genome-wide predictions. *Nat. Rev. Genet.* 15, 272–86.
- Shubin, N., Tabin, C. and Carroll, S. (2009). Deep homology and the origins of evolutionary novelty. *Nature* 457, 818–23.
- Sinha, S. and Chen, J. K. (2006). Purmorphamine activates the Hedgehog pathway by targeting Smoothened. *Nat. Chem. Biol.* 2, 29–30.
- Snyder, R. C., Ray, R., Blume, S. and Miller, D. M. (1991). Mithramycin blocks transcriptional initiation of the c-myc P1 and P2 promoters. *Biochemistry* 30, 4290–7.
- Su, W., Jackson, S., Tjian, R. and Echols, H. (1991). DNA looping between sites for

- transcriptional activation: self-association of DNA-bound Sp1. *Genes Dev.* 5, 820.
- Suske, G., Bruford, E. and Philipsen, S. (2005). Mammalian SP/KLF transcription factors: bring in the family. *Genomics* 85, 551–6.
- Talamillo, A., Delgado, I., Nakamura, T., de-Vega, S., Yoshitomi, Y., Unda, F., Birchmeier, W., Yamada, Y. and Ros, M. a (2010). Role of Epiprofin, a zinc-finger transcription factor, in limb development. *Dev. Biol.* 337, 363–74.
- Tannous BA, Kim DE, Fernandez JL, Weissleder R, Breakefield XO. 2005. Codon-optimized Gaussia luciferase cDNA for mammalian gene expression in culture and in vivo. *Mol Ther* 11:435-443.
- te Welscher, P., Zuniga, A., Kuijper, S., Drenth, T., Goedemans, H. J., Meijlink, F. and Zeller, R. (2002). Progression of vertebrate limb development through SHH-mediated counteraction of GLI3. *Science* 298, 827-830.
- ten Berge D, Brugmann SA, Helms JA, Nusse R. 2008. Wnt and FGF signals interact to coordinate growth with cell fate specification during limb development. *Development* 135:3247-3257.
- Towers, M., Mahood, R., Yin, Y. and Tickle, C. (2008). Integration of growth and specification in chick wing digit-patterning. *Nature* 452, 882-886.
- Treichel, D., Schöck, F., Jäckle, H., Gruss, P. and Mansouri, A. (2003). mBtd is required to maintain signaling during murine limb development. *Genes Dev.* 17, 2630–5.
- Trevino C, Anderson R, Landry M, König G, Tonthat B, Shi C, Muneoka K. 1993. MPLB-2: a posterior signaling cell line derived from the mouse limb bud. *Prog Clin Biol Res* 383A:295-304.
- Van Dyke, M. W. and Dervan, P. B. (1983). Chromomycin, mithramycin, and olivomycin binding sites on heterogeneous deoxyribonucleic acid. Footprinting with (methidiumpropyl-EDTA)iron(II). *Biochemistry* 22, 2373–7.
- Vargesson, N., Clarke, J. D., Vincent, K., Coles, C., Wolpert, L. and Tickle, C. (1997). Cell fate in the chick limb bud and relationship to gene expression. *Development* 124, 1909–18.
- Verheyden, J. M. and Sun, X. (2008). An Fgf/Gremlin inhibitory feedback loop triggers termination of limb bud outgrowth. *Nature* 454, 638-641.
- Visel, A., Carson, J., Oldekamp, J., Warnecke, M., Jakubcaková, V., Zhou, X., Shaw, C. a, Alvarez-Bolado, G. and Eichele, G. (2007). Regulatory pathway analysis by high-throughput in situ hybridization. *PLoS Genet.* 3, 1867–83.
- Vokes, S. A., Ji, H., Wong, W. H. and McMahon, A. P. (2008). A genome-scale analysis of the cis-regulatory circuitry underlying sonic hedgehog-mediated patterning of the mammalian limb. *Genes Dev* 22, 2651-2663.
- Wang, B., Fallon, J. F. and Beachy, P. A. (2000). Hedgehog-regulated processing of Gli3 produces an anterior/posterior repressor gradient in the developing vertebrate limb. *Cell* 100, 423-434.
- Wang, C., Pan, Y. and Wang, B. (2010). Suppressor of fused and Spop regulate the stability, processing and function of Gli2 and Gli3 full-length activators but not their repressors. *Development* 137, 2001-2009.

- Wang, C., Ruther, U. and Wang, B. (2007). The Shh-independent activator function of the full-length Gli3 protein and its role in vertebrate limb digit patterning. *Dev Biol* 305, 460-469.
- Wang, C. C., Chan, D. C. and Leder, P. (1997). The mouse formin (Fmn) gene: genomic structure, novel exons, and genetic mapping. *Genomics* 39, 303-311.
- Wen, X., Lai, C. K., Evangelista, M., Hongo, J. A., de Sauvage, F. J. and Scales, S. J. (2010). Kinetics of hedgehog-dependent full-length Gli3 accumulation in primary cilia and subsequent degradation. *Mol Cell Biol* 30, 1910-1922.
- Welten, M., Pavlovska, G., Chen, Y., Teruoka, Y., Fisher, M., Bangs, F., Towers, M. and Tickle, C. (2011). 3D expression patterns of cell cycle genes in the developing chick wing and comparison with expression patterns of genes implicated in digit specification. *Dev. Dyn.* 240, 1278–88.
- Whiting, J., Marshall, H., Cook, M., Krumlauf, R., Rigby, P. W., Stott, D. and Allemann, R. K. (1991). Multiple spatially specific enhancers are required to reconstruct the pattern of Hox-2.6 gene expression. *Genes Dev* 5, 2048-2059.
- Wilson, C. W. and Chuang, P.-T. (2010). Mechanism and evolution of cytosolic Hedgehog signal transduction. *Development* 137, 2079–94.
- Yang, Y., Drossopoulou, G., Chuang, P. T., Duprez, D., Marti, E., Bumcrot, D., Vargesson, N., Clarke, J., Niswander, L., McMahon, A., et al. (1997). Relationship between dose, distance and time in Sonic Hedgehog-mediated regulation of anteroposterior polarity in the chick limb. *Development* 124, 4393-4404.
- Yokoyama, S., Ito, Y., Ueno-Kudoh, H., Shimizu, H., Uchibe, K., Albin, S., Mitsuoka, K., Miyaki, S., Kiso, M., Nagai, A., et al. (2009). A systems approach reveals that the myogenesis genome network is regulated by the transcriptional repressor RP58. *Dev. Cell* 17, 836–48.
- Yoo, J., Jeong, M.-J., Kwon, B.-M., Hur, M.-W., Park, Y.-M. and Han, M. Y. (2002). Activation of dynamin I gene expression by Sp1 and Sp3 is required for neuronal differentiation of N1E-115 cells. *J. Biol. Chem.* 277, 11904–9.
- Yu, J., Valerius, M. T., Duah, M., Staser, K., Hansard, J. K., Guo, J.-J., McMahon, J., Vaughan, J., Faria, D., Georgas, K., et al. (2012). Identification of molecular compartments and genetic circuitry in the developing mammalian kidney. *Development* 139, 1863–73.
- Yuen CM, Rodda SJ, Vokes SA, McMahon AP, Liu DR. 2006. Control of transcription factor activity and osteoblast differentiation in mammalian cells using an evolved small-molecule-dependent intein. *J Am Chem Soc* 128:8939-8946.
- Zeller, R., López-Ríos, J. and Zuniga, A. (2009). Vertebrate limb bud development: moving towards integrative analysis of organogenesis. *Nat. Rev. Genet.* 10, 845–58.
- Zhang, B., Kirov, S. and Snoddy, J. (2005). WebGestalt: an integrated system for exploring gene sets in various biological contexts. *Nucleic Acids Res.* 33, W741–8.
- Zhang, Y., Hassan, M. Q., Xie, R.-L., Hawse, J. R., Spelsberg, T. C., Montecino, M., Stein, J. L., Lian, J. B., van Wijnen, A. J. and Stein, G. S. (2009). Co-stimulation of the bone-related Runx2 P1 promoter in mesenchymal cells by SP1 and ETS

- transcription factors at polymorphic purine-rich DNA sequences (Y-repeats). *J. Biol. Chem.* 284, 3125–35.
- Zhao, C. and Meng, A. (2005). Sp1-like transcription factors are regulators of embryonic development in vertebrates. *Dev. Growth Differ.* 47, 201–11.
- Zhu, J., Nakamura, E., Nguyen, M. T., Bao, X., Akiyama, H. and Mackem, S. (2008). Uncoupling Sonic hedgehog control of pattern and expansion of the developing limb bud. *Dev Cell* 14, 624–632.
- Zhulyn, O., Li, D., Deimling, S., Vakili, N. A., Mo, R., Puvindran, V., Chen, M.-H., Chuang, P.-T., Hopyan, S. and Hui, C.-C. (2014). A switch from low to high shh activity regulates establishment of limb progenitors and signaling centers. *Dev. Cell* 29, 241–9.
- Zuniga, A., Haramis, A. P., McMahon, A. P. and Zeller, R. (1999). Signal relay by BMP antagonism controls the SHH/FGF4 feedback loop in vertebrate limb buds. *Nature* 401, 598–602.
- Zuniga, A., Laurent, F., Lopez-Rios, J., Klasen, C., Matt, N. and Zeller, R. (2012). Conserved cis-regulatory regions in a large genomic landscape control SHH and BMP-regulated Gremlin1 expression in mouse limb buds. *BMC Dev Biol* 12, 23.
- Zuniga, A., Michos, O., Spitz, F., Haramis, A. P., Panman, L., Galli, A., Vintersten, K., Klasen, C., Mansfield, W., Kuc, S., et al. (2004). Mouse limb deformity mutations disrupt a global control region within the large regulatory landscape required for Gremlin expression. *Genes Dev* 18, 1553–1564.
- Zúñiga, A. and Zeller, R. (1999). Gli3 (Xt) and formin (ld) participate in the positioning of the polarising region and control of posterior limb-bud identity. *Development* 126, 13–21.